AD-A133 918 NONLINEAR OSCILLATIONS OF A FLUTTERING PANEL IN A TRANSONIC AIRSTREAM(U) DAYTON UNIV OH SCHOOL OF ENGINEERING F E EASTEP APR 83 UDR-TR-83-43 1/2

UNCLASSIFIED AFOSR-TR-83-0858 AFOSR-81-0134 F/G 20/4 NL

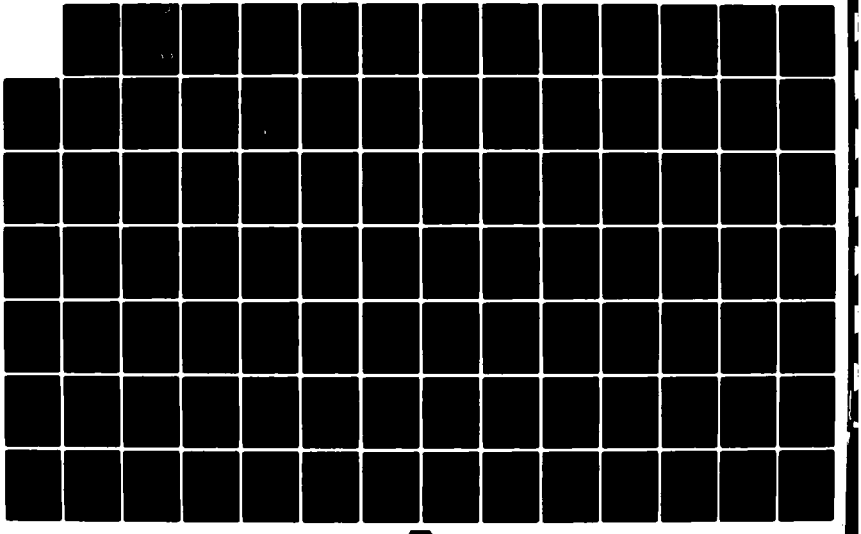

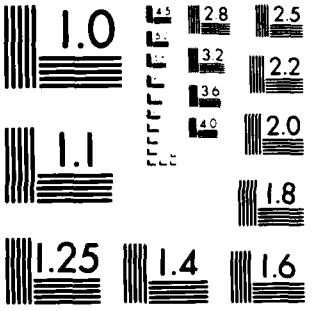

AFOSR-TR- 83-0858

AD-A133918

NONLINEAR OSCILLATIONS OF A FLUTTERING PANEL IN A TRANSONIC AIRSTREAM

Franklin E. Eastep
School of Engineering
University of Dayton
Dayton, OH 45469

April 1983

FINAL REPORT

Distribution is unlimited.

Prepared for

Air Force Office of Scientific Research
Bolling Air Force Base, D.C.

Unclassified

SECURITY CLASSIFICATION OF THIS PAGE (When Data Entered)

REPORT DOCUMENTATION PAGE	READ INSTRUCTIONS BEFORE COMPLETING FORM
1. REPORT NUMBER AFOSR-TR- 83-0858 / 2. GOVT ACCESSION NO. A133 918	3. RECIPIENT'S CATALOG NUMBER
4. TITLE (and Subtitle) NONLINEAR OSCILLATIONS OF A FLUTTERING PANEL IN A TRANSONIC AIRSTREAM	5. TYPE OF REPORT & PERIOD COVERED Final Report 1 May 81 - 1 May 82
	6. PERFORMING ORG. REPORT NUMBER UDR-TR-83-43
7. AUTHOR(s) Franklin E. Eastep	8. CONTRACT OR GRANT NUMBER(s) AFOSR-81-0134
9. PERFORMING ORGANIZATION NAME AND ADDRESS School of Engineering University of Dayton Dayton, Ohio 45469	10. PROGRAM ELEMENT, PROJECT, TASK AREA & WORK UNIT NUMBERS 61102F 2307/D9
11. CONTROLLING OFFICE NAME AND ADDRESS AFOSR/NA Bolling Air Force Base, D.C. 20332	12. REPORT DATE April 1983
	13. NUMBER OF PAGES 98
14. MONITORING AGENCY NAME & ADDRESS(if different from Controlling Office)	15. SECURITY CLASS. (of this report) Unclassified
	15a. DECLASSIFICATION/DOWNGRADING SCHEDULE

16. DISTRIBUTION STATEMENT (of this Report)

Approved for public release; distribution unlimited.

17. DISTRIBUTION STATEMENT (of the abstract entered in Block 20, if different from Report)

18. SUPPLEMENTARY NOTES

19. KEY WORDS (Continue on reverse side if necessary and identify by block number)

Aeroelasticity
Panel Flutter
Nonlinear Response
Unsteady Transonic Aerodynamics

20. ABSTRACT (Continue on reverse side if necessary and identify by block number)

A flutter analysis has been conducted on a simply supported panel to demonstrate the successful combining of the panel (Von Karman) large deflection equations with a linear aerodynamic (Piston) theory for determining the panel response. The panel response was determined by coupling a Galerkin modal representation with a numerical time integration scheme. The time integration scheme was also successfully used to obtain the linear

DD FORM 1 JAN 73 1473

Unclassified

SECURITY CLASSIFICATION OF THIS PAGE (When Data Entered)

structural (small-deflection) response to a nonlinear aerodynamic pressure. Here, the simultaneous time integration scheme was used to determine the aeroelastic response of the linear pitching or plunging of an airfoil to the nonlinear lift and moment obtained from the NLR-LTRAN2 computer code. An analysis was also initiated to study the nonlinear panel response to a nonlinear aerodynamic pressure using the simultaneous time integration scheme; but, numerical instabilities within the computer code NLR-LTRAN2 have hampered the progress.

Because the representation of the nonlinear panel response by a linear superposition of linear mode shapes is very questionable, the Von Karman large deflection equations were replaced by a large deflection finite-element representation. The nonlinear panel response of the finite-element model was obtained using Piston theory aerodynamics and it is recommended that the finite-element response be determined for a nonlinear aerodynamic pressure.

TABLE OF CONTENTS

LIST OF FIGURES

LIST OF FIGURES (continued)

LIST OF TABLES

LIST OF SYMBOLS

a	Chord
b	Semichord
C	Damping
C_ℓ	Coefficient of lift
C_m	Coefficient of moment
D	Plate stiffness
E	Modulus of elasticity
F	Airy stress function
h	Plate thickness
I	Bending inertia
I_α	Mass moment of inertia
K	Stiffness
k_a	Reduced frequency, $\frac{a\omega}{V}$
M	Mach number
$\bar{m}$	Mass
N	Number of assumed modes
$\bar{N}$	Axial load
P	Pressure
$\bar{P}$	Force
q	Dynamic pressure, $1/2\ \rho V^2$
t	Time
U	Unknown coefficients of time
V	Velocity
W	Transverse deflection

LIST OF SYMBOLS (continued)

x	Spatial coordinate
y	Spatial coordinate
α	Pitching angle
γ	Specific heat
δ	Plunging displacement
μ'	Airfoil - air mass moment of inertia ratio, $I_\alpha/\pi\rho b^4$
$\bar{\mu}$	Airfoil - air mass ratio, $M/\pi\rho b^2$
ρ	Density
ω	Frequency
ϕ	Displacement functions
$\bar{\phi}$	Velocity potentials

Subscripts

i	Mode Number
m	Material
x	Spatial direction
y	Spatial direction
∞	Infinity condition

SECTION 1

INTRODUCTION

Panel flutter is a self-induced oscillation of a thin-walled structure caused by an increase of aerodynamic forces resulting from panel deformation in an airstream. Panel flutter does differ from wing flutter in that the nature of panel flutter is generally not as catastrophic as wing flutter. Linear flutter prediction techniques allow one to determine the locus of neutrally stable oscillations which is called the flutter boundary. Nonlinear panel flutter; however, is characterized by a periodic oscillation of finite amplitude at and above the linear flutter boundary. Presently, the two methods available for nonlinear flutter prediction are theoretical analysis and experimental determination.

At the present time there is poor correlation between experimental and theoretical flutter prediction in the transonic Mach number regime. In the past, the theoretical prediction of panel flutter has been overly conservative due to simplifying assumptions made because of the complexity of panel flutter. However, these assumptions are usually so restrictive that there is great variance between experimental results and theoretical predictions at transonic speeds.

The theoretical studies have been restricted by use of a simplified linear aerodynamic theory and an imprecise idealization of the panel support conditions which result when the

nonlinear midplane stresses (i.e., use of small amplitude oscillation) are neglected. This study removes the above two simplifying assumptions in that the large deflection equations of a panel in a nonlinear transonic airstream with shocks present, are formulated for solution.

Dowell[1] has presented a study of the nonlinear flutter of a flat panel using a Galerkin procedure wherein he numerically integrates the resulting ordinary differential equation of motion in the time variable. Dowell[2] has also used a nonlinear plate theory but a linear aerodynamic theory in the form of both a quasi-steady and a full unsteady theory. The availability of such an analysis permits the consideration of the panel post-flutter behavior only over the subsonic and supersonic Mach number range. In the transonic range it is necessary to use a nonlinear aerodynamic theory since the governing differential equation is nonlinear and contains both subsonic and supersonic regions together with shocks.

The method to be used herein will be briefly outlined. The equations of motion for the transverse oscillation of a panel are obtained. It is assumed that the large deformations can be adequately described by use of the Von-Karman large strain-displacement relations. The flutter motion of the panel is described by a simple two mode approximation. Galerkin's method is used to obtain the differential equation in time governing the panel response to a time dependent aerodynamic pressure field. The aerodynamic pressure is to be transonic and as such is governed by the small-disturbance, potential transonic flow differential

equation. The solution to the nonlinear transonic differential equation is obtained using a finite difference method developed by Ballhaus and Goorjian[3] and modified for large values of reduced frequency by Huizing and van der Vooren[4]. This time dependent response investigation requires simultaneous integration of the panel large deflection equation and the transonic aerodynamic equations in time.

Objectives

The main objective of this investigation is to determine a procedure for the prediction of the large deflection response of a structural panel situated in a transonic airstream. Von-Karman large deflection equations are to be integrated simultaneously with solutions of the nonlinear transonic equations obtained from a finite difference, alternating direction implicit scheme referred to as LTRAN2. The prime task then is to incorporate this integration scheme into a modified version of LTRAN2 called NLR-LTRAN2. This procedure will yield theoretical predictions of flutter speed which should compare with experimentally determined speeds within the transonic Mach number region.

Large Deflection Equations for Panel Oscillation

Consider the isotropic thin-walled panel shown in Figure 1. It is exposed to a transonic airstream in which shocks may occur and is subjected to a longitudinal axial load. It is assumed that the large oscillations of the panel in the presence of mid-surface stresses are governed by the nonlinear Von-Karman strain displacement relations. These relations are given as:

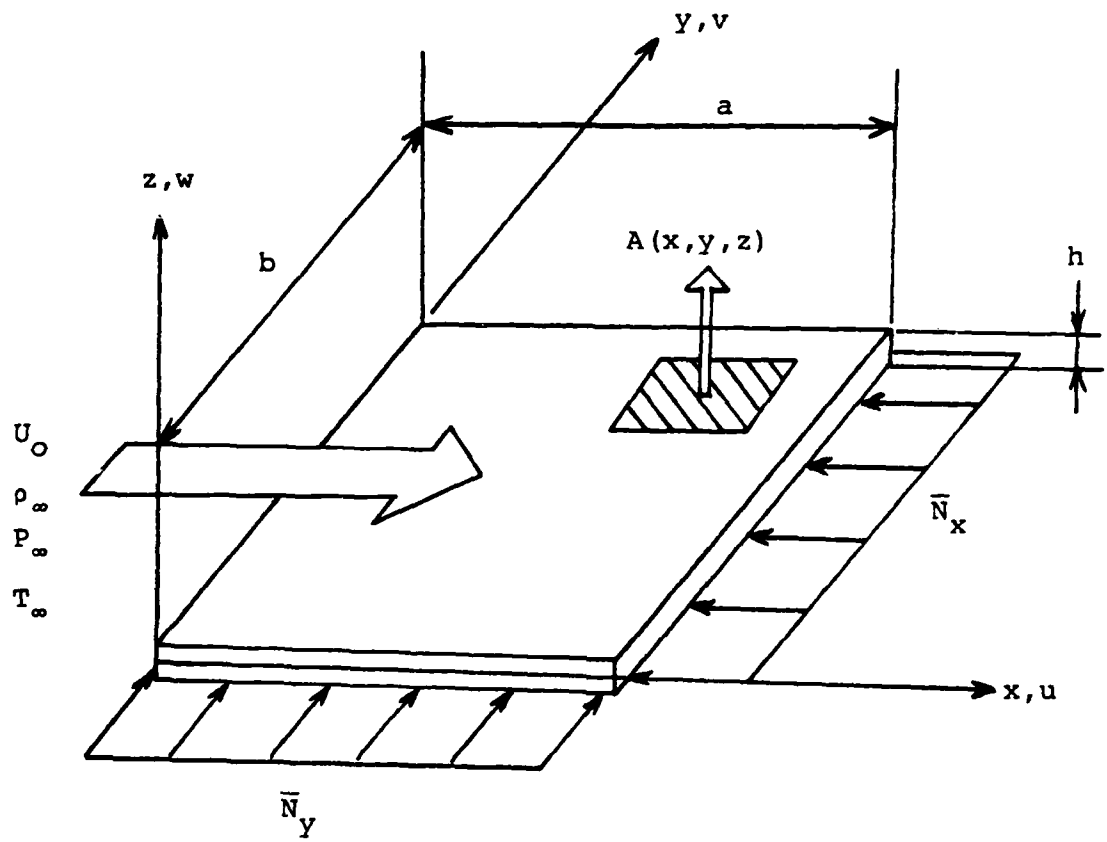

ρ - plate density

$E = 10 \times 10^6$ lb/in^2
h = 0.03 in
a = b = 10 in

Plate edges are simply supported

Figure 1. A Thin Uniform Elastic Plate Exposed to a Transonic Airstream

$$\epsilon_x = \frac{\partial u}{\partial x} + \frac{1}{2}\left(\frac{\partial w}{\partial x}\right)^2 - z\frac{\partial^2 w}{\partial x^2} \tag{1a}$$

$$\epsilon_y = \frac{\partial u}{\partial y} + \frac{1}{2}\left(\frac{\partial w}{\partial y}\right)^2 - z\frac{\partial^2 y}{\partial y^2} \tag{1b}$$

$$\gamma_{xy} = \frac{\partial u}{\partial y} + \frac{\partial v}{\partial x} + \frac{\partial w}{\partial x}\frac{\partial w}{\partial y} - 2z\frac{\partial^2 w}{\partial x \partial y} \tag{1c}$$

where z is measured from the midsurface of the panel. Equation (1) is a modification of a small deflection theory to include the first order effects of midsurface stretching necessary to investigate large deflections.

Now Hamilton's variational principle is enforced to obtain the partial differential equations of panel motion. For a three-dimensional plate, Von-Karman's large deflection equations (see Eastep and McIntosh[5] for a derivation) are:

$$D\nabla^4 w - h\frac{\partial^2 F}{\partial y^2}\frac{\partial^2 w}{\partial x^2} - 2\frac{\partial^2 F}{\partial x \partial y}\frac{\partial^2 w}{\partial x \partial y} + \frac{\partial^2 F}{\partial x^2}\frac{\partial^2 w}{\partial y^2} + \bar{N}_x\frac{\partial^2 w}{\partial x^2} + \frac{\partial^2 w}{\partial x^2}$$

$$+ \bar{N}_y\frac{\partial^2 w}{\partial y^2} = -\rho h\frac{\partial^2 w}{\partial t^2} + A(w,t) \tag{2}$$

and

$$\frac{\nabla^4 F}{E} = \left(\frac{\partial^2 w}{\partial x \partial y}\right)^2 - \frac{\partial^2 w}{\partial x^2}\frac{\partial^2 w}{\partial y^2} \tag{3}$$

where w is the plate transverse deflection while F is the Airy stress function. The aerodynamic pressure loading, A, is the

increased incremental aerodynamic pressure caused by the panel deformation and is given by:

$$A(w,t) = -\rho_\infty \left[\frac{\partial \phi}{\partial t} + U_o \frac{\partial \phi}{\partial x}\right] \tag{4}$$

where the velocity potential ϕ must satisfy the small disturbance transonic differential equation:

$$(1-M_\infty^2)\frac{\partial^2 \bar{\phi}}{\partial x^2} - (\gamma + 1) M_\infty^2 \frac{\partial \bar{\phi}}{\partial x}\frac{\partial^2 \bar{\phi}}{\partial x^2} - 2M_\infty^2 \frac{\partial^2 \bar{\phi}}{\partial t^2} - 2M_\infty^2 \frac{\partial^2 \bar{\phi}}{\partial t \partial x}$$

$$+ \frac{\partial^2 \bar{\phi}}{\partial y^2} = 0 \tag{5}$$

The numerical computation method used for determining the unsteady transonic flow field is based on the alternating direction implicit (ADI)[3] procedure modified to consider flows of moderately high reduced frequencies and panel deformations. The procedure is referred to as NLR-LTRAN2.[4]

The system of Equations (2) through (5) will be solved by the Galerkin method for a simply supported plate undergoing cylindrical bending. That is:

$$W(x,t) = h\left[C_1(t)\sin\frac{\pi x}{a} + C_2(t)\sin\frac{2\pi x}{a}\right] \tag{6}$$

SECTION 2

APPROACH

Two-Dimensional Flow

Consider for simplification the flow about a two-dimensional wing panel of given thickness undergoing an assumed chordwise deformation and the prediction of the oscillatory aerodynamic pressures in the transonic speed regime. Figure 2 shows a panel that is simple supported at both ends. For this study the aerodynamic loading was assumed to act only on one side of the panel. The undeformed shape of the panel was represented by a half-sine wave for both the upper and lower surfaces. With a chord of 10 inches, the thickness to chord ratio of the panel was 0.003.

For two-dimensional flow, all derivatives with respect to y are zero. Therefore, th Von-Karman large deflection plate equation becomes:

$$D \frac{\partial^4 w}{\partial w^4} - \bar{N}_x \frac{\partial^2 w}{\partial x^2} + \rho_m h \frac{\partial^2 w}{\partial t^2} = - (P - P\infty) \qquad (7)$$

where the longitudinal axial load $\bar{N}_x$ is defined as:

$$N_x = \frac{Eh}{2a} \int_0^a \left(\frac{\partial w}{\partial x}\right)^2 dx$$

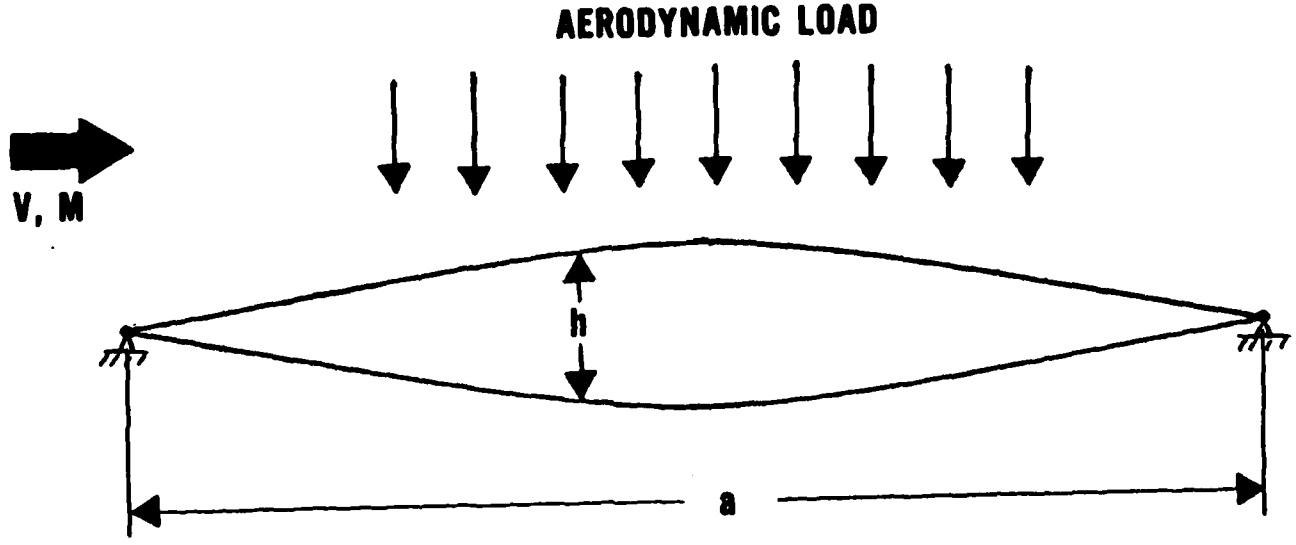

Figure 2. Plate Exposed to Aerodynamic Forces on One Side

Galerkin's Method

The procedure used in solving Equation (7) was to apply Galerkin's Method and a step-by-step time integration method. Galerkin's Method is an assumed mode technique which reduces a partial differential equation with independent variables x and t to a set of simultaneous ordinary differential equations with independent variable t.

For the Galerkin procedure, a series of displacment functions which satisfy both the geometric and force boundary conditions are assumed. In practice, the more terms used in the series, the more accurate the answer will become. For the simple supported beam, the geometric boundary conditions imposed on the problem are:

$$w(x,t) \Big|_{o}^{a} = 0, \text{ for all time} \tag{8}$$

and the force boundary conditions are:

$$EI \frac{\partial^2 w(x,t)}{\partial x^2} \Big|_{o}^{a} = 0, \text{ for all time} \tag{9}$$

The transverse deflection w(x,t) can then be approximated by a series of displacement functions weighted by unknown coefficients of time. Therefore,

$$w(x,t) \approx \bar{w}(x,t) = h \sum_{i=1}^{N} C_i(t)\phi_i(x), \tag{10a}$$

or

$$\bar{w}(x,t) = h\left(C_1(t)\sin\frac{\pi x}{a} + C_2(t)\sin\frac{2\pi x}{a} + \ldots\right.$$

$$\left. + C_N(t)\sin\frac{N\pi x}{a}\right) \qquad (10b)$$

where the displacement functions are defined as:

$$\phi_i(x) = \sin\frac{i\pi x}{a} \qquad (10c)$$

The basic procedure in applying the Galerkin Method is to substitute Equation (10a) into Equation (7); multiply the resulting equation by $\phi_i(x)$, i = 1,...N; and integrate over the domain of the problem. This can be expressed in equation form as:

$$\int_o^a \left(hD\frac{\partial^4\bar{w}}{\partial x^4} - h\bar{N}_x\frac{\partial^2\bar{w}}{\partial w^2} + \rho_m h^2\frac{\partial^2\bar{w}}{\partial t^2} + \right.$$

$$\left. h(P - P\infty)\right)\sin\frac{i\pi x}{a}\,dx = 0 \text{ for } i = 1,\ldots N \qquad (11)$$

This will result in N simultaneous ordinary differential equations with unknowns $C_i(t)$.

Piston Theory Aerodynamics

To become familiar with using the Von-Karman large displacement equations and to check the resulting equations after applying Galerkin's Method, a simple aerodynamic theory was used as the forcing function. For this study, Piston Theory aerodynamics was used because of the ease in which (P - P∞) can be calculated, and secondly because of the availability of previous

studies conducted by Prof. Dowell[1,2]. In the development of Piston Theory, the flow was assumed to be highly supersonic or:

$$\beta = \sqrt{M_\infty^2 - 1} \approx M_\infty \tag{12}$$

With this assumption, the pressure distribution could be expressed as:

$$(P - P_\infty) = \frac{2q}{\beta}\left[\frac{\partial w}{\partial x} + \frac{1}{V}\frac{\partial w}{\partial t}\right] \tag{13}$$

Time Integration Procedure

After applying Galerkin's Method and transforming the equation into a nondimensional form, the set of simultaneous differential equations can be obtained from Equation (11):

$$[M]\{\ddot{U}\} + [C]\{\dot{U}\} + [K]\{U\} = \{\bar{P}\} \tag{14}$$

where [M], [C], and [K] are the mass, damping and stiffness matrices respectively, {U} is the vector of the unknown coefficients of time, and {P} is a vector of the aerodynamic loads. The time derivatives are with respect to the nondimensional time.

The nondimensional variables used in obtaining Equation (14) include:

$$\lambda = \frac{2qa^3}{\beta D} \; ; \; \mu = \frac{\rho a}{\rho_m h} \; ; \; k = \frac{a\omega}{V} \; ; \; \tau = \omega t \tag{15}$$

The solution of Equation (14) was obtained using a step-by-step time integration finite difference approach[6]. Assuming a linear variation of acceleration, the velocities and displacements at the end of a small time interval can be expressed as:

$$\{\dot{U}\}_\tau = \{\dot{U}\}_{\tau-\Delta\tau} + \frac{\Delta\tau}{2}\left(\{\ddot{U}\}_{\tau-\Delta\tau} + \{\ddot{U}\}_\tau\right) \tag{16}$$

$$\{U\}_t = \{U\}_{\tau-\Delta\tau} + \Delta\tau\{\dot{U}\}_{\tau-\Delta\tau} + \frac{\Delta\tau^2}{3}\left(\{\ddot{U}\}_{\tau-\Delta\tau} + \tfrac{1}{2}\{\ddot{U}\}_\tau\right) \tag{17}$$

where $\Delta\tau$ is the time step and $\tau-\Delta\tau$ is the previous time. Substitution of Equations (16) and (17) into Equation (14) gives the acceleration at the new time step as:

$$\{\ddot{U}\}_\tau = [F]\left[\{\bar{P}\}_\tau - [C]\{v\} - [K]\{w\}\right] \tag{18}$$

where

$$[F] = \left[[M] + \frac{\Delta\tau}{2}[C] + \frac{\Delta\tau^2}{6}[K]\right]^{-1} \tag{19}$$

$$\{v\} = \{\dot{U}\}_{\tau-\Delta\tau} + \frac{\Delta\tau}{2}\{\ddot{U}\}_{\tau-\Delta\tau} \tag{20}$$

$$\{w\} = \{U\}_{\tau-\Delta\tau} + \Delta\tau\{\dot{U}\}_{\tau-\Delta\tau} + \frac{\Delta\tau^2}{3}\{\ddot{U}\}_{\tau-\Delta\tau} \tag{21}$$

Equation (18) can then be used to find the velocity (Equation 16) and displacement Equation (17) at the new time step.

The vector {P} is obtained numerically by solving the governing aerodynamic equations. The displacment and velocities

needed for computing {P} are based on the values obtained at the old time tep. The time step was chosen small enough such that no numerical instabilities would occur during the solution. In general, {P} can be shown to be:

$$\{P\} = \frac{-\left(\frac{w}{M}\right)Ma}{K^2 h} \begin{Bmatrix} \int_0^1 \left(\frac{P-P_\infty}{q}\right) \sin \pi \frac{x}{a} \frac{dx}{a} \\ \vdots \\ \int_0^1 \left(\frac{P-P_\infty}{q}\right) \sin 2\pi \frac{x}{a} \frac{dx}{a} \\ \vdots \\ \int_0^1 \left(\frac{P-P_\infty}{q}\right) \sin n\pi \frac{x}{a} \frac{dx}{a} \end{Bmatrix} \qquad (22)$$

where $(P - P_\infty)$ can be determind from either Piston Theory or LTRAN2.

Transonic Aerodynamic Pressures

The problem of interest is the flow about a wing panel of given thickness undergoing an assumed chordwise deformation (herein selected to be two modes) and the prediction of the oscillatory aerodynamic pressures in the transonic speed regime. The numerical computation method used for the unsteady flow field is based on the alternating direction implicit (ADI) procedure first formulated by Ballhaus and Goorjian[3]. The procedure was modified by van der Vooren[4] to consider flows of moderately high reduced frequencies and panel deformations. The small disturbance velocity potential equation can be derived for transonic flow by assuming an inviscid isentropic fluid with only weak shocks existing. The resulting moderately high reduced frequency differential equation solved in the code NLR-LTRAN2 is Equation

(5) with the ϕ_{tt} term dropped. In addition NLR-LTRAN2 retained necessary unsteady terms in the boundary conditions on the panel and the wake condition of zero pressure differential in the wake. These modifications of the original LTRAN2 code of Reference 3 allowed reduced frequencies up to k = 0.8 to be considered. The unsteady two-dimensional, transonic small disturbance equation solved in the code NLR-LTRAN2 is:

$$-2kM_\infty^2\phi_{xt} + [1-M_\infty^2 - (\gamma+1)M_\infty^2\phi_x]\phi_{xx} + \phi_{yy} = 0 \qquad (23)$$

where $\phi(x,y,t)$ is the small disturbance velocity potential resulting from the panel deformation $w(x,t)$. The boundary conditions which must be satisfied are:

$$\phi_y(x,y=0,t) = \frac{\partial w}{\partial x} + \frac{k\partial w}{\partial t} \text{ on the panel surface} \qquad (24)$$

and

$$\Delta Cp(x,y=0,t) = \Delta(\phi_x + k\phi_t) = 0 \text{ across the wake} \qquad (25)$$

where $w(x,t)$ is the panel deformation. At large distances away from the panel we require that:

$$\phi_x^2 + \phi_y^2 \to 0 \qquad (26)$$

For a prescribed panel deformation $w(x,t)$ then NLR-LTRAN2 can be used to determine the velocity potential from Equation (23) using

the AID scheme of Reference 3. With the velocity potential thus determined, the pressure field and hence the pressure difference of the panel can be obtained from:

$$C_p = -2(\phi_x + k\phi_t) \tag{27}$$

The panel considered in this study is a symmetric section composed of sinusoidal arcs of max thickness ratio as shown in Figure 2. This panel is placed at zero angle of incidence in a transonic airstream of Mach number 0.85. The chord deformation is selected by the two-mode assumption as given in Equation (10) where the maximum slope of the chord deformation is limited to 1 degree. The code NLR-TRAN2 is used to calculate the steady state initial conditions for the 10% thick panel and plot of the upper surface coefficient of pressure shown in Figure 3. The occurrence of the shock wave can be detected at the 70% chord location. In addition, shown in Figure 4, is the upper surface coefficient of pressure for the first mode at nondimensional time of 4. The shock wave has now moved to the new location of 90% chord location. For assumed values of the modal coefficients C_1 and C_2 then the transonic aerodynamic pressure, P, required in Equation (22) can be obtained from NLR-LTRAN2. However, in general, the determination of the modal coefficients must result from a simultaneous integration of the panel equations and the transonic aerodynamic equations as described in the previous section on the time integration procedure.

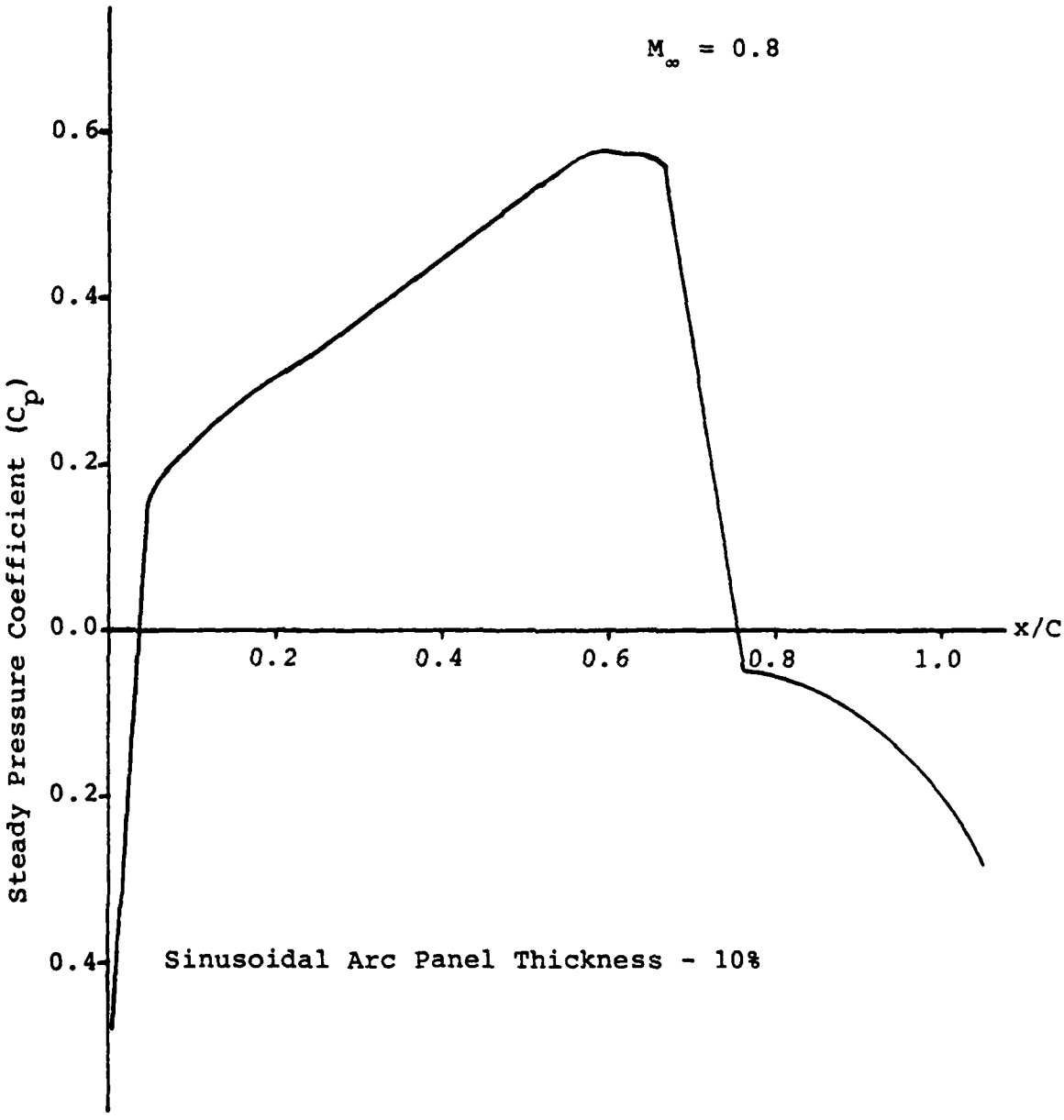

Figure 3. Upper Surface Steady Pressure Coefficient for a 10% Thick Sinusoidal Arc Panel

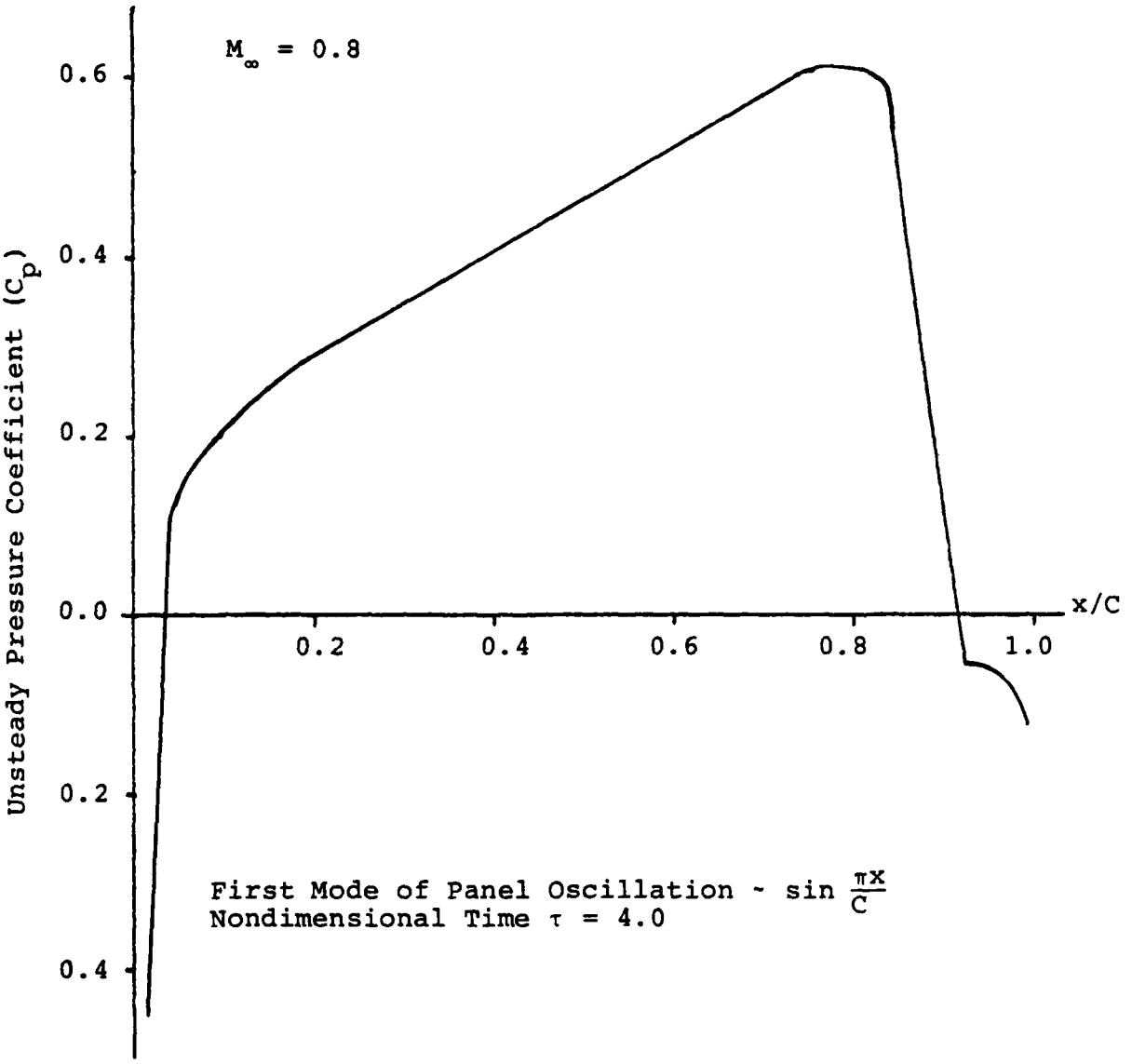

Figure 4. Upper Surface Unsteady Pressure Coefficient for a Panel Oscillating in the Fundamental Mode

SECTION 3

RESULTS

The results are presented as two tasks; the first task involves the use of the Von-Karman large deflection equations and Piston Theory aerodynamics. The second task involves the use of two single-degree-of-freedom models being loaded by transonic aerodynamics.

Large Displacement Equations and Piston Theory

Assuming a two mode series solution for the Galerkin procedure (with no damping, [C] = 0), the mass and stiffness matrices of Equation (19) are:

$$[\bar{M}] = \begin{bmatrix} 1 & 0 \\ 0 & 1 \end{bmatrix} \tag{28}$$

and

$$[K] = \frac{\pi^4 (\frac{\mu}{M}) M}{k^2 \lambda \beta} \begin{bmatrix} 1 + 3(C_1^2 + 4C_2^2) & 0 \\ 0 & 16 + 22(C_1^2 + 4C_2^2) \end{bmatrix} \tag{29}$$

The mass became the identity matrix as a result of the nondimensional form of the final equations of motion. Also, the stiffness is nonlinear since it is a function of the square of the panel displacements C_1 and C_2.

The value $(P - P_\infty)$ can be found as a function of the panel displacement and velocities. The variation of $(P - P_\infty)$ across

the chord of the panel can then be weighted by each of the assumed modes and integrated to obtain the force vector.

Assuming a two-term representation for the panel displacement and using Piston Theory, the panel deflection at limit cycle for increasing dynamic pressure is shown in Figure 5 as a solid line. The dash lines represent similar calculations performed by Prof. Dowell at Princeton several years earlier. Point solutions were also made with a four-term and six-term representation of the panel displacement. For all cases, the present analysis correlates very well with previous calculations.

The panel mode shape is a function of the aerodynamic loading and is presented in Figure 6. Once again, the data agrees very well with Dowell's results. The maximum deflection of the panel was shown to occur near the 70% chord point for all variations in the aerodynamic loading.

Aeroelastic Response of a Single Degree of Freedom Airfoil

For this task, the aeroelastic response of an airfoil constrained to deflect in either pitch or plunge was determined using the NLR-LTRAN2[4] computer code. The equation of motion for an airfoil pitching about its midchord is:

$$\ddot{\alpha} + A_1\dot{\alpha} + A_2\alpha = \frac{8C_m}{\pi\mu' K_a^2} \qquad (30)$$

For this case, $A_1 = .5$, $A_2 = 1.5$ and, $\mu' = 1000$. These data were selected so that the predictions could be correlated with similar results found in Reference 7.

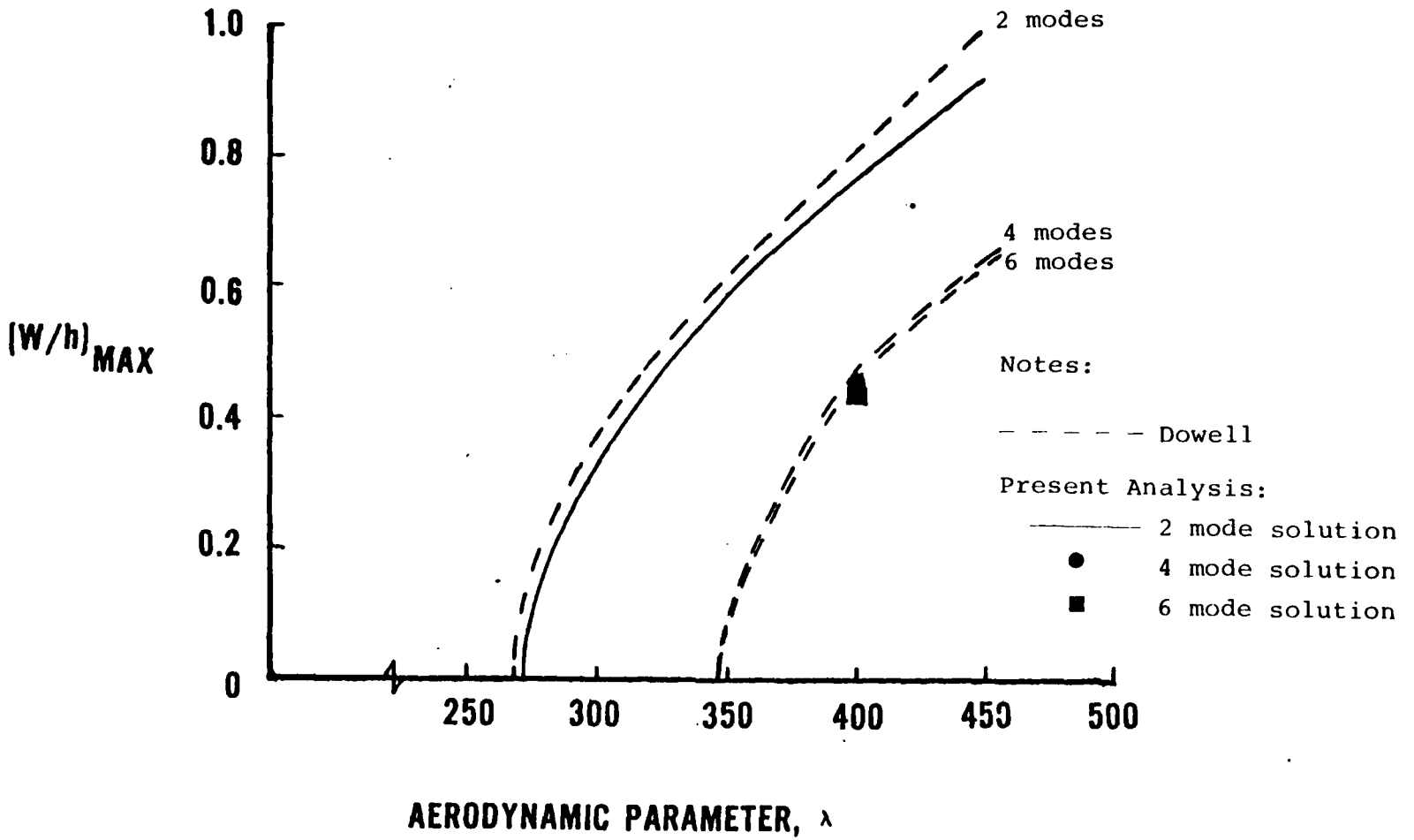

Figure 5. Panel Displacement at Limit Cycle

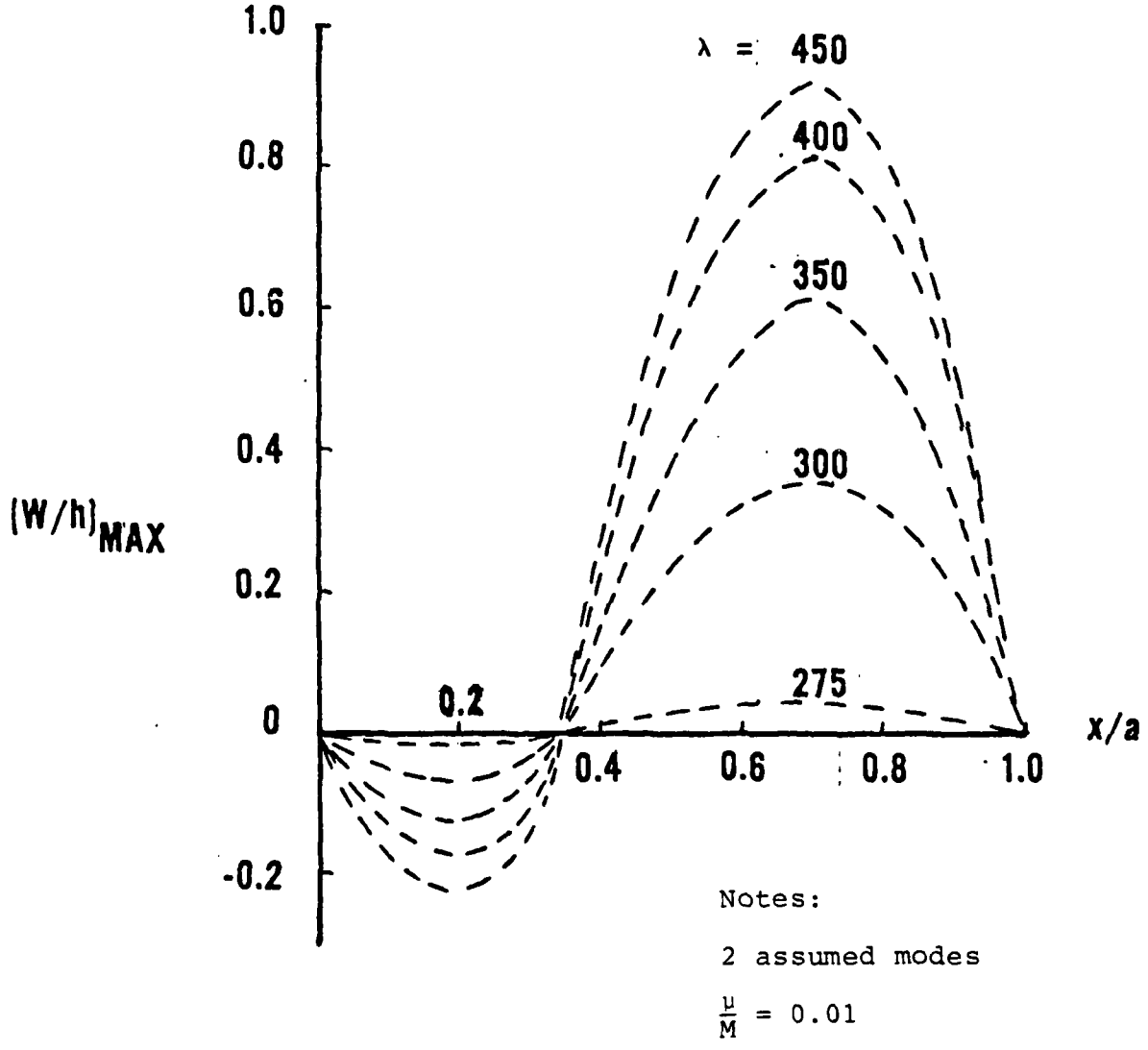

Figure 6. Panel Mode Shape at Limit Cycle

The dynamic response of the flat plate pitching about the mid-chord at a Mach number of 0.7 was obtained for a reduced frequency of 0.1. The aerodynamic equation was integrated in time for two cycles by forcing a sinusoidal variation of pitching angle with amplitude of 0.01 radians. The free motion was started at the end of the second cycle. The pitching moment coefficient, C_m, was determined by LTRAN2 at each time interval and used in Equation (30) to determine the time history. A converging type response was obtained for both the pitching angle and the pitching moment indicating that the flight conditions are below the instability speed. The results provided in Figure 7 compared very well with data from Reference 7.

Similarly, for a flat plate plunging, the equation of motion is:

$$\ddot{\delta} + B_1\dot{\delta} + B_2\delta = \frac{-2C_\ell}{\pi\mu' K_a^2} \tag{31}$$

To obtain data for correlation with Reference 7, the coefficients B_1, B_2 and μ' were selected to be 0., 1.0 and 100 respectively. Under similar starting conditions as discussed for the pitching airfoil case, the plunging response and the coefficient of lift variation with time is presented in Figure 8 for a Mach number of 0.7 and a reduced frequency of 0.1. Both the plunging displacement and lift coefficient agreed very well with the Reference 7 results.

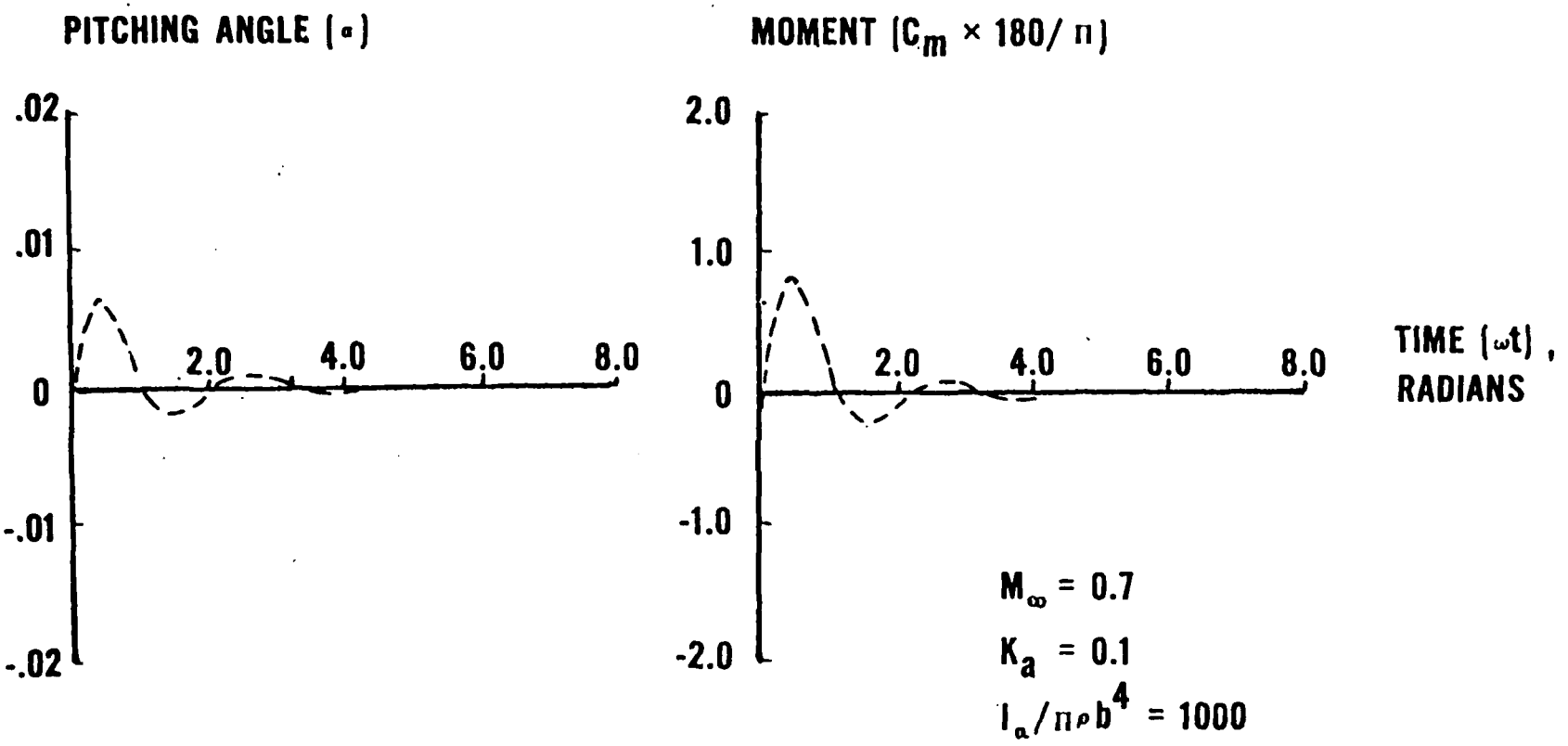

Figure 7. Flat Plate Pitching in a Transonic Airstream

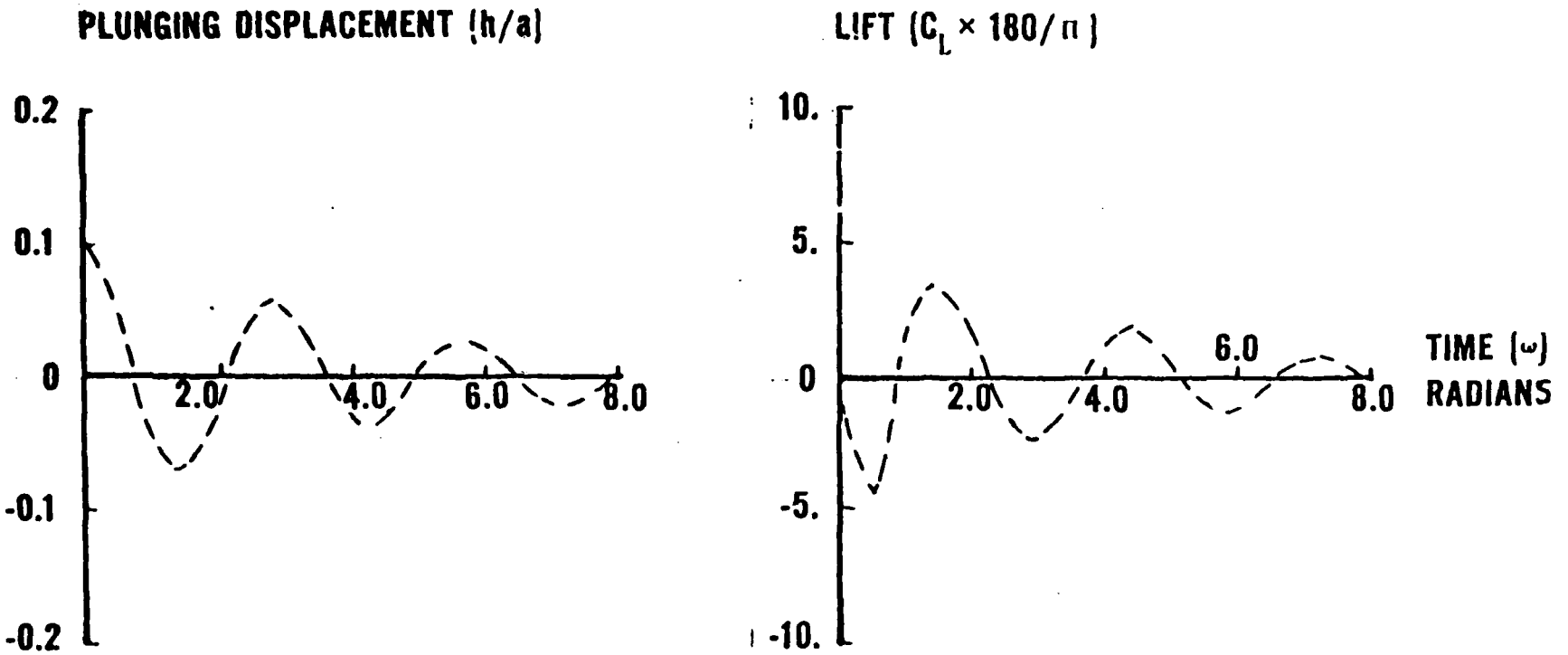

Figure 8. Flat Plate Plunging in a Transonic Airstream

SECTION 4

CONCLUSIONS AND RECOMMENDATIONS

Flutter analyses have been conducted on a simply supported panel to demonstrate the successful combining of panel Von Karman large deflection equations with a simple linear aerodynamic theory (Piston) for determining panel response. The panel response was determined from a numerical time integration scheme which reproduced the results presented previously by Dowell.[2] In addition, the time integration scheme was successfully used to insure the simultaneous integration of a set of linear structural equations and nonlinear aerodynamic equations. Here, the simultaneous integration scheme was used to determine the aeroelastic response of the linear pitching or plunging of an airfoil to the nonlinear aerodynamic lift and moment obtained from the NLR-LTRAN2 computer code. The response obtained for pitching or plunging compared favorably to those obtained by Yang, et al.[7]

An analysis was also initiated to study the panel response represented by a nonlinear structural equation (Von Karman's large deflection) and a nonlinear aerodynamic equation represented by NLR-LTAN2. Here, the panel response was represented with an assumed modal series combination even though both the structural equations and aerodynamic equations are nonlinear. However, to date, numerical instabilities with the computer code NLR-LTRAN2 have hampered the progress and obtaining of final results.

It is recommended that the analysis of the nonlinear response of a panel in a transonic airstream be continued using the simultaneous integration of structural and aerodynamic equations described herein. Further, it is recommended that the assumed modal technique used here with nonlinear equations be investigated. Toward this end, the replacement of the Von Karman large deflection equations with a finite-element representation is described in Appendix A. Unfortunately, only Piston Theory aerodynamics have been investigated with the finite element model so it suggested that the nonlinear aerodynamic theory obtained from NLR-LTRAN2 be coupled with the element model of Appendix A for analyses.

RFERENCES

1. Earl H. Dowell, "Nonlinear Oscillations of a Fluttering Plate," AIAA Paper No. 66-79, AIAA 3rd Aerospace Sciences Meeting, New York, NY, Jan. 24-26, 1966.

2. Earl H. Dowell, "Nonlinear Oscillations of a Fluttering Plate II," AIAA Paper No. 67-13, AIAA 5th Aerospace Sciences Meeting, New York, NY, Jan. 23-26, 1967.

3. W. F. Ballhaus and P. M. Goorjian, "Implicit Finite Difference Computations of Unsteady Transonic Flows About Airfoils, Including the Treatment of Irregular Shock-Wave Motions," AIAA Journal, Vol. 15, Dec. 1977.

4. G. W. Huizing and J. van der Vooren, "Users Manual for NLR-LTRAN2; A Programme for the Calculation of Inviscid Transonic Flow About Thin Airfoils in Moderately Slow Unsteady Motion," NLR-Memo W-79-003, National Aerospace Laboratory NLR, The Netherlands, June 20, 1979.

5. F. E. Eastep and S. C. McIntosh, "Analysis of Nonlinear Panel Flutter and Response Under Random Excitation or Nonlinear Aerodynamic Loading," AIAA Journal, Vol. 9, No. 3, Mar. 1971.

6. K. J. Bathe and E. L. Wilson, Numerical Methods in Finite Element Analysis, Prentice-Hall, Inc., Englewood Cliffs, New Jersey, 1976.

7. T. Y. Yang, P. Guruswamy, and A. G. Striz, "Aeroelastic Response Analysis of Two-Dimensional, Single and Two Degree of Freedom Airfoils in Low Frequency, Small-Disturbance Unsteady Transonic Flow," Technical Report AFFDL-TR-79-3077, Air Force Flight Dynamics Laboratory, Wright-Patterson Air Force Base, Ohio, June 1979.

8. R. A. Brockman, "MAGNA (Materially and Geometrically Nonlinear Analysis), General Description and Summary of Capabilities," Technical Memorandum UDR-TM-80-27, Apr. 1981.

9. R. A. Brockman, "MAGNA Computer Program User's Manual," Technical Memorandum UDR-TR-80-107, Nov. 1980.

APPENDIX A

PANEL RESPONSE OF A FINITE ELEMENT MODEL AT POST FLUTTER CONDITIONS USING PISTON THEORY

Introduction

Panel flutter is a self-induced oscillation of a thin-walled structure caused by increasing aerodynamic pressures resulting from the panel deformation in an airstream. Nonlinear panel flutter is characterized by a periodic oscillation of finite amplitude commonly referred to as limit cycle. Theoretical studies in the past have been restricted by the use of a simplified linear aerodynamic theory and an inaccurate representation of the panel support conditions which result when the nonlinear midplane stresses are neglected (assumption of small amplitudes). References 1, 2 and 5 present some of the large amount of work completed in this technical area. Some details have been extracted from these references for use in the study presented here.

The main objective of this investigation is to determine a procedure for the prediction of the large deflection response of structural panels in a transonic airstream. The Von Karman large deflection equations are to be integrated simultaneously with the solutions of the nonlinear transonic equations. Since this approach requires an extremely large amount of computation, the Von Karman large deflection equations will be used in conjunction with Piston Theory aerodynamics. This section presents only the

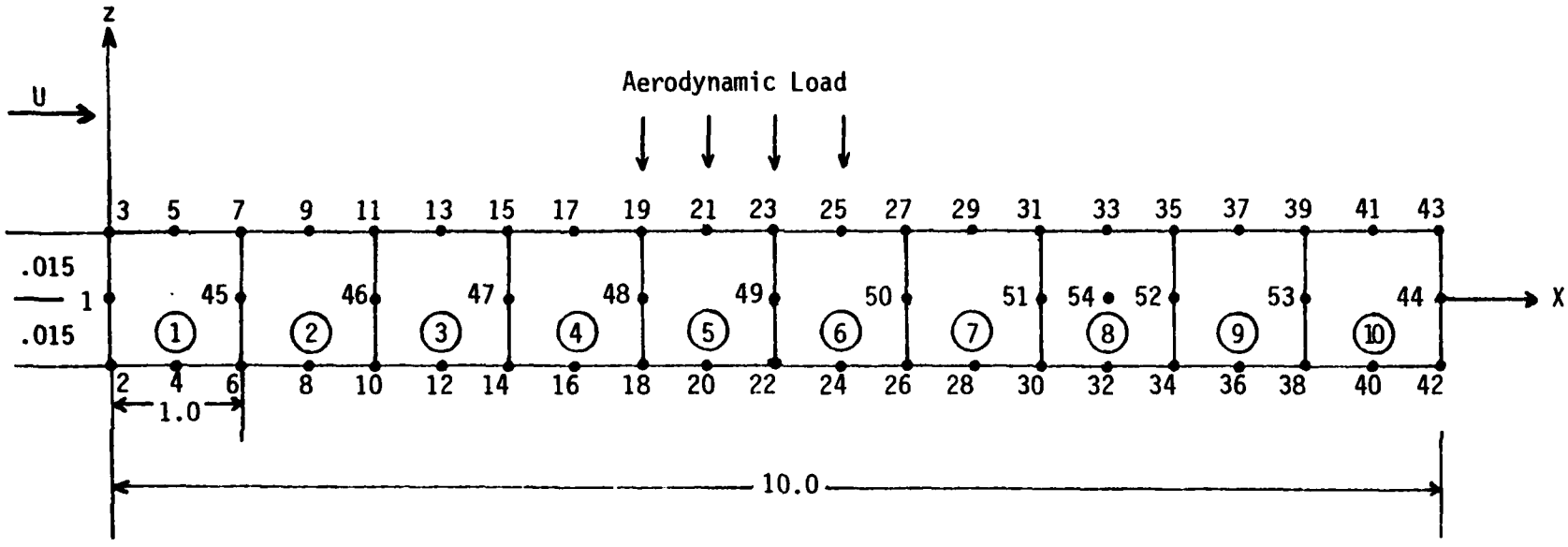

Figure A-1. Thin Two-Dimensional Plate Exposed to Aerodynamic Loads on One Side

results of the calculations with Piston Theory and a finite element model.

The thin two-dimensional plate shown in Figure A-1 has been selected as the configuration to be investigated in this study. The transverse aerodynamic load acting on only one side of the panel is of known spatial and temporal distribution. A finite element representation was selected to eliminate the modal approximations necessary in the previous investigation because of the nonlinear Von Karman large deflection equation. The plate is represented as consisting of twin variable node plane-strain elements each of unit length. A thickness of 0.03 inches and the material properties of aluminum are used because of studies completed on similar plates in References 1, 2 and 5. The plate consists of 54 nodes; nodes #1 and #44 are simply supported (constrained in the x, y and z directions), while the other nodes are only constrained from moving in the y direction. Node #54 represents the three-quarter span of the plate.

It is assumed that the large displacements of the plate are governed by the nonlinear Von Karman large deflection equations.

$$\bar{D}\nabla^4 w - h\left[\frac{\partial^2 \bar{F}}{\partial y^2}\frac{\partial^2 w}{\partial x^2} - 2\frac{\partial^2 \bar{F}}{\partial x \partial y}\frac{\partial^2 w}{\partial x \partial y} + \frac{\partial^2 \bar{F}}{\partial x^2}\frac{\partial^2 w}{\partial y^2}\right]$$

$$+ \bar{N}_x \frac{\partial^2 w}{\partial x^2} + \bar{N}_y \frac{\partial^2 w}{\partial y^2} = -\rho h \frac{\partial^2 w}{\partial t^2} + A(x,t) \qquad \text{(A-1)}$$

and from the compatibility equation:

$$\frac{\nabla^4 \bar{F}}{E} = \left(\frac{\partial^2 w}{\partial x \partial y}\right)^2 - \left(\frac{\partial^2 w}{\partial x^2}\right)\left(\frac{\partial^2 w}{\partial y^2}\right) \qquad \text{(A-2)}$$

where w is the plate transverse deflection and F is the Airy stress function. The aerodynamic pressure loading, A(x,t), is the increased incremental aerodynamic pressure caused by the plate displacement. As mentioned previously, A(x,t) for this study is obtained from Piston Theory. These equations are solved in a computer code referred to as MAGNA, Materially and Geometrically Nonlinear Analysis[5,6] using a finite element procedure.

Discussion

This section briefly describes the MAGNA computer program capabilities, and presents a derivation of a subroutine for MAGNA for calculating Piston Theory aerodynamic pressures.

MAGNA Computer Program

The MAGNA computer program is a large scale, general purpose finite element system intended for the nonlinear (large deflection) analysis of complex engineering structures. MAGNA has been developed primarily for the efficient solution of three-dimensional problems involving many degrees of freedom and large bandwidth. Isoparametric modeling techniques and state-of-the-art numerical solution methods are combined in MAGNA to provide effective analytical capabilities for finite strains, arbitrary rotations, and elastic-plastic behavior. Both static and transient dynamic solution options may be performed with the program, as well as natural frequency/mode shape calculations. Features such as user subroutine interfaces, post-analysis

graphics, and analysis restart capabilities are included in MAGNA.

For the problem investigated herein, a two-dimensional large displacement element, referred to in MAGNA as Element #9, has been used following a modification for obtaining plane-strain. This modification required a user subroutine which is presented in Appendix B.

The MAGNA finite element program is operational on the CDC 6000 series, CYBER-74, and CYBER-175 computers with cupport CCL (CYBER control language) procedures and the segmentation loader. An example of the job control language (JCL) used for executing the program during the investigations reported herein is presented in Figure A-2. This JCL attaches permanent files which include the input data (MAGNADATA), the user subroutines (TNMAGNA), and a dynamic analysis restart file. It also forms a post-processing file for plotting the plate response (Tape L06296) and forms the next dynamic analysis restart file (Tape L06091) following execution of the program.

The nonlinear dynamic response investigation was started by first performing a static displacement analysis to obtain an initial displacement (ID) for the initial transient dynamic analysis. In the time plots of the section entitled, "Analysis Results", time zero is indicated by t = 2.0 because of the static analysis increments required for a converge solution. The first dynamic analysis used the static restart file. After a specified number of time increments, a dynamic restart tape was formed for

```
100=NT2,T1200,IO3200,CM10500,GE2    D800956,NOLL,56832
110=SET=R1=MFL
120=ATTACH,A,MAGNADATA,CY=5
130=ATTACH,B,TNMAGNA,CY=3
140=REWIND,A,B
150=COPY,A,TAPES
160=COPY,B,USRSUB
170=RETURN,A,B
180=REWIND,TAPES,USRSUB
190=ATTACH,OLDTAP,TDF1,CY=2
200=REWIND,OLDTAP
210=SKIPK,OLDTAP,11,0,B
220=COPYBR,OLDTAP,TAPE23
230=REWIND,TAPE23
240=RETURN,OLDTAP
250=REQUEST,MPOST,GE,RING,VSN=L06296
260=REQUEST,NRSTAP,GE,RING,VSN=L06091
270=ATTACH,P,MAGNAJCL,ID=BROCKMAN,MR=1
280=BEGIN,XMAGNA,P,,USRSUB,R1+B
290=UNLOAD,MPOST,NRSTAP
```

Figure A-2. Job Control Language for Executing MAGNA

the next dynamic analysis. The results of each analysis were placed on a post-processing file for plotting.

The dynamic restart file was then used to continue the analysis, again forming both post-processing and restart files. This procedure could be repeated until the panel response versus time was constant (limit cycle had been reached). Figure A-3 presents a procedure for using the post-processing data file to obtain panel nodal point displacements plotted versus time. Figure A-4 presents typical output results using the FDL/FIBRC IMLAC in a Tecktronic Mode of generating one-line plots of panel response.During this investigation, all MAGNA computer runs and plotting were accomplished using terminal inputs.

Piston Theory Aerodynamics

Piston Theory aerodynamics was used in this study to load the panel. For Piston Theory, the unsteady aerodynamic pressures are defined as:

$$A(x,t) = \frac{-2q}{\beta}\left[\frac{\partial w}{\partial x} + \frac{1}{U}\frac{\partial w}{\partial t}\right] \qquad (A-3)$$

Using the nondimensional aerodynamic parameters defined in References 1 and 2, that is:

$$\lambda = \frac{2qa^3}{\beta D}, \text{ and } \frac{\mu}{M}\frac{\rho a}{\rho_m h M}$$

Equation (A-3) can be expressed as:

```
100=.PROC,NOLL.
110=ATTACH,PROCFIL,ID=D800236.
120=BEGIN,NOSFILE.
130=GET,WRTFIL,ID=D800236.
140=FTN,I=WRTFIL,L=0.
150=ATTACH,TAPE99,POSTPR,CY=1.
160=LGO.
170=RETURN,PROCFIL,WRTFIL,LGO,TAPE99.
180=FET,XYPLOT,ID=D800236.
190=FTN,I=XYPLOT,L=0.
200=ATTACH,LIB1,TEKLIB,ID=LIBRARY,SN=ASD.
210=ATTACH,LIB2,PLOT3D,ID=KING.
220=LIBRARY,LIB1,LIB2.
230=LGO.
240=RETURN,LGO,LIB1,LIB2,XYPLOT,TAPE2,TAPE30.
250=REVERT.
260=XEOR
270=XEOF
```

Figure A-3. Procedure File for Executing MAGNA Plot Capability

```
BEGIN, NOLL, PROCNOLL
 AT CY=001 SN=AFFDL
 PFN IS
 PROCFIL:
 AT CY=001 SN=AFFDL
         NOSFILE VERSION 3 READY.
       OTHER PROCFIL OPTIONS
       EDTFILE, ALLFILE, TEKFILE, HPFILE
 FILE NAME WRTFIL    HAS BEEN RETRIEVED
       .360 CP SECONDS COMPILATION TIME

 MAGNA POST FILE TRANSLATOR FOR XYPLOT

 WRITE DISPLACEMENT OR STRESS DATA (D,9).....D
 HOW MANY CURVES WILL BE PLOTTED?1
 ENTER NODE NUMBER AND DISPLACEMENTS1.2

 FOR CURVE NO. 1 WANT THE FIRST POINT TO BE AT 3.0,0.0?N
     STOP
     033000 MAXIMUM EXECUTION FL.
      8.071 CP SECONDS EXECUTION TIME.
 FILE NAME XYPLOT     HAS BEEN RETRIEVED
 PLOT ON HP OR TEKTRONIX (1=HP,2=TEK).......:
   UNSATISFIED EXTERNAL REF -- SETIN
      NON-FATAL LOADER ERRORS -
   UNSATISFIED EXTERNAL REF -- SETUU  2
 READ DATA FROM FILE OR TERMINAL (1=FILE,2=TERM).:1
 NEED CONVERSION OPTION FOR DATA SET NO. 1?......:N
 HOW MANY CURVES DO YOU WISH TO PLOT.............:1

 WHICH SETS OF DATA DO YOU WISH TO PLOT..........:1
 LABELS FOR THIS PLOT ARE COMPUTED TO BE:
 X-MAXIMUM =        2.08
 Y-MAXIMUM =         .04
 X-MINIMUM =        1.99
 Y-MINIMUM =        -.05
 CHANGE THESE VALUES (Y,N).....................:Y

 ENTER MAXIMUM X-LABEL.........................:2.08
 ENTER MAXIMUM Y-LABEL.........................:.04
 ENTER MINIMUM X-LABEL.........................:2.
 ENTER MINIMUM Y-LABEL.........................:-.04
 INTERVAL SIZE ON X-AXIS.......................:.01
 INTERVAL SIZE ON Y-AXIS.......................:.01

 ENTER X-AXIS LABEL, (MAX. 40 CHAR.)...........:TIME,SEC

 ENTER Y-AXIS LABEL, (MAX. 40 CHAR.)...........:NODAL PT 51 DISPLACEMENT,IN

 FOR DATA SET NUMBER  1
 LINE OPTIONS ARE:
 SOLID LINE CURVE, NO SYMBOL, TYPE -1
 DASH LINE, NO SYMBOL, TYPE -2
 SYMBOL AT EACH POINT, TYPE 1
 SYMBOLS CONNECTED WITH SOLID LINE, TYPE 2
 SYMBOLS CONNECTED WITH DASH LINE, TYPE 3.
 ENTER CURVE TYPE..............................:-1
```

Figure A-4. Example Output of MAGNA Plot Routine Using Procedure File

$$A(x,t) = \frac{-\lambda D}{a^3}\left(\frac{\partial w}{\partial x} + \sqrt{\frac{a^2\left(\frac{\mu}{M}\right)M\rho_m h}{\beta D\lambda}}\ \frac{\partial w}{\partial t}\right) \qquad (A-4)$$

By grouping the dimensional and material properties of the panel, the aerodynamic pressure can be represented as a function of only λ, μ/M, and $\underline{M}$ as:

$$A(x,t) = C_1\lambda\ \frac{\partial w}{\partial x} + C_1C_2\sqrt{\frac{\left(\frac{\mu}{M}\right)\lambda M}{\beta}}\ \frac{\partial w}{\partial t} \qquad (A-5)$$

and

$$C_1 = \frac{-D}{a^3} \text{ and } C_2 = \sqrt{\frac{a^2\rho_m h}{D}}$$

Using an aluminum plate $\left(\rho_m = \frac{.000259 \text{ lb sec}^2}{\text{in}} \text{ and } E = 10^7 \text{ psi}\right)$ and assuming that the plate stiffnes, $\underline{D}$, equals $Eh^3/12$, the aerodynamic pressure becomes:

$$A(x,t) = -.0225\lambda\ \frac{\partial w}{\partial x} - .0001322\sqrt{\frac{\left(\frac{\mu}{M}\right)\lambda M}{\beta}}\ \frac{\partial w}{\partial t} \qquad (A-6)$$

Now it is necessary to define the nodal point slopes, $\partial w/\partial x$, and velocities, $\partial w/\partial t$, for Equation (A-6). The nodal point displacements in an element local coordinate system (referring to the sketch below) are defined as:

$$w(\xi) = N_1w_A + N_2w_B + N_3w_C = N^Tw \qquad (A-7)$$

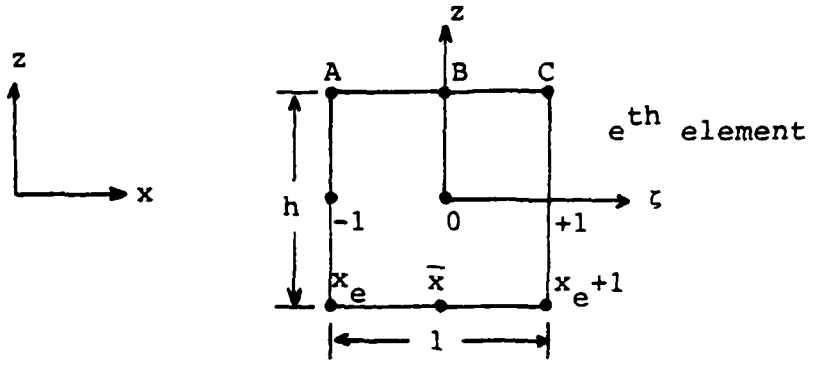

The shape functions in Equation (A-7) are defined as:

$$N_1 = -(\zeta/1)(1-\zeta);\ N_2 = (1-\zeta^2);\ \text{and}\ N_3 = (\zeta/2)(1+\zeta) \qquad \text{(A-8)}$$

These shape functions provided parabolic displacement approximation across the element. Since:

$$x = \left(\frac{x_e+x_{e+1}}{2}\right) + \zeta\left(\frac{x_{e+1}-x_e}{2}\right) = \bar{x}_e + \frac{\zeta}{2} \qquad \text{(A-9)}$$

then the slope of a node becomes:

$$\frac{\partial w}{\partial x}(\zeta) = 2\left[\frac{w_C-w_A}{2} + (w_A - 2w_B + w_C)\zeta\right] \qquad \text{(A-10)}$$

and the node velocity becomes:

$$\frac{\partial w}{\partial t}(\zeta) = N_1\dot{w}_A + N_2\dot{w}_B + N_3\dot{w}_C \qquad \text{(A-11)}$$

From the Principle of Virtual Work, the work done by the aerodynamic pressure A(x,t) was equated to the work done by the nodal

forces moving through the nodal displacements. In other words, for a particular element, the work done is:

$$W = \int_{x_e}^{x_{e+1}} A(x,t)w(x)dx = \begin{Bmatrix} F_A \\ F_B \\ F_C \end{Bmatrix}^T \begin{Bmatrix} w_A \\ w_B \\ w_C \end{Bmatrix} \qquad \text{(A-12)}$$

or

$$W = \tfrac{1}{2} \int_{-1}^{1} A(\zeta,t)w(\zeta)d\zeta = \begin{Bmatrix} F_A \\ F_B \\ F_C \end{Bmatrix}^T \begin{Bmatrix} w_A \\ w_B \\ w_C \end{Bmatrix}$$

With $w(\zeta) = N^T \begin{Bmatrix} w_A \\ w_B \\ w_C \end{Bmatrix}$, $\quad A(\zeta,t) = N^T \begin{Bmatrix} P_A \\ P_B \\ P_C \end{Bmatrix}$

and

$P_A = A(-1,t)$,

$P_B = A(0,t)$,

$P_C = A(1,t)$ for the e^{th} element,

substitution into Equation (A-12) gives:

$$\tfrac{1}{2} \int_{-1}^{1} N^T \begin{Bmatrix} P_A \\ P_B \\ P_C \end{Bmatrix} N^T \begin{Bmatrix} w_A \\ w_B \\ w_C \end{Bmatrix} = \begin{Bmatrix} F_A \\ F_B \\ F_C \end{Bmatrix}^T \begin{Bmatrix} w_A \\ w_B \\ w_C \end{Bmatrix}$$

or

$$\begin{Bmatrix} F_A \\ F_B \\ F_C \end{Bmatrix} = \tfrac{1}{2} \begin{Bmatrix} P_A \\ P_B \\ P_C \end{Bmatrix} \int_{-1}^{1} NN^T d\zeta \qquad \text{(A-13)}$$

By evaluating the integral for the shape functions N_1, N_2, and N_3, Equation (A-13) becomes:

$$\begin{Bmatrix} F_A \\ F_B \\ F_C \end{Bmatrix} = \frac{1}{60} \begin{bmatrix} 8 & 4 & -2 \\ 4 & 32 & 4 \\ -2 & 4 & 8 \end{bmatrix} \begin{Bmatrix} P_A \\ P_B \\ P_C \end{Bmatrix} \qquad \text{(A-14)}$$

Now using the nodal point displacement and velocities, the pressures evaluated at the element nodal points become:

$$P_A = C_1\lambda \left[(-3w_A + 4w_B - w_C) + C_2 \sqrt{\frac{(\frac{\mu}{M})M}{\beta\lambda}}\, \dot{w}_A \right] \qquad \text{(A-15a)}$$

$$P_B = C_1\lambda \left[(w_C - w_A) + C_2 \sqrt{\frac{(\frac{\mu}{M})M}{\beta\lambda}}\, \dot{w}_B \right] \qquad \text{(A-15b)}$$

$$P_C = C_1\lambda \left[(w_A - 4w_B + 3w_C) + C_2 \sqrt{\frac{(\frac{\mu}{M})M}{\beta\lambda}}\, \dot{w}_C \right] \qquad \text{(A-15c)}$$

By substituting these expressions into Equation (A-14) we obtain an equation which now relates the nodal point forces to the nodal point displacements and velocities. Equation (A-16) becomes:

$$\begin{Bmatrix} F_A \\ F_B \\ F_C \end{Bmatrix} = \frac{C_1\lambda}{6} \begin{bmatrix} -3 & 4 & -1 \\ -4 & 0 & 4 \\ 1 & -4 & 3 \end{bmatrix} \begin{Bmatrix} w_A \\ w_B \\ w_C \end{Bmatrix} +$$

$$\frac{C_1C_2}{30}\sqrt{\frac{(\frac{\mu}{M})\lambda M}{\beta}} \begin{bmatrix} 4 & 2 & -1 \\ 2 & 16 & 2 \\ -1 & 2 & 4 \end{bmatrix} \begin{Bmatrix} \dot{w}_A \\ \dot{w}_B \\ \dot{w}_C \end{Bmatrix} \qquad \text{(A-16)}$$

At common nodal points between two elements, the nodal forces are added. Equation (A-16) was programmed in the ULOAD subroutine for calculating the nodal point forces based on Piston Theory aerodynamics. Appendix C presents a listing of ULOAD.

Analysis Results

This section presents the results of a vibration analysis and a nonlinear static analysis, and briefly summarizes the results of the nonlinear transient dynamic analyses. Some of the response data provided herein are sketches of (w/h) versus a non-dimensional time, τ, defined as:

$$\tau = t(D/\rho_m h a^4)^{1/2}$$

For the plate used in this study, $\tau = 17.02t$. These sketches were made prior to obtaining on-line plot capability. The sketches are somewhat rough in that there was no attempt to obtain an accurate time history; only the peaks and zeros of the time history were plotted. All on-line plots present w versus real time, t, with time zero beginning at t = 2.0 secs as described earlier. The time increment jump from 0.0 to 2.0 was

caused during the generation of the static restart tape which required two increments for convergence (2.0 secs). Therefore, the first dynamics run, using a static restart file, would begin at t = 2.0 secs.

Vibration Analysis

The eigenvalue solution option of MAGNA was used to obtain the first five mode shapes and natural frequencies of the plate. These data are found in Table A-1. The mode shapes are presented for the nodal points through the center of the plate (nodes #45-#54 and the simply supported edges #1 and #44). A consistent mass representation was selected for this analysis. MAGNA uses a vector iteration procedure for obtaining the desired eigenvalues and eigenvectors.

For a simply supported beam, the natural frequencies of the beam can be represented as:

$$\omega_n = (n\pi/a)^2 (Eh^2/12\rho_m)^{1/2}, \quad n = 1,2,....$$

This expression gives 26.73 Hz, 106.92 Hz, and 240.57 Hz for the first three natural frequencies. These results are in good agreement with the frequencies found in Table A-1. All the beam results are lower, as expected. The mode shapes, which are presented with only three decimal digits, all appear reasonable with respect to the mode shapes of a simply supported beam.

Nonlinear Static Analysis

The static analysis input data to MAGNA are presented in Figure A-5. The static analysis was required to obtain an initial displacement (ID) for the nonlinear transient dynamic analyses. Four initial displacements were investigated during

TABLE A-1

NATURAL FREQUENCIES AND MODE SHAPES

Mode No.:	1	2	3	4	5
Freq (Hz)	28.04	112.13	252.69	451.18	711.25

Modal PT	Mode Shapes				
	1	2	3	4	5
1	.000	.000	.000	.000	.000
45	-.309	.588	-.809	-1.000	-1.000
46	-.588	.951	-.951	-.618	.000
47	-.809	.951	-.309	.618	1.000
48	-.951	.588	.588	1.000	.000
49	-1.000	.000	1.000	.000	-1.000
50	-.951	-.588	.588	-1.000	.000
51	-.809	-.951	-.309	-.618	1.000
54	-.707	-1.000	-.706	.000	.698
52	-.588	-.951	-.951	.618	.000
53	-.309	-.587	-.809	1.000	-1.000
44	.000	.000	.000	.000	.000

```
NONLINEAR PANEL FLUTTER   POST FLUTTER RESPONSE
PISTON THEORY UNSTEADY AERODYNAMICS
STATIC LOADS FOR INITIAL DISPLACEMENT, NODAL LOAD = .01071 LB
    1    1    1    2
    2
1.
0
0
    2    2   15
RESTART          0                1 INID    2
COORDINATES          54
     1          0.0          1.0
    45          1.5          1.0
    53          1 9.0        2.0
     2          6.0          -.015
    42          2 10.        -.015
     3          6.0           .015
    43          2 10.0        .015
    44         10.0          1.0
    54          7.5          1.0
0
     9    1   10
      10.E6  0.3       .000259
     1    1    2          2    6    7    3    4   45    5    1
     2    1    2          6   10   11    7    8   46    9   45
     3    1    2         10   14   15   11   12   47   13   46
     4    1    2         14   18   19   15   16   48   17   47
     5    1    2         18   22   23   19   20   49   21   48
     6    1    2         22   26   27   23   24   50   25   49
     7    1    2         26   30   31   27   28   51   29   50
     8    1    3         30   34   35   31   32   52   33   51   54
     9    1    2         34   38   39   35   36   53   37   52
    10    1    2         38   42   43   39   40   44   41   53
0
0
     2    2
     2   43    1
     3
    45   53    1
     3
     1    2    3
     1   44
     3
    54
     1
     1    2 NODAL LOAD = .01071 LB
0.0          .01071          10.0          .01071
    23    2    1    -1.
0
```

Figure A-5. MAGNA Data Input for Nonlinear Static Load Analysis

the course of this study. The static load and the resulting plate displacements that were used are shown in Table A-2. For these analyses, a static load was placed at the center of the plate (nodal point #23). A nonlinear large displacement formulation was assumed in these analyses. For the results defined in the section entitled, "Nonlinear Transient Dynamic Analyses", all time histories have a specific initial displacement associated with it. These ID's are defined in Table A-2. For a simply supported beam, the deflection at the center can be defined as:

$$w_{49} = Fa^3/4Eh^3.$$

This expression gives results which are in good agreement with ID #1 of Table A-2. The other loads result in MAGNA predicted deflections which are considered to be "large deflections". The beam expression was derived assuming small displacements, therefore, correlation with ID #2, ID #3, and ID #4 would be expected to worsen.

Nonlinear Transient Dynamic Analyses

The nonlinear transient dynamic analyses were conducted for three different Mach numbers; 3.0, 1.2, and 0.8. When the Mach number of 0.8 was used, β was redfined as $(1-M^2)^{1/2}$. Figure A-6 presents a sample of the data input to MAGNA for these analyses. Any variations to λ, μ/M, or Mach number were accomplished in the ULOAD subroutine.

TABLE A-2

INITIAL DISPLACEMENTS USED FOR
TRANSIENT DYNAMIC ANALYSES

Nodal PT	Static Load at PT 23 (lbs) .00357	.00714	.01071	.02570
	ID#1 (in)	ID#2 (in)	ID#3(in)	ID#4 (in)
1	.0	.0	.0	.0
45	-.00087	-.00162	-.00224	-.00396
46	-.00166	-.00311	-.00430	-.00762
47	-.00232	-.00434	-.00601	-.01070
48	-.00276	-.00517	-.00718	-.01284
49	-.00292	-.00548	-.00761	-.01365
50	-.00276	-.00517	-.00718	-.01283
51	-.00231	-.00433	-.00600	-.01069
54	-.00201	-.00376	-.00521	-.00926
52	-.00166	-.00311	-.00431	-.00764
53	-.00087	-.00162	-.00224	-.00396
44	.0	.0	.0	.0

```
NONLINEAR PANEL FLUTTER; POST FLUTTER RESPONSE
PISTON THEORY UNSTEADY AERODYNAMICS
TRANSIENT DYNAMIC ANALYSIS
    1    2    1    2    1    1                    1    1
 720  30
.300 2          2.0726       3.0
0
0
     3
RESTART          1 TOF1   360      1 TOF2    30
COORDINATES          54
     1          0.0          0.0
    45          1.0          0.0
    53      1   9.0          0.0
     2          0.0          -.0015
    42      2  10.           -.0015
     3          0.0           .0015
    43      2  10.0           .0015
    44         10.1          0.0
    54          7.5          0.0
0
     9    1   10
      10.E6  0.3        .000259
     1     1     2          2     6     7     3     4    45     5     1
     2     1     2          6    10    11     7     8    46     9    45
     3     1     2         10    14    15    11    12    47    13    46
     4     1     2         14    18    19    15    16    48    17    47
     5     1     2         18    22    23    19    20    49    21    48
     6     1     2         22    26    27    23    24    50    25    49
     7     1     2         26    30    31    27    28    51    29    50
     8     1     3         30    34    35    31    32    52    33    51    54
     9     1     2         34    38    39    35    36    53    37    52
    10     1     2         38    42    43    39    40    44    41    53
0
0
     2     2
     2    43     1
     3
    45    53     1
     3
     1     2     3
     1    44
     3
    54
     1
     1     2 AERO LOADS (ULOAD)
0.0          0.0          10.0         0.0
    23     2     1     -1.
0
```

Figure A-6. MAGNA Data Input for Nolinear Transient Dynamic Analysis

Mach Number = 3.0

Figures A-7, A-8, and A-9 present time history plots of nodal point #54 (3/4 span) for initial displacements ID #1, ID #2 and ID #3 and for λ, μ/M and M equal to 400, .01 and 3.0, respectively. The figures present nondimensional displacement, (w/h), versus nondimensional time, τ. As described earlier, the plots are approximate and only show trends. As can be seen from the figures, the displacements are approaching the thickness of the plate. The frequency of the oscillation is about 83 Hz. Since the objective of this study is ultimately to investigate transonic effects, the studies at M 3.0 were not continued to limit cycle.

Mach Number = 1.2

For a Mach number of 1.2, the aerodynamic parameters, λ and μ/M, were selected to be 300 and 0.013, respectively. Two different initial displacements wer investigated at these conditions. Figure A-10 presents the time history results for ID #4, and Figure A-11 presents results for ID #3. These figures present the time histories of the nodal point displacement, w, versus real time, t, for the points through the center of the plate (points #45-#54). Nodal point #54 represents the 3/4 span location of the plate and is positioned correctly for increasing x within the figures (between points #51 and #52). The nodal point is described in the ordinate label of each time history plot. Also note that in Figure A-10, there is a change in ordinate scale after t = 2.7 secs.

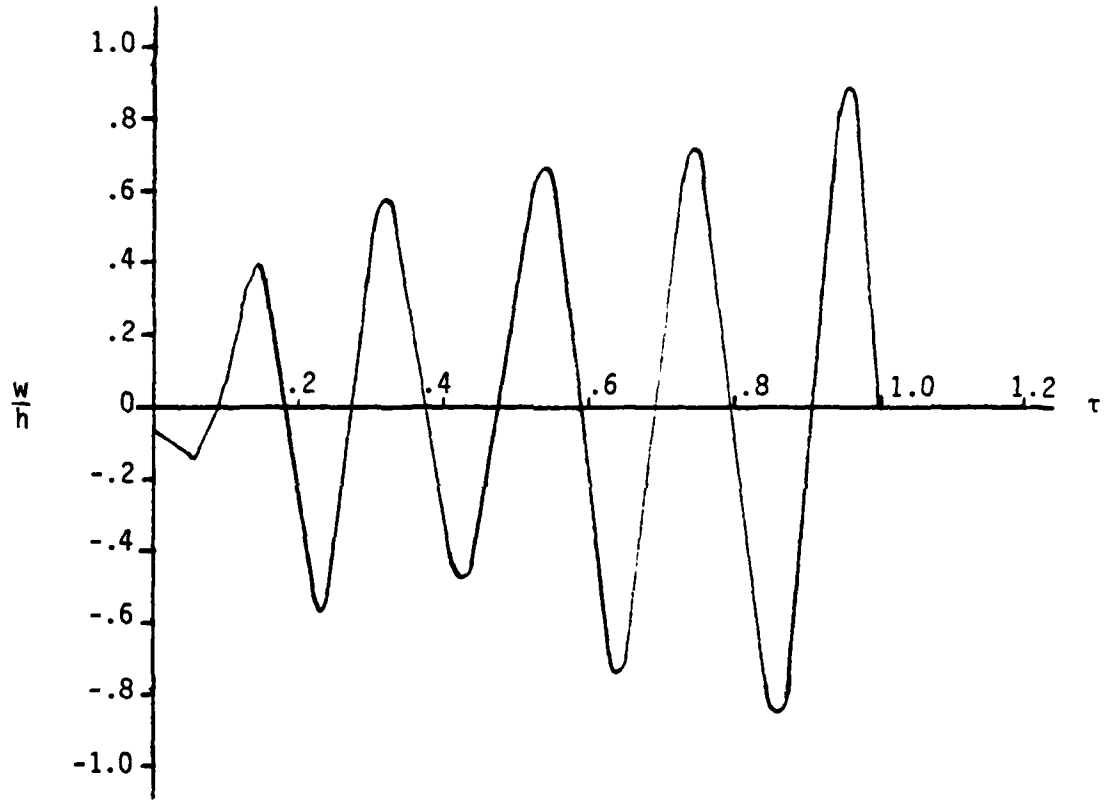

Figure A-7. Transient Dynamic Response to Initial Displacement #1, PT.54, (λ = 400, μ/M = .01, M = 3.0)

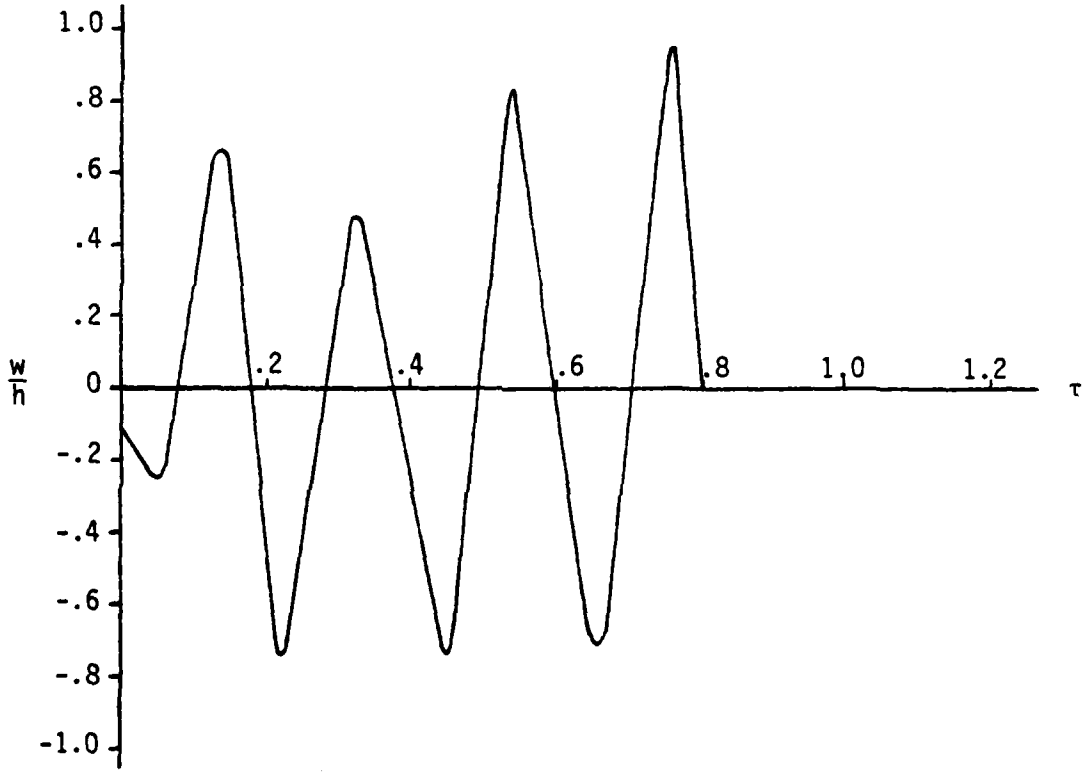

Figure A-8. Transient Dynamic Response to Initial Displacement #2, PT.54, (λ = 400, μ/M = .01, M = 3.0)

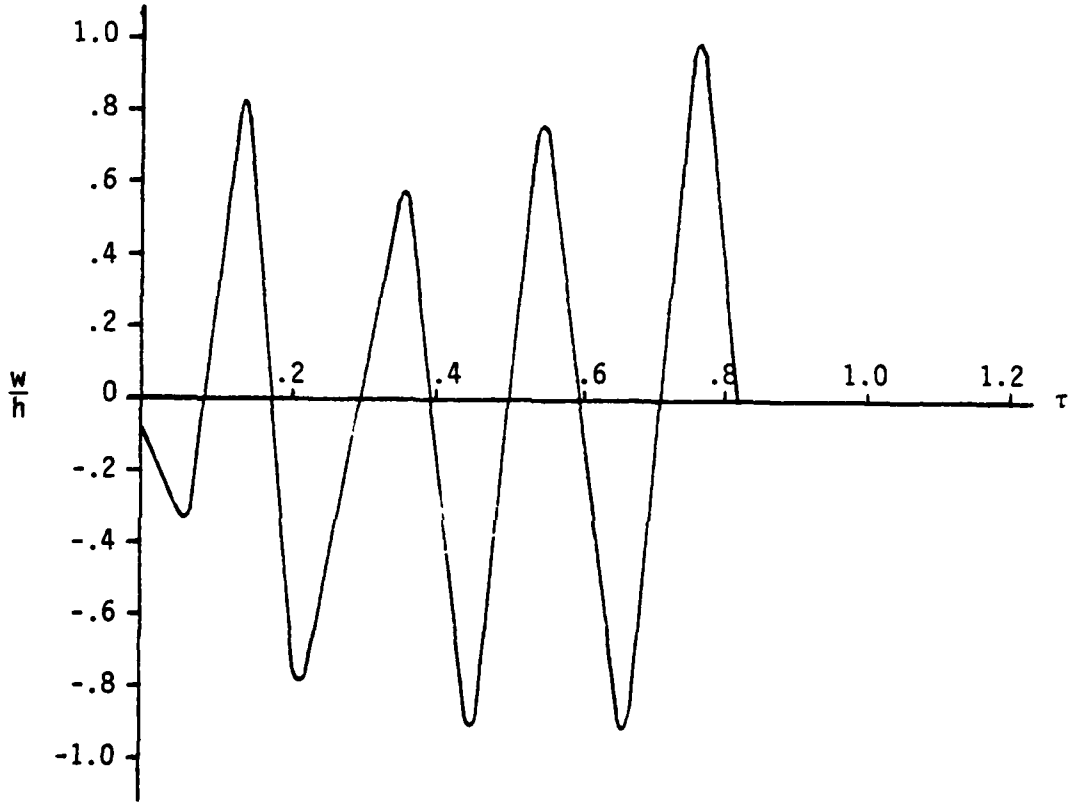

Figure A-9. Transient Dynamic Response to Initial Displacement #3, PT.54, (λ = 400, μ/M = .01, M = 3.0)

After three dynamic restart cycles, the time history for ID #4 (Figure A-10) reaches a limit cycle near t = 2.21 secs (.21 secs). The magnitude of the displacement at point #54 is ±.0144 inches or, in nondimensional form, (w/h) = ±.480. For ID #3 (Figure A-11), the time history shows limit cycle after two dynamic restart cycles. At point #54, the displacement of the limit cycle is ±.012 inches (w/h ±.400) at t = 2.13 (.13 secs). This information indicates that the limit cycle amplitude is dependent not only on Mach number, μ/M and λ, but also on initial displacement. The maximum amplitude of the motion occurs at about ξ = .7 (70% span); the displacement then falls off to zero at nodal points #1 and #44. The frequency of the oscillation is about 65 Hz.

Mach Number = 0.8

Figure A-12 presents the transient dynamic analysis results for a Mach number of 0.8 and initial displacement ID #3, again with λ = 300, and μ/M = .013. The results are similar to that discussed in the section entitled, "Mach Number = 1.2". Motion that was very near the limit cycle was reached at t = 2.21 (.21 secs). The amplitude of the motion at point #54 was ±.017 inches (w/h ±.580). Again, the frequency of the oscillation is about 65 Hz.

A summary plot which presents the deflection of the plate during limit cycle for Mach numbers of 0.8 and 1.2, is shown in Figure A-13. The response at M = 0.8 is larger across the plate than the response at M = 1.2.

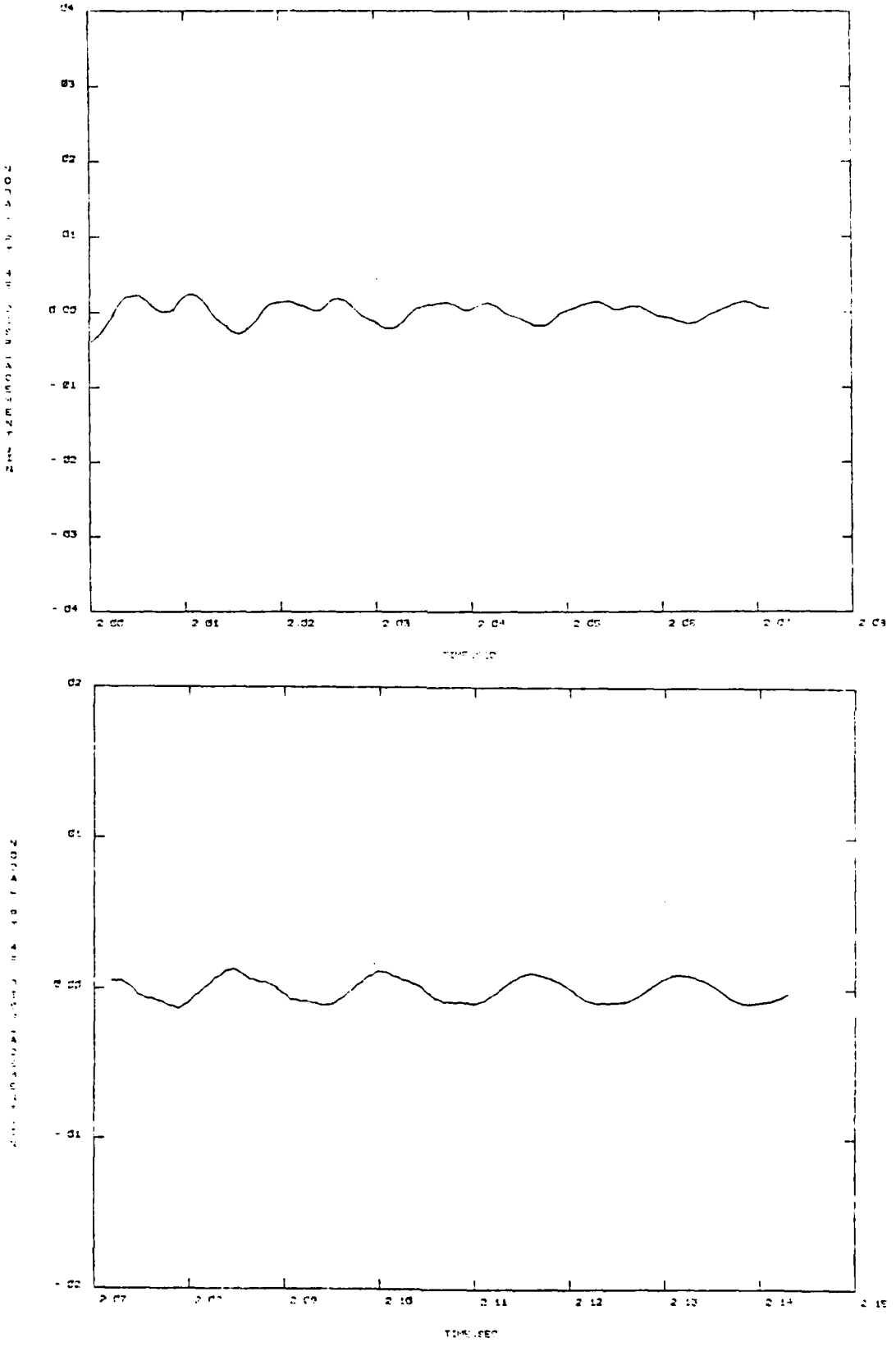

Figure A-10. Transient Dynamic Response to ID#4
(λ = 300, μ/M = .013, M = 1.2)

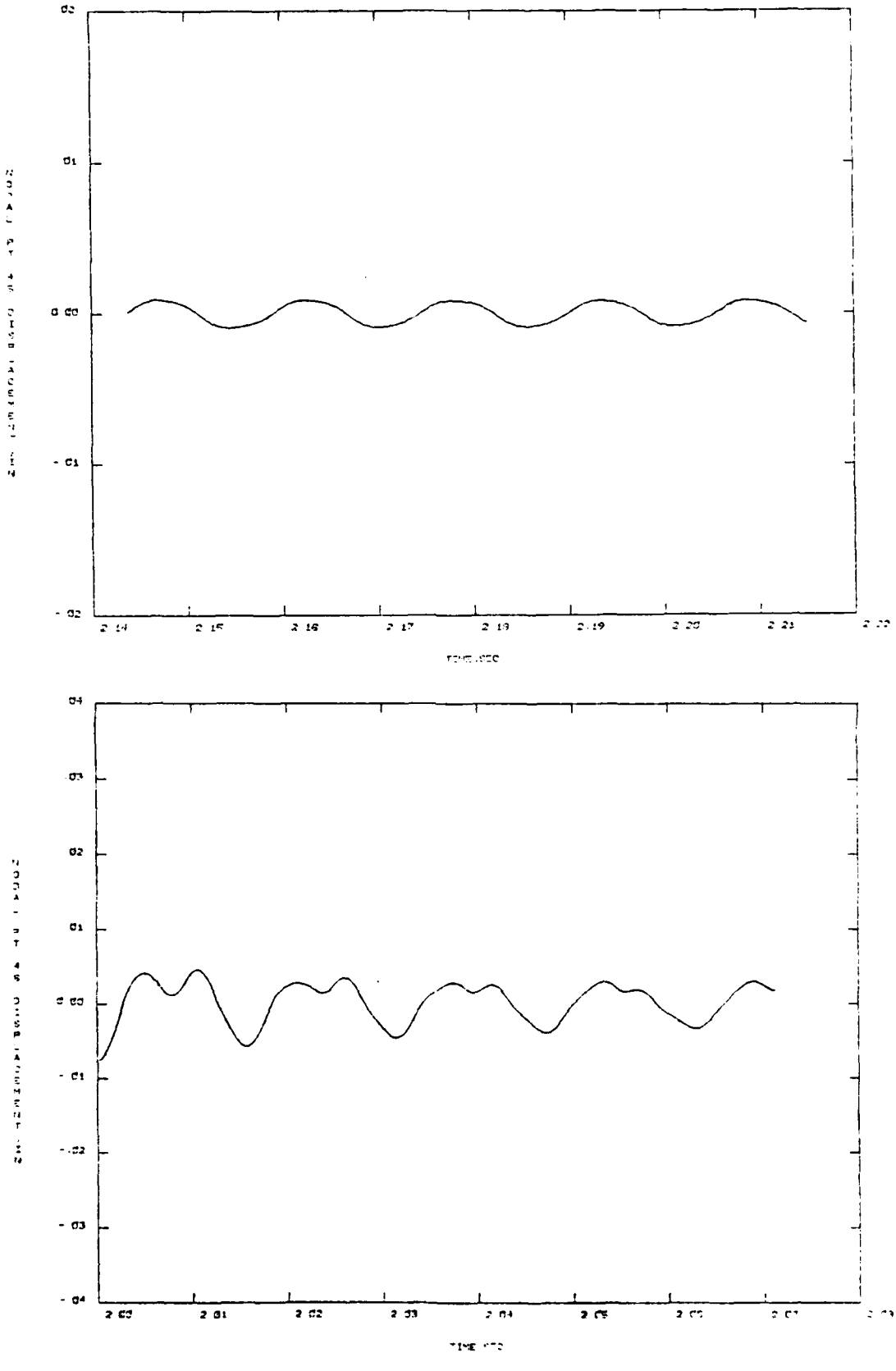

Figure A-10. (continued)

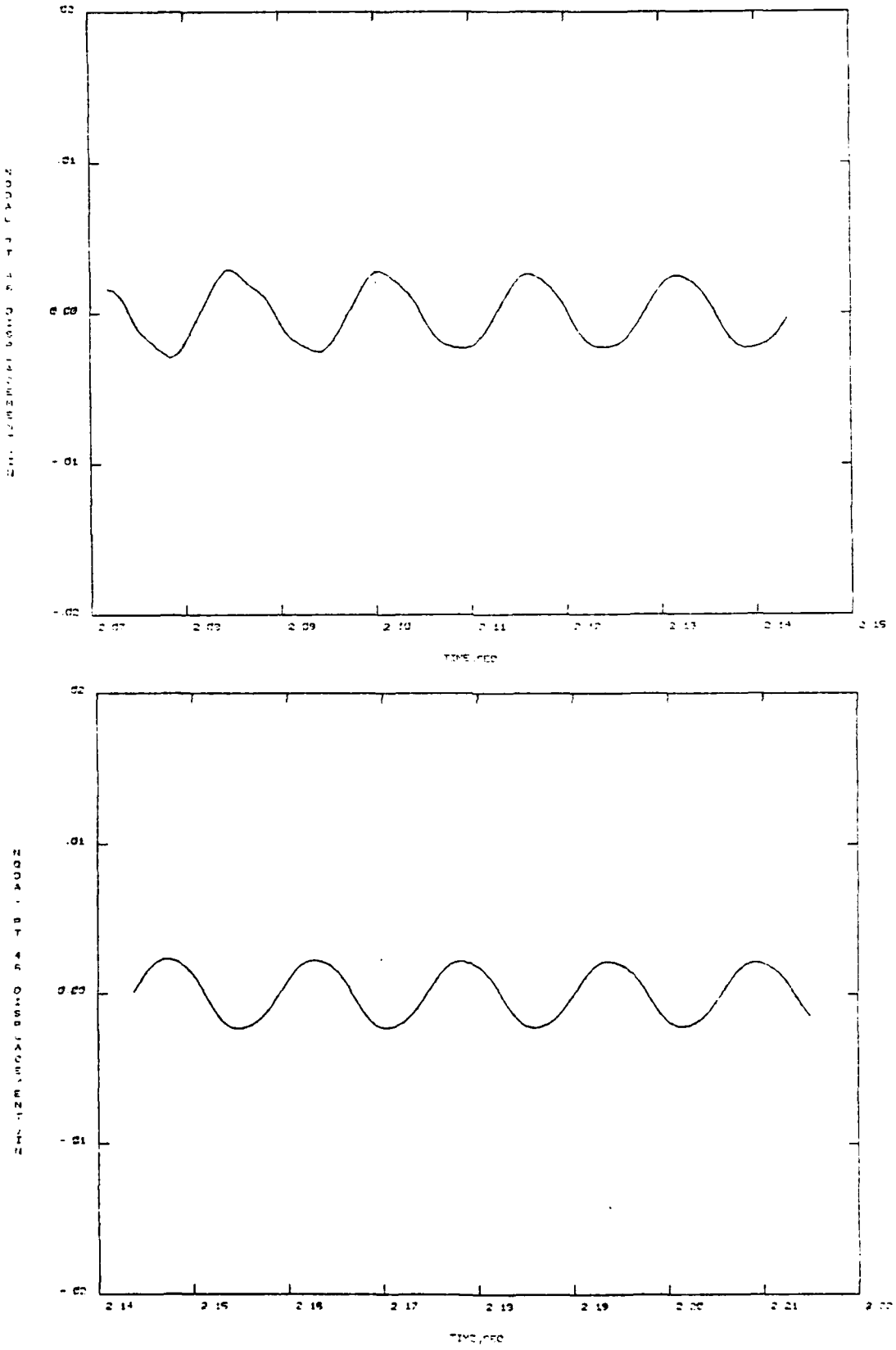

Figure A-10. (continued)

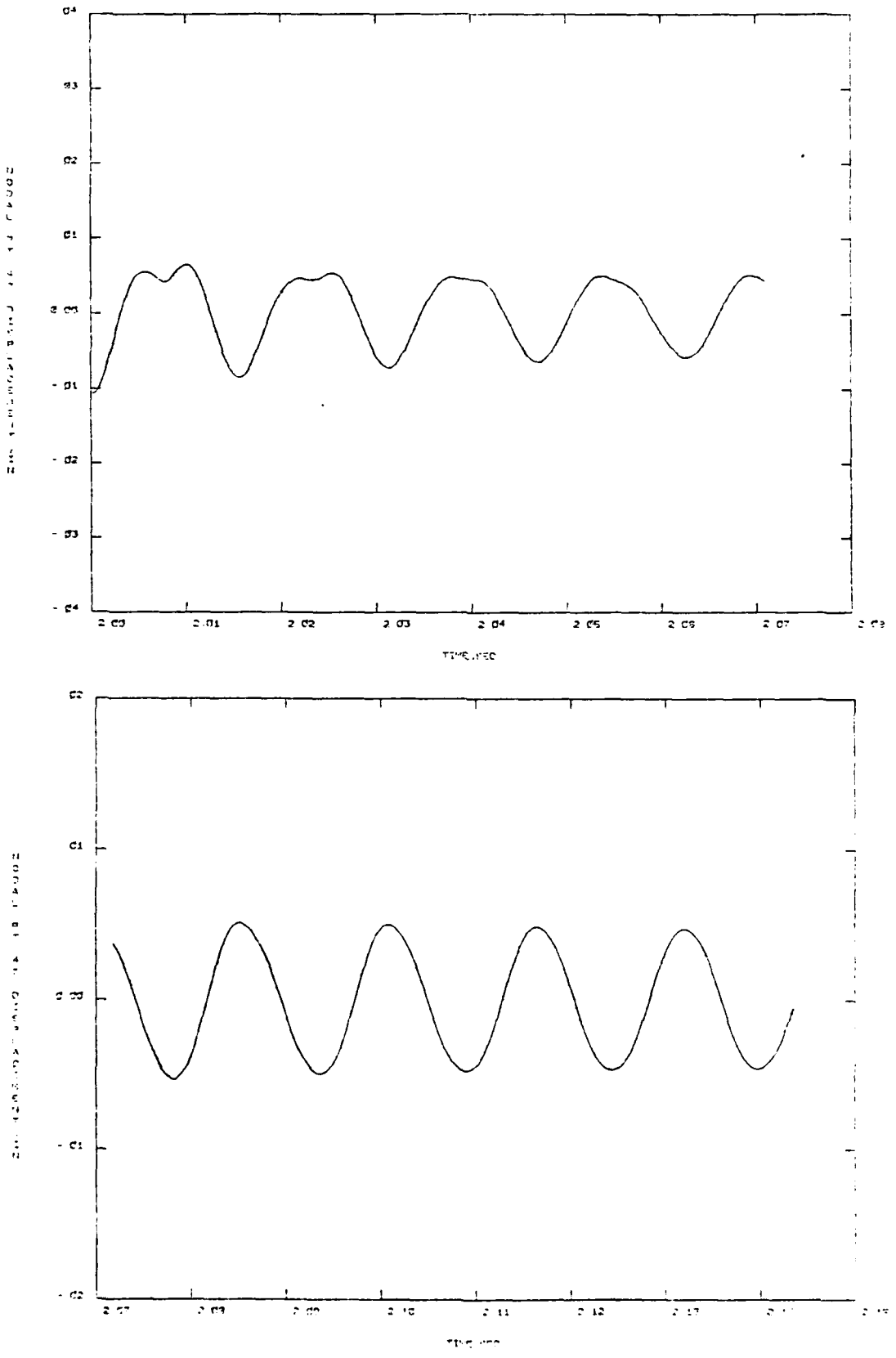

Figure A-10. (continued)

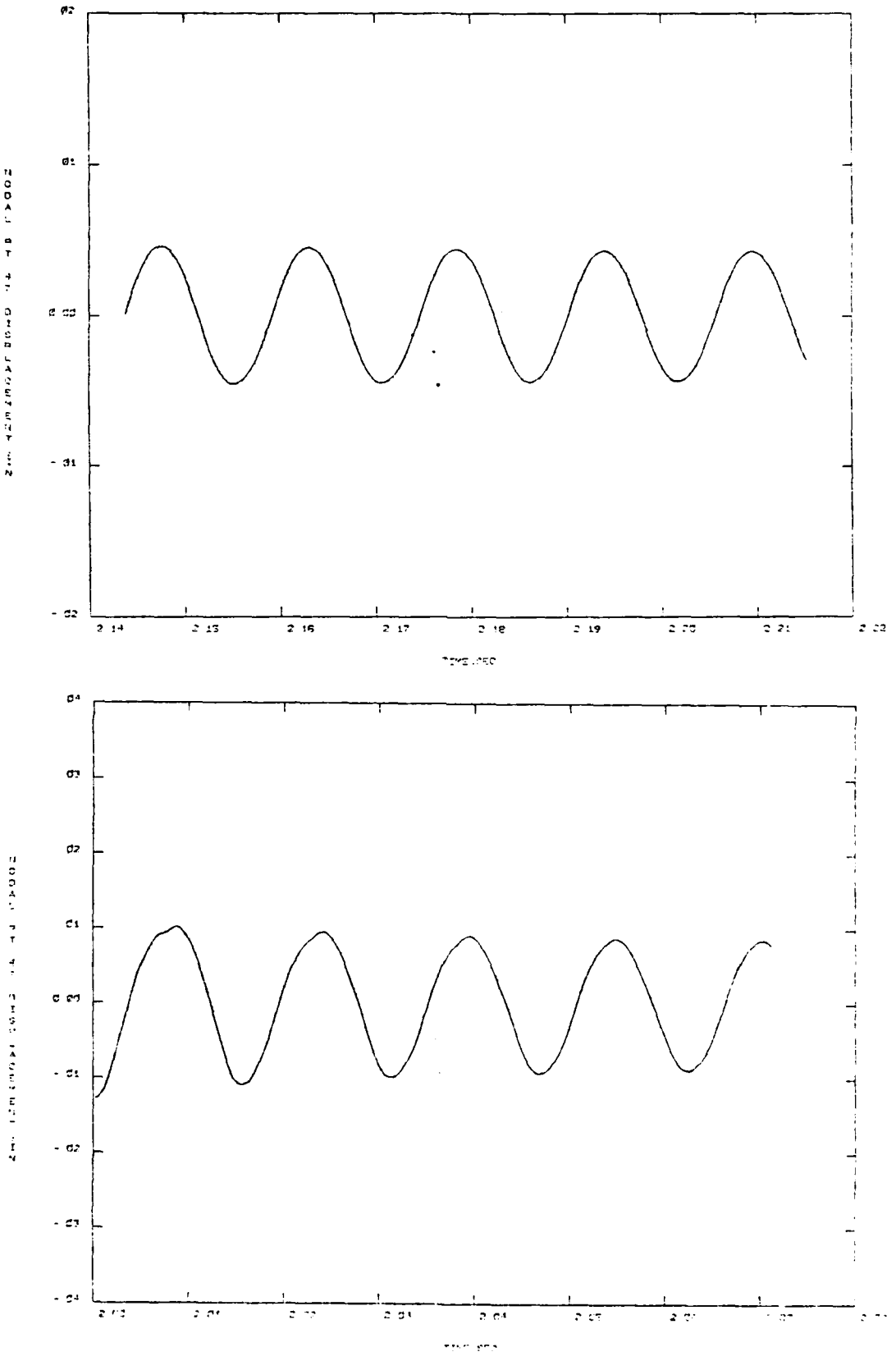

Figure A-10. (continued)

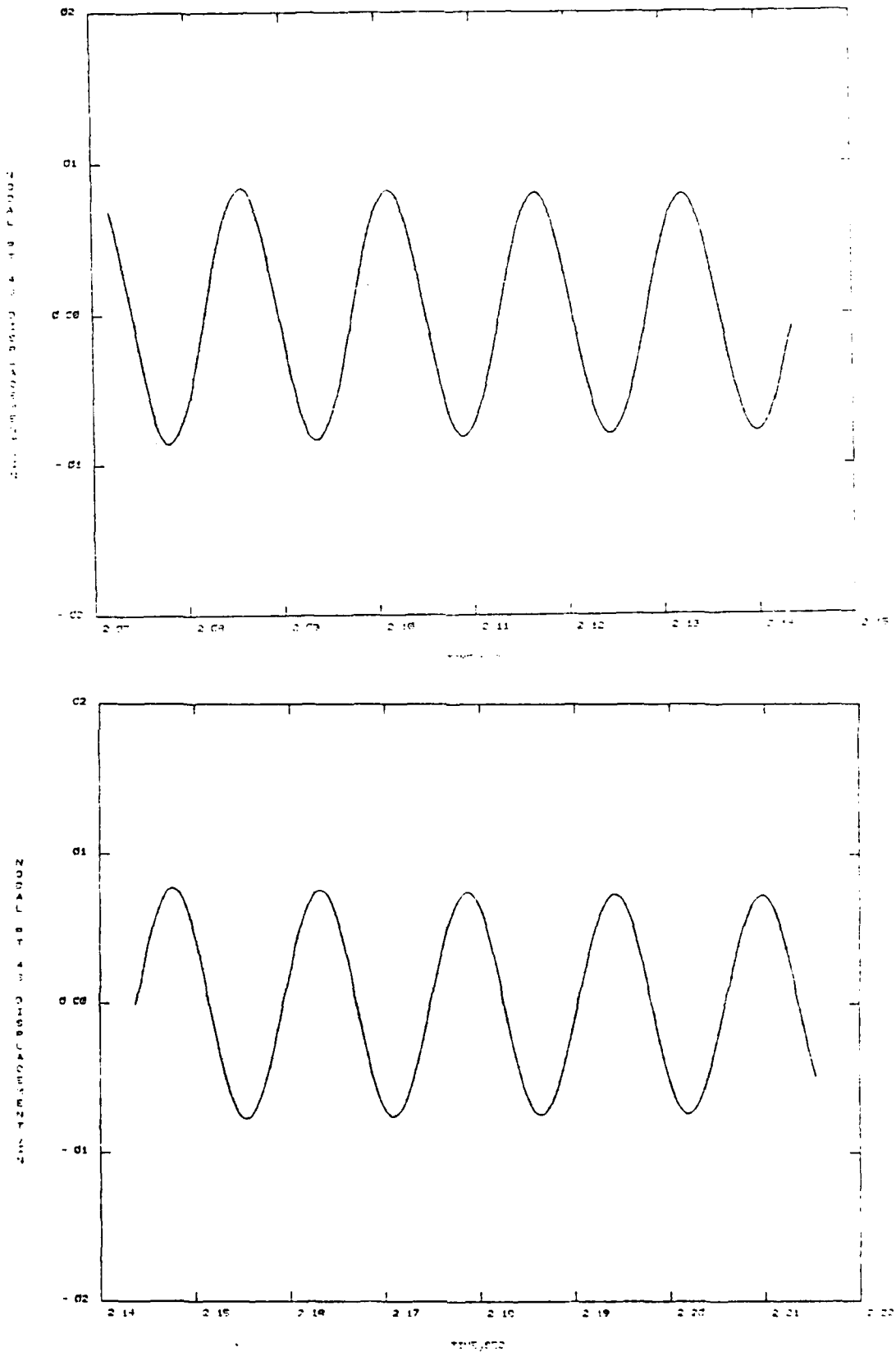

Figure A-10. (continued)

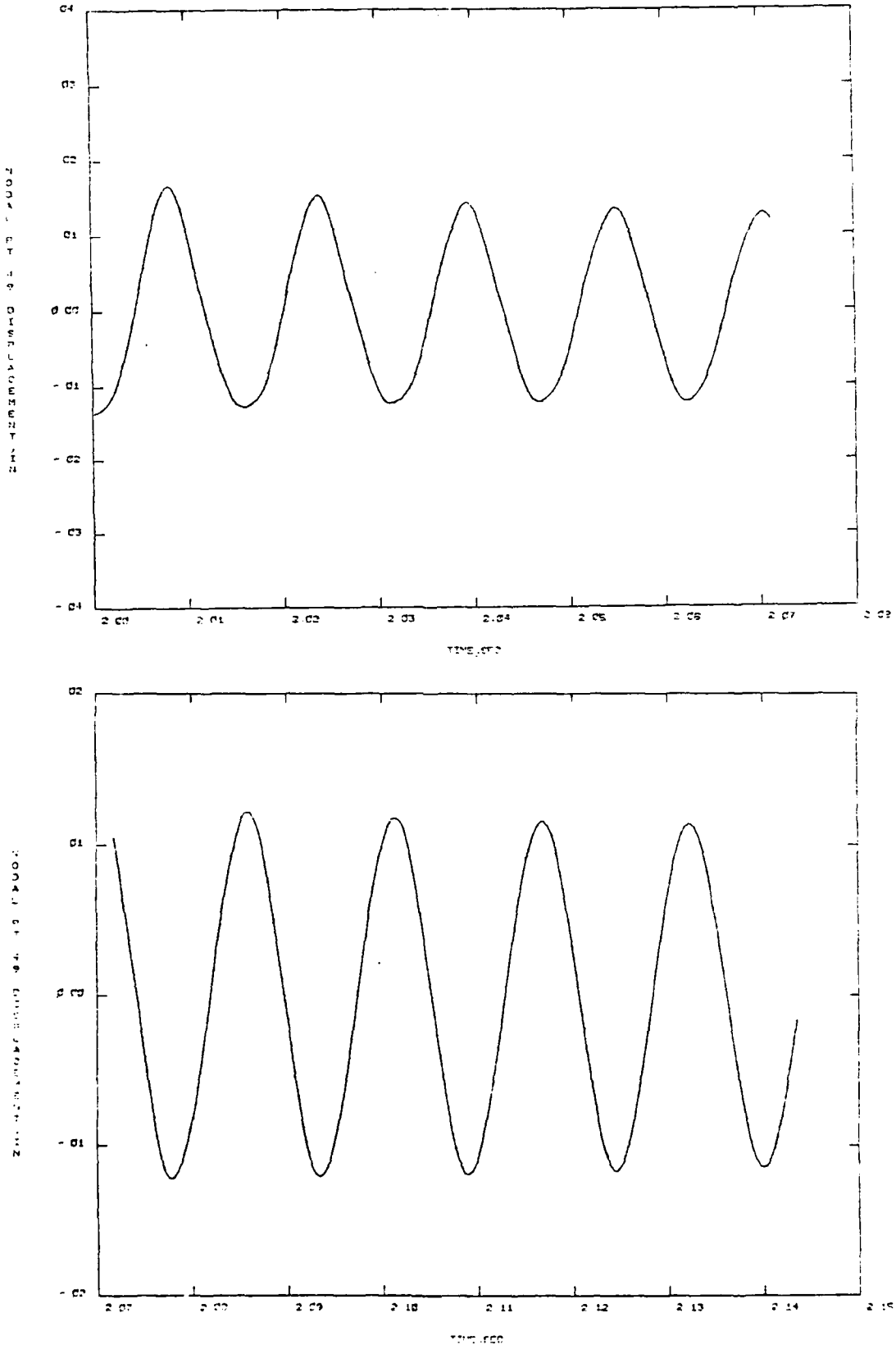

Figure A-10. (continued)

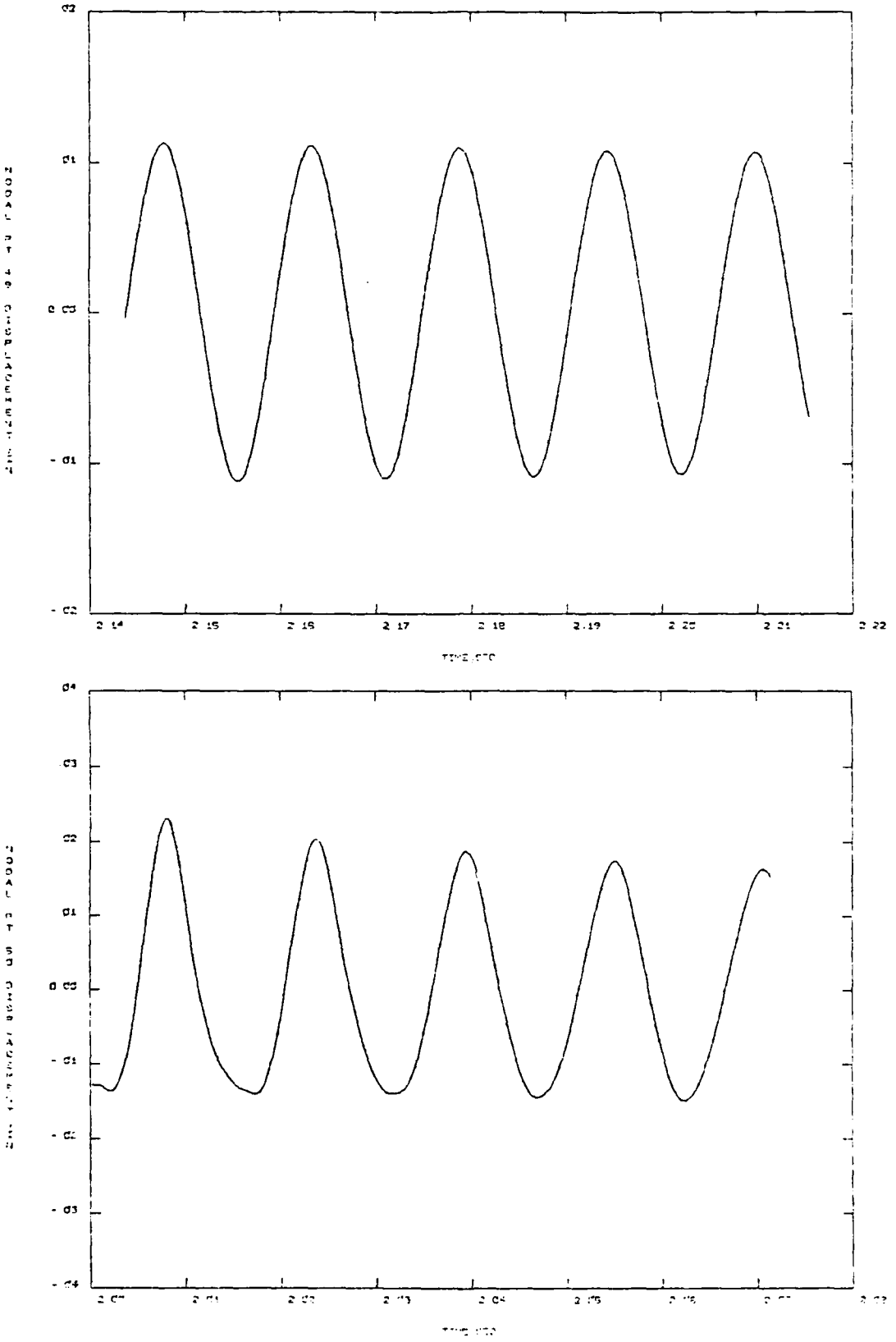

Figure A-10. (continued)

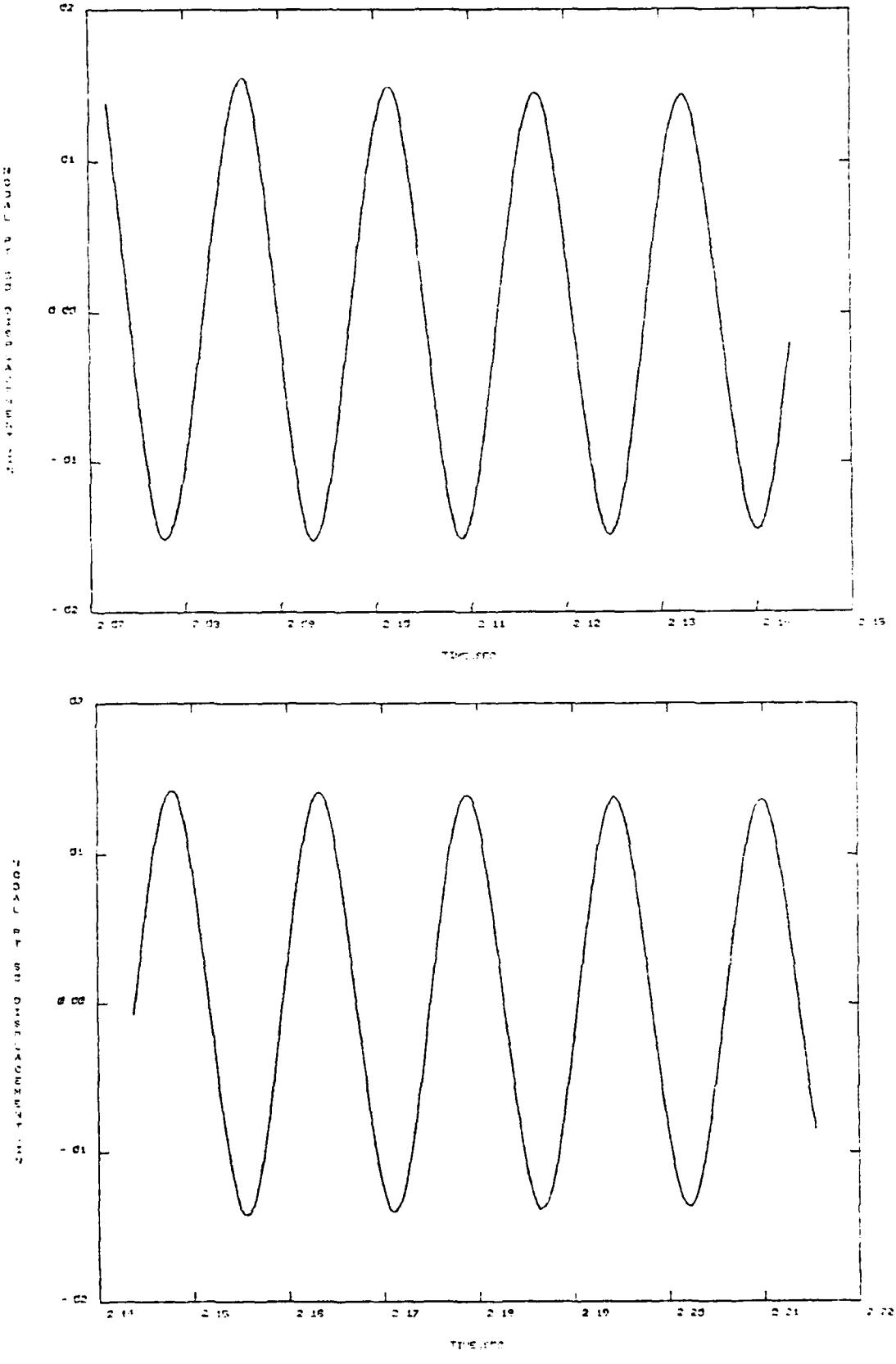

Figure A-10. (continued)

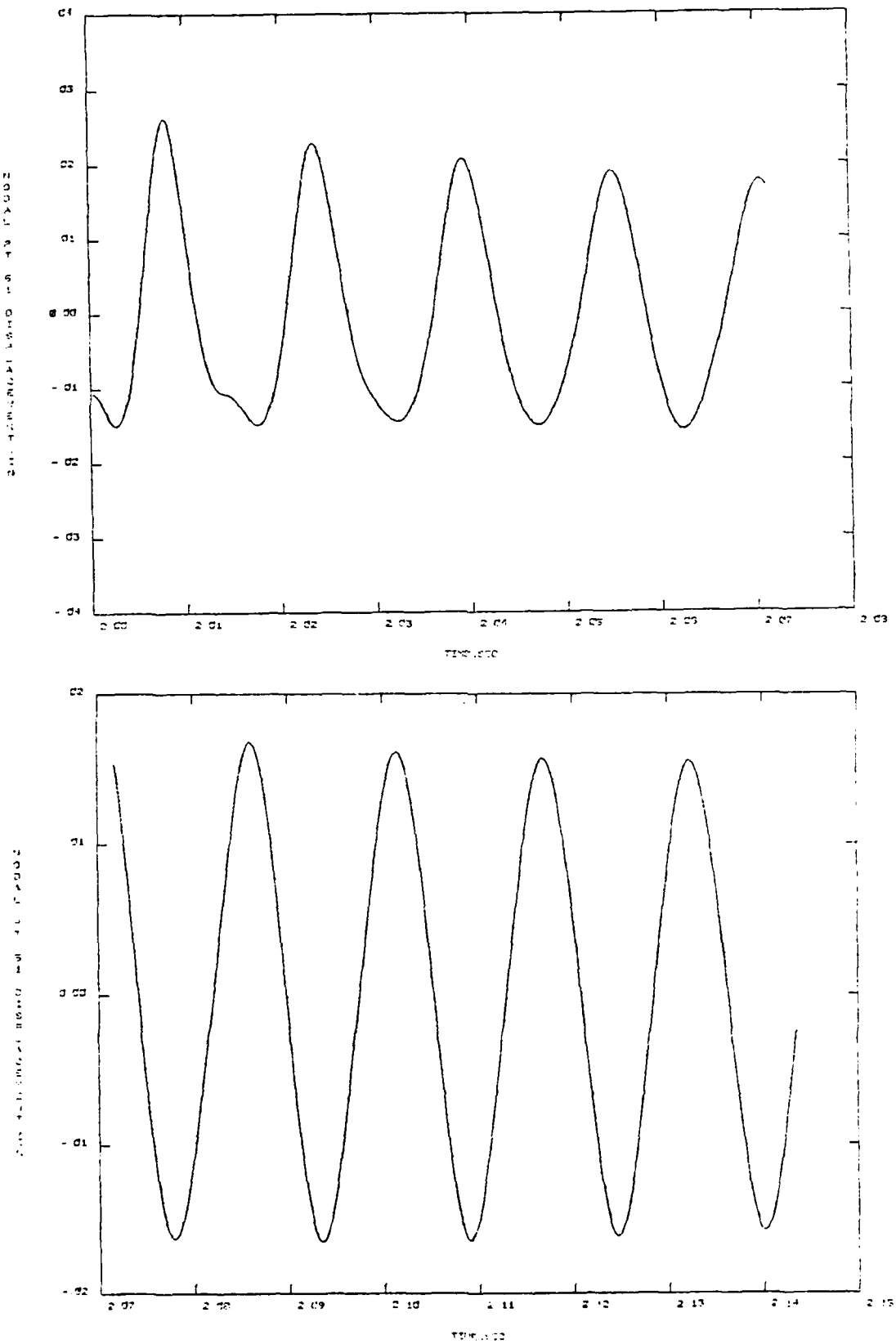

Figure A-10. (continued)

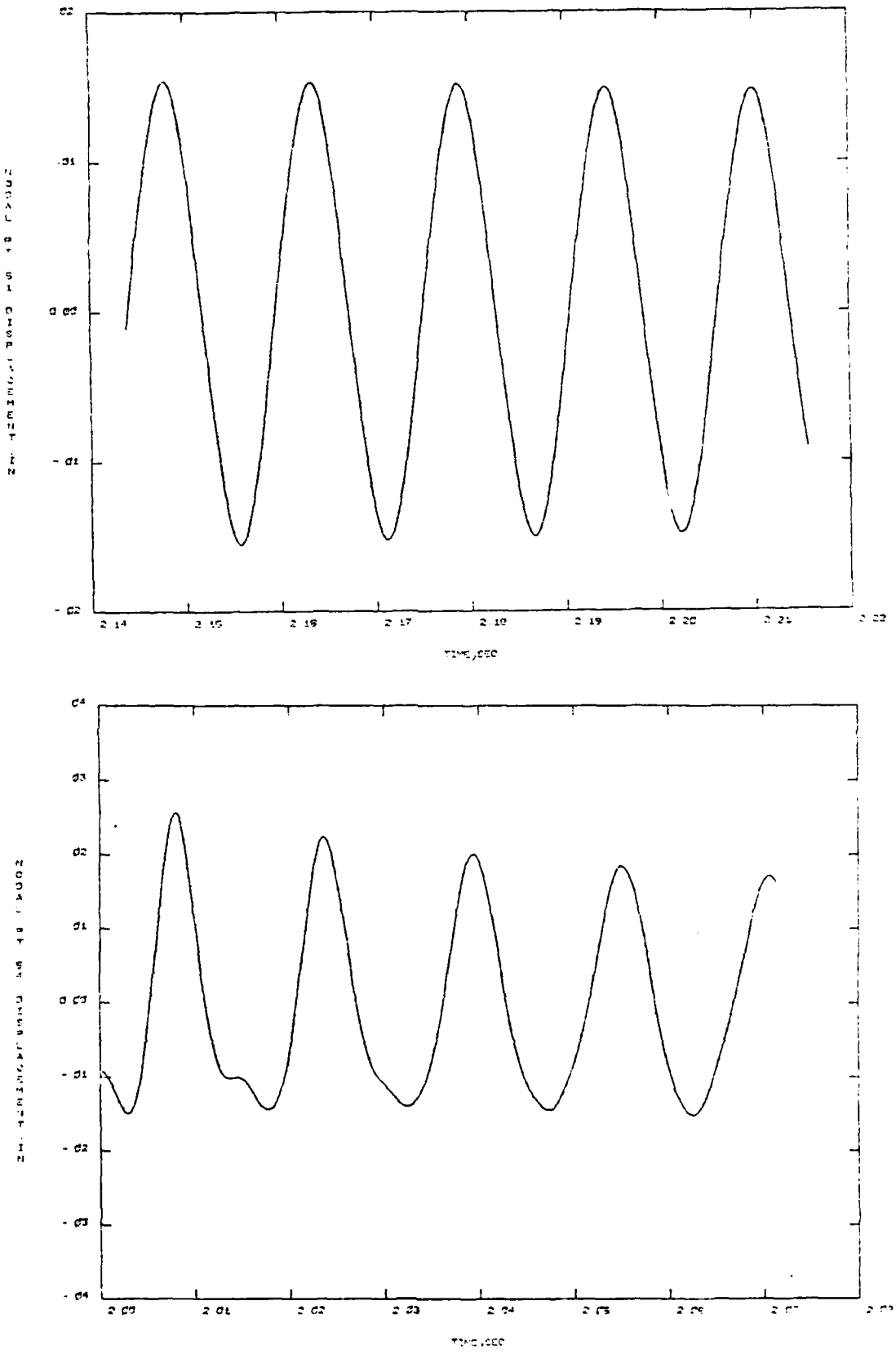

Figure A-10. (continued)

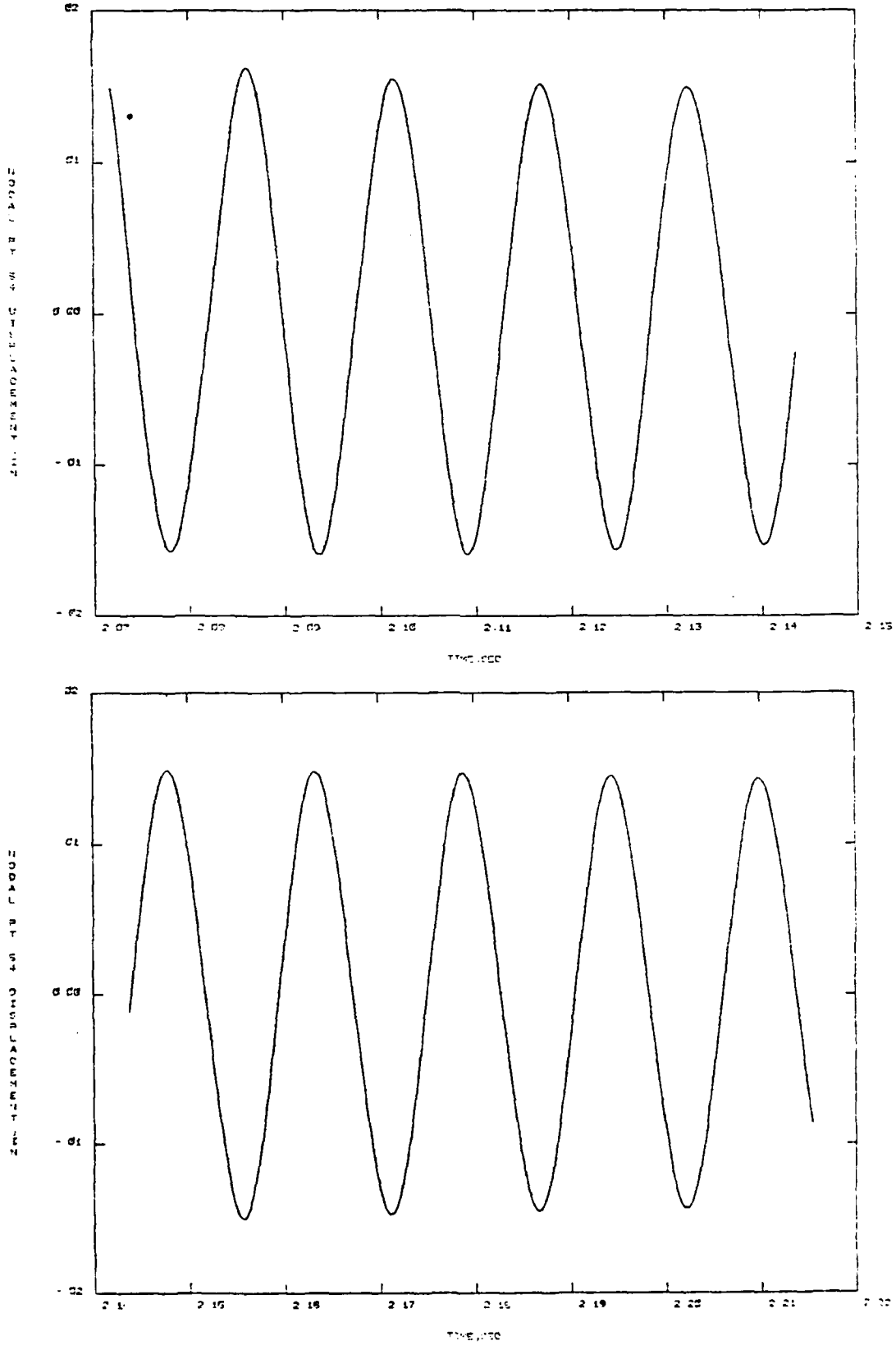

Figure A-10. (continued)

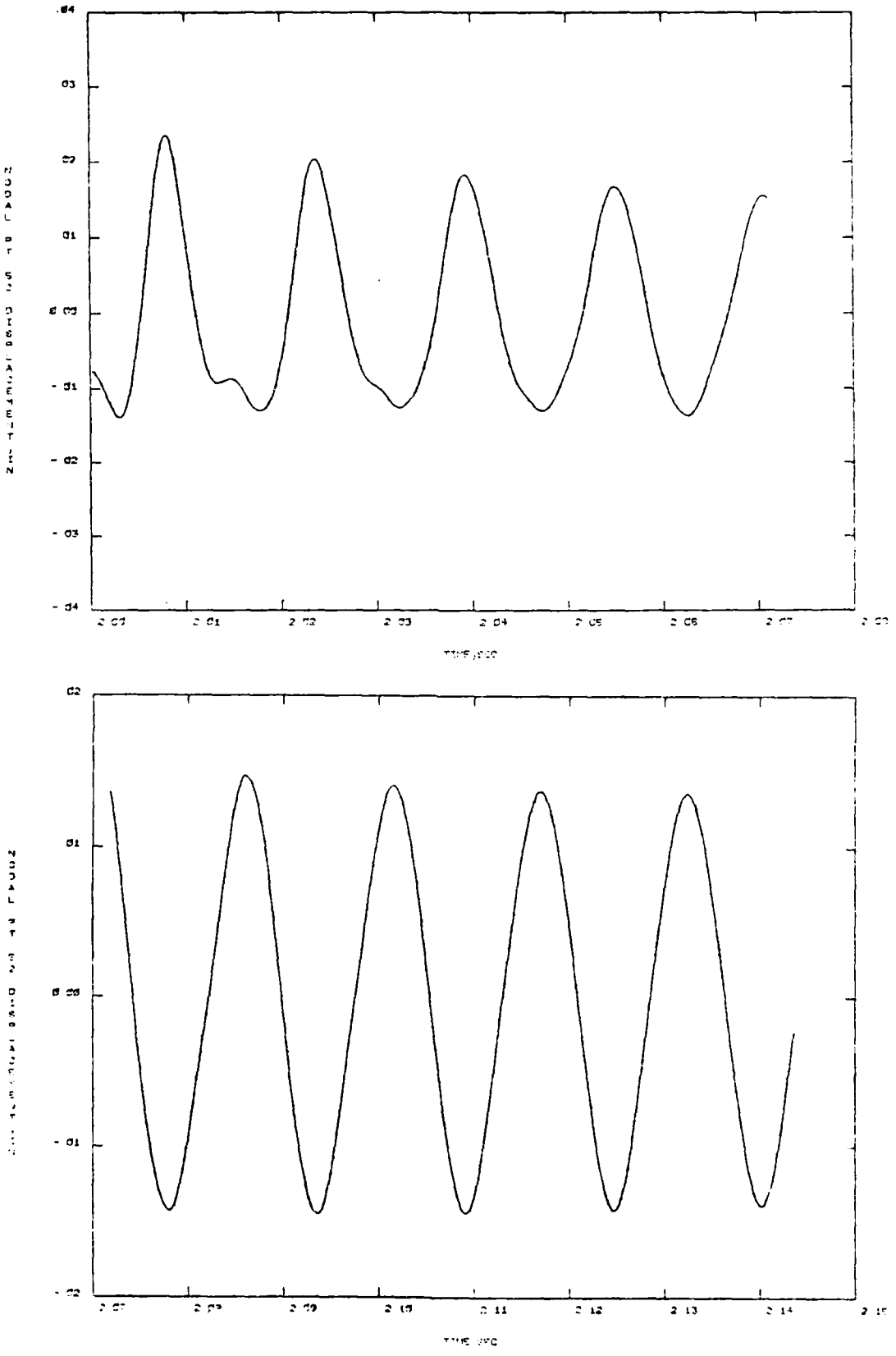

Figure A-10. (continued)

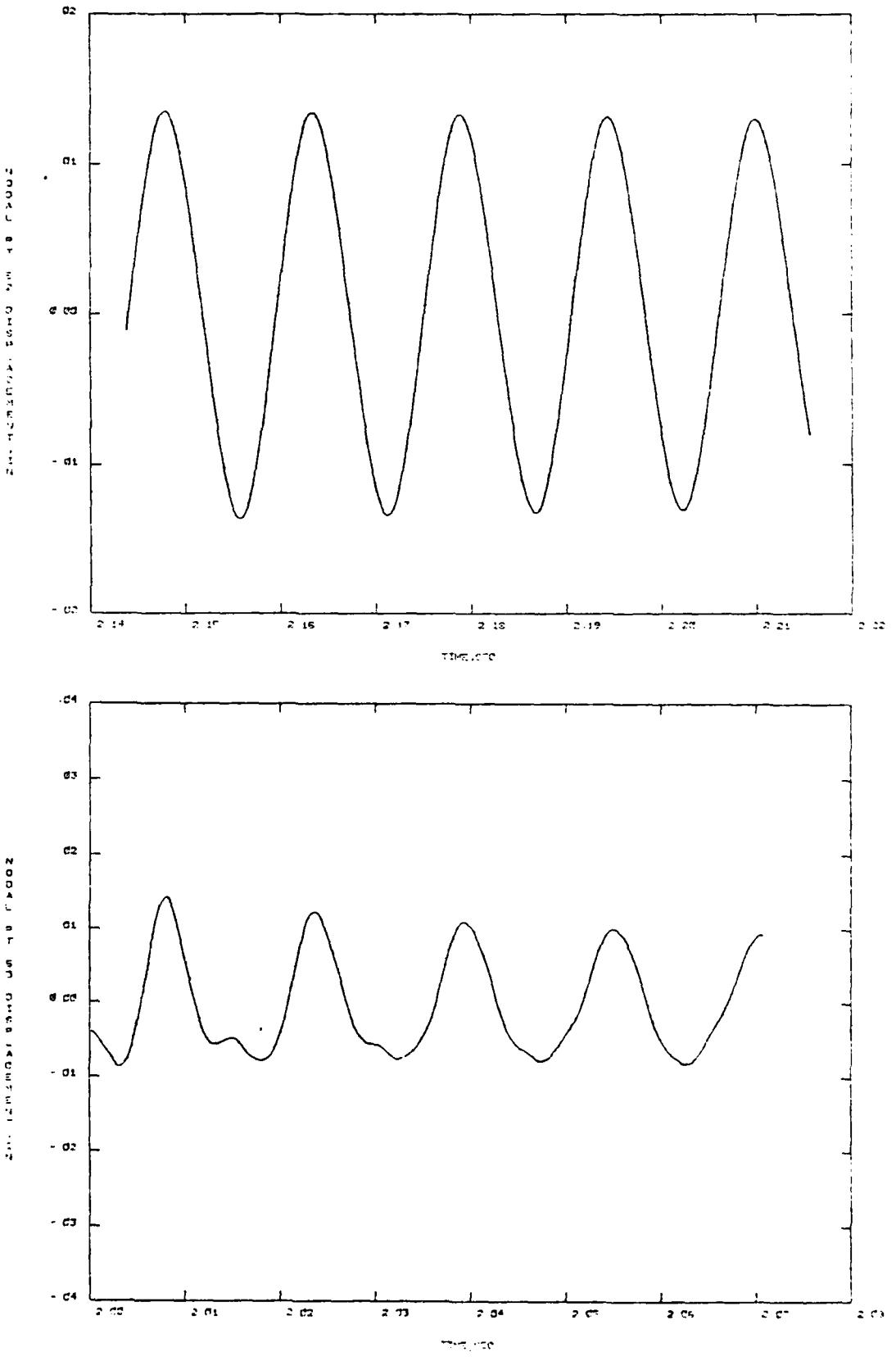

Figure A-10. (continued)

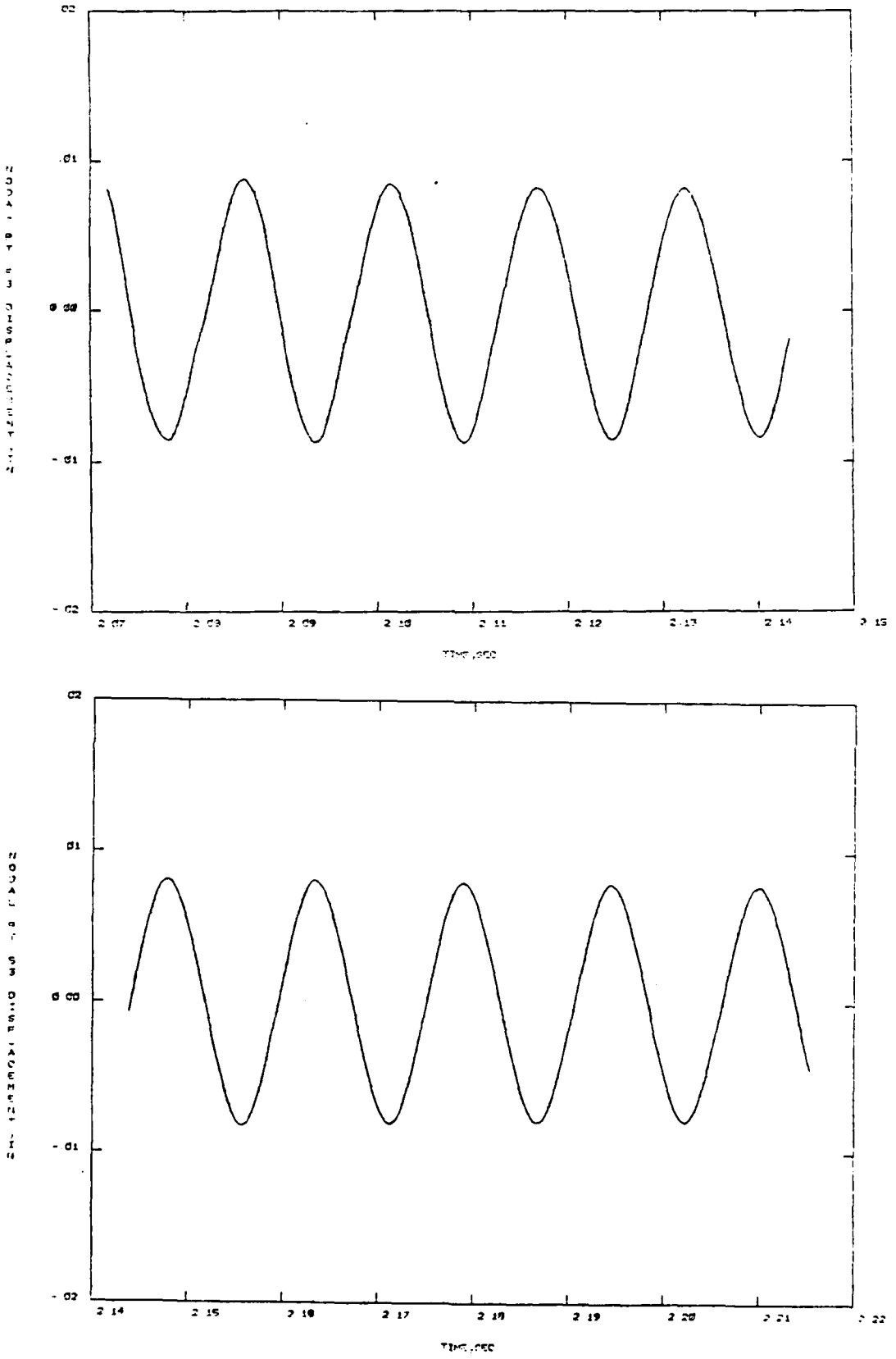

Figure A-10. (continued)

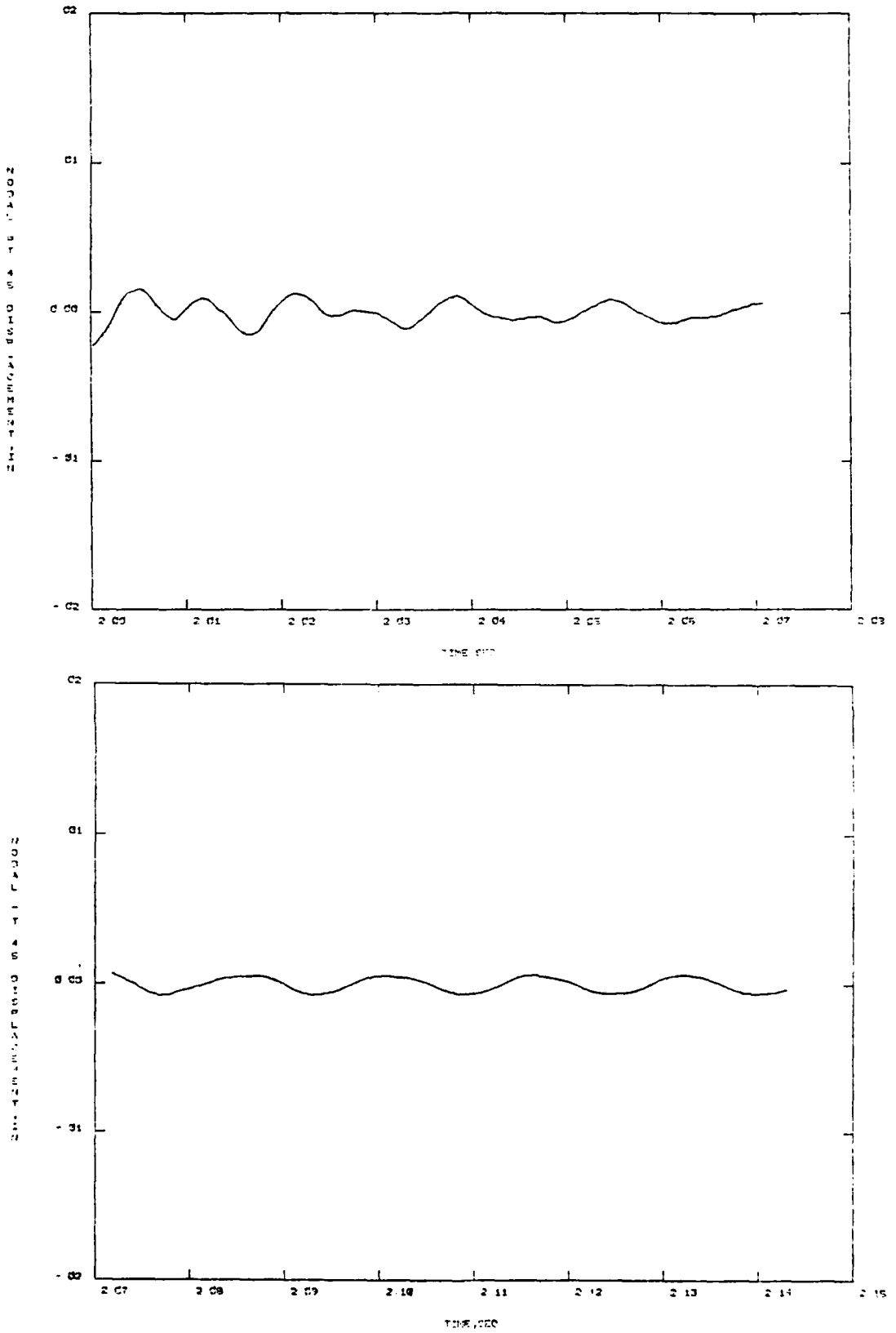

Figure A-11. Transient Dynamic Response to ID#3
(λ = 300, μ/M = .013, M = 1.2)

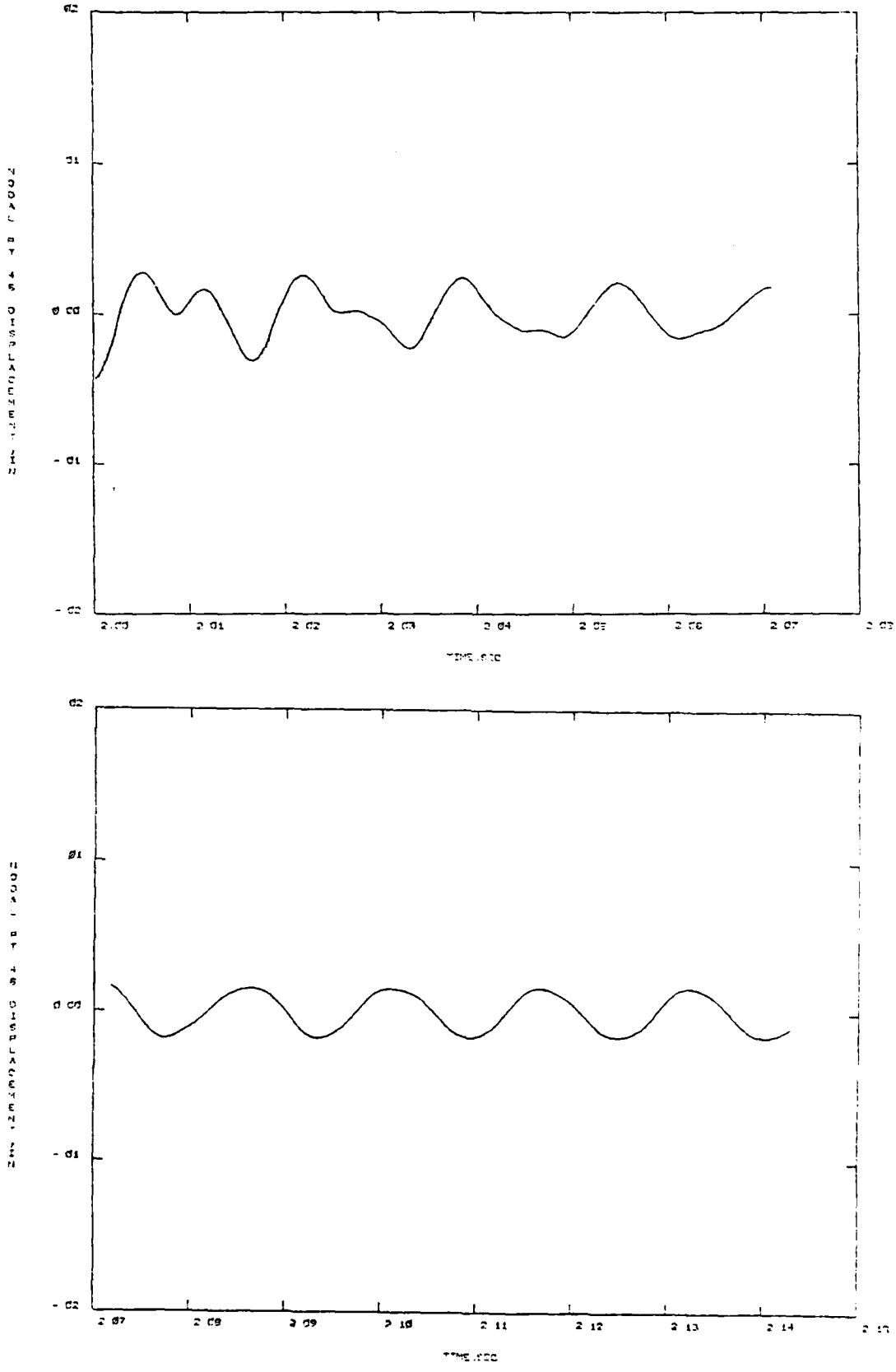

Figure A-11. (continued)

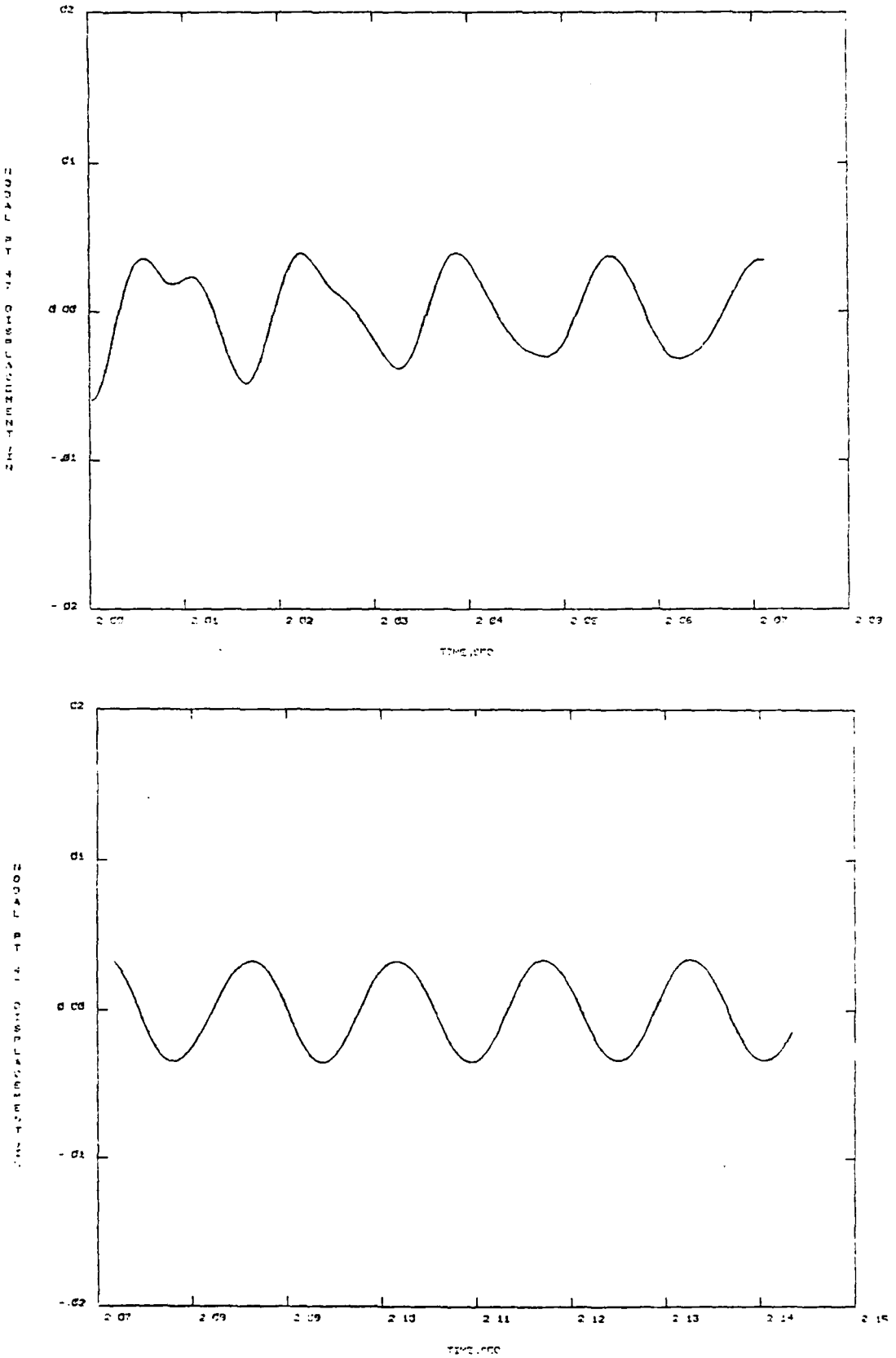

Figure A-11. (continued)

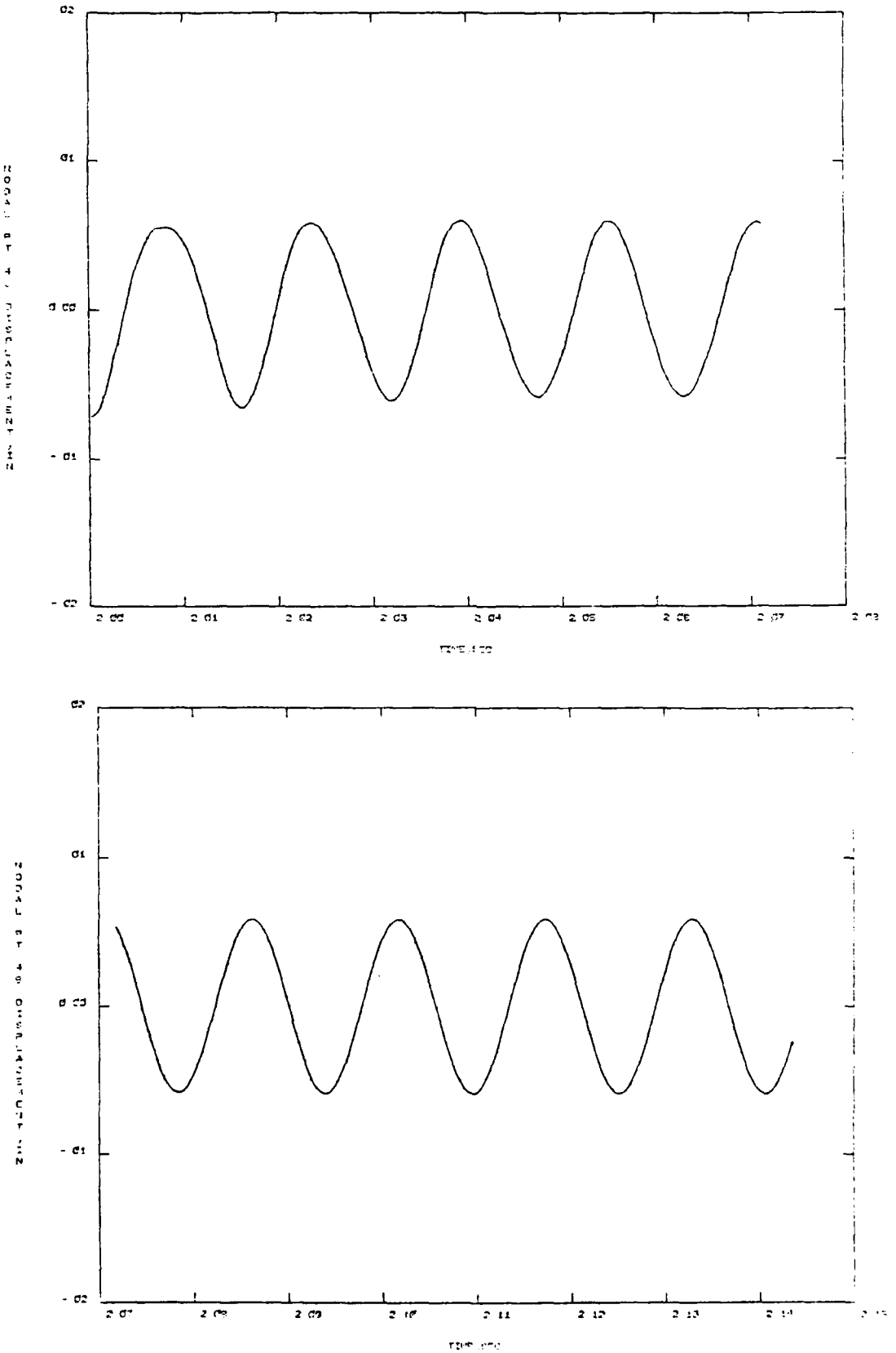

Figure A-11. (continued)

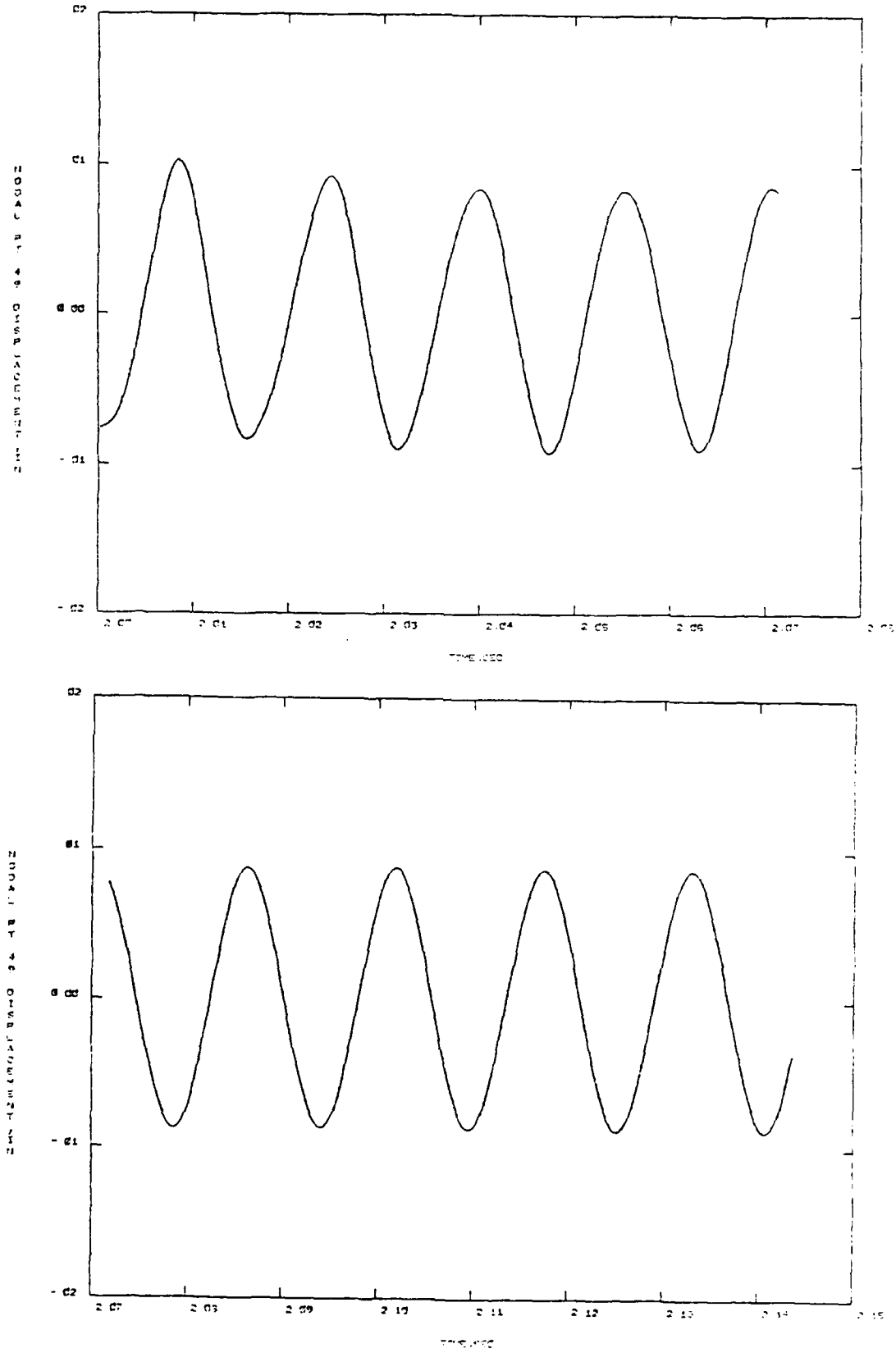

Figure A-11. (continued)

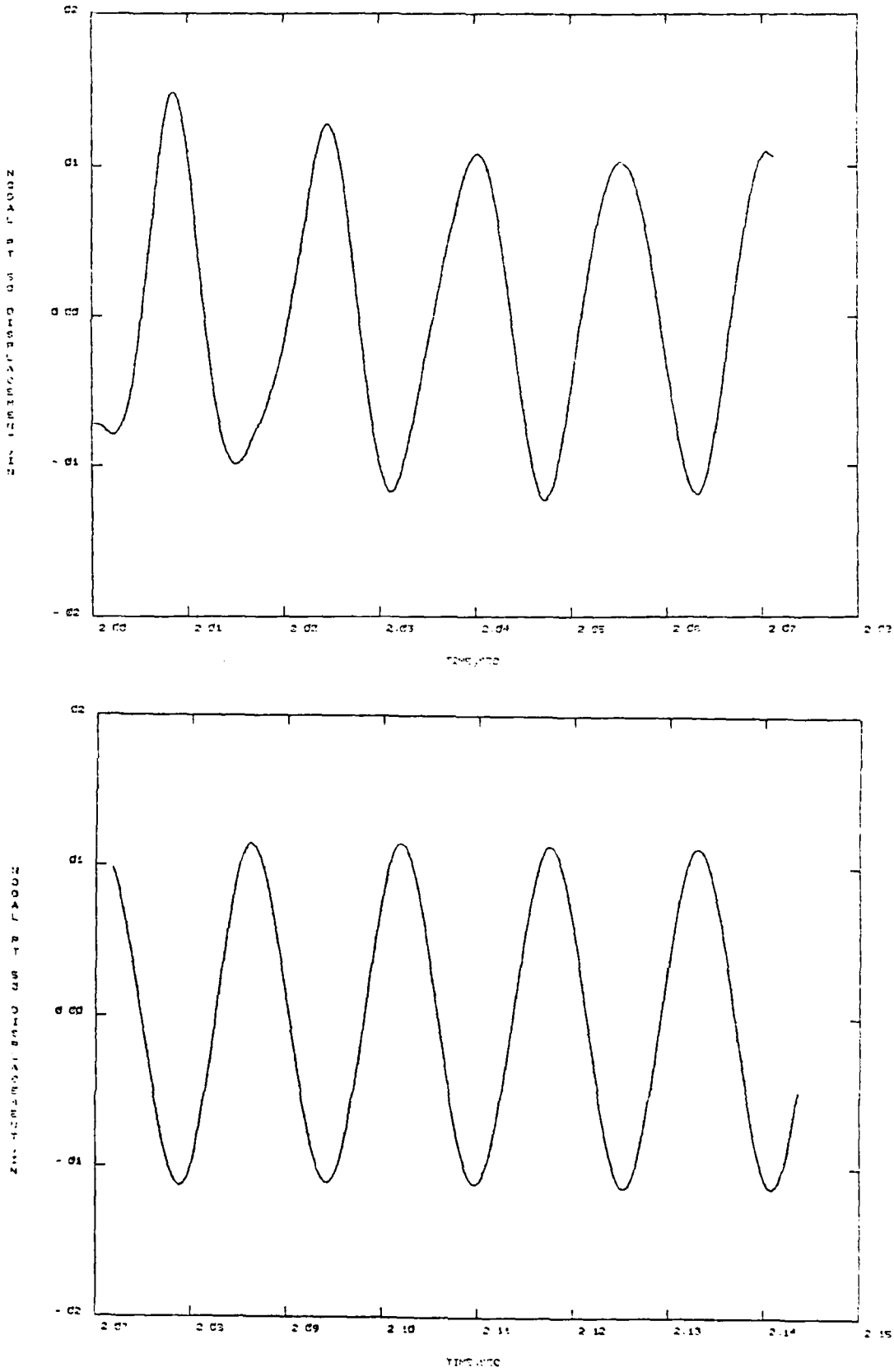

Figure A-11. (continued)

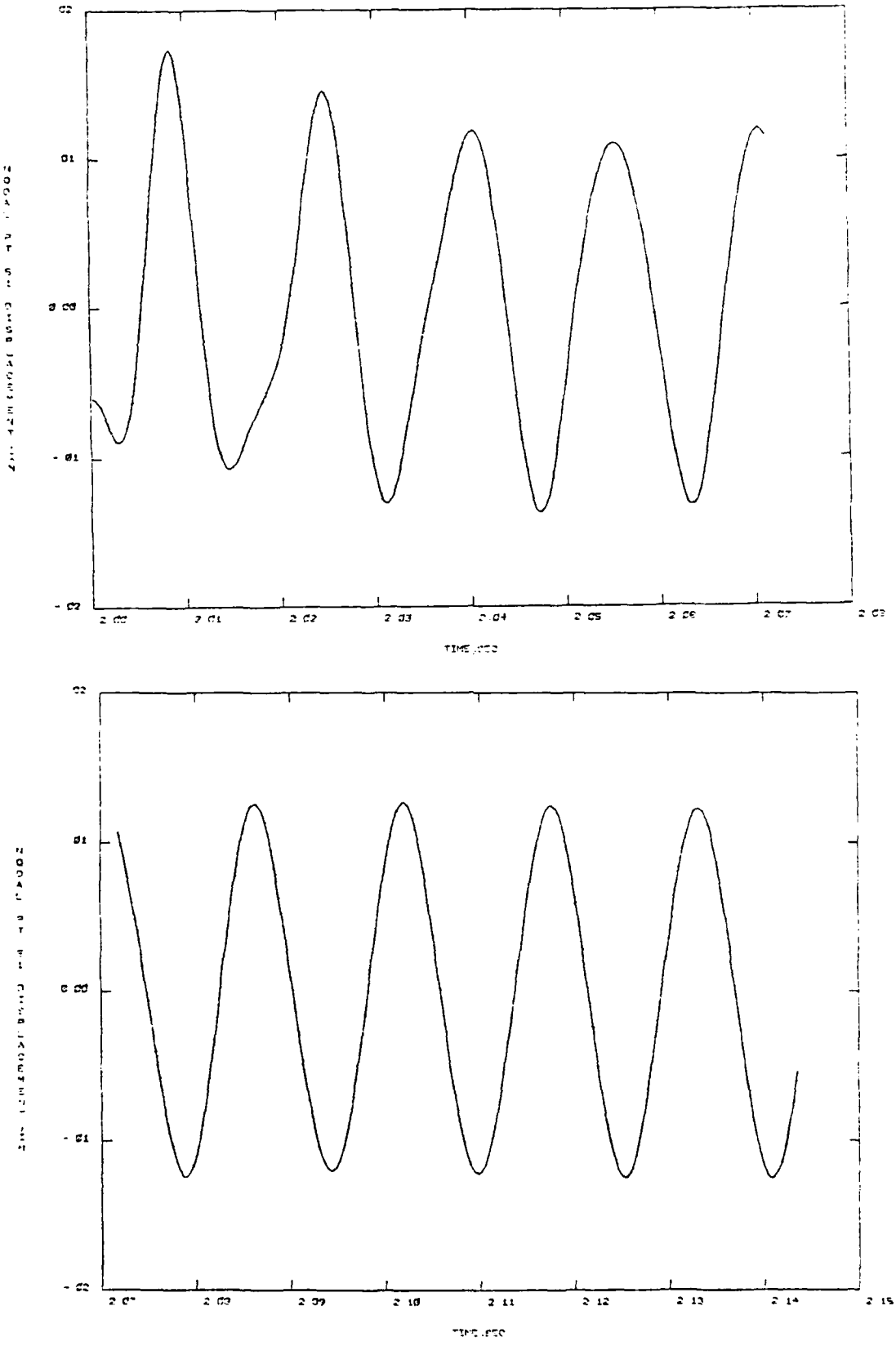

Figure A-11. (continued)

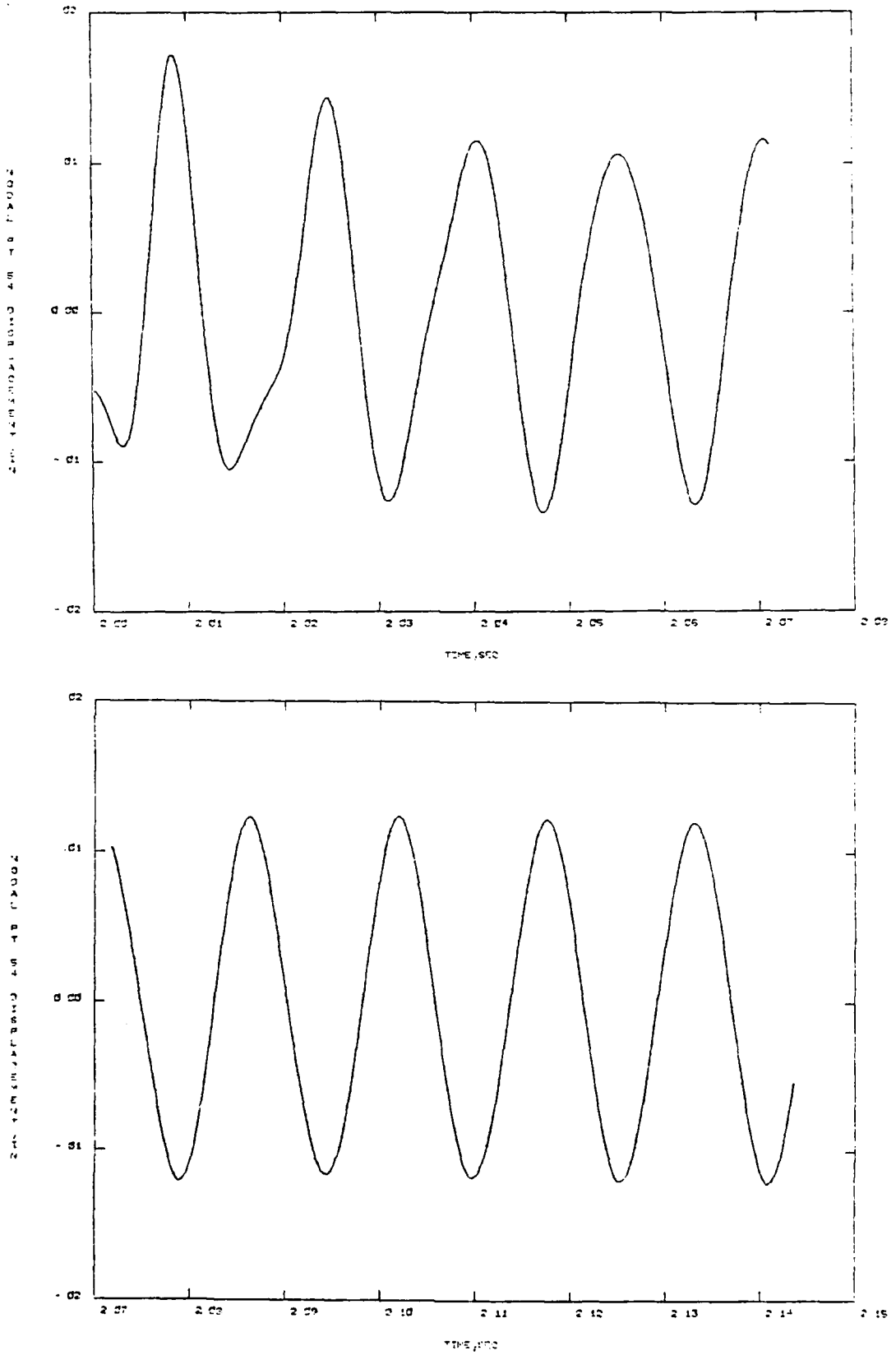

Figure A-11. (continued)

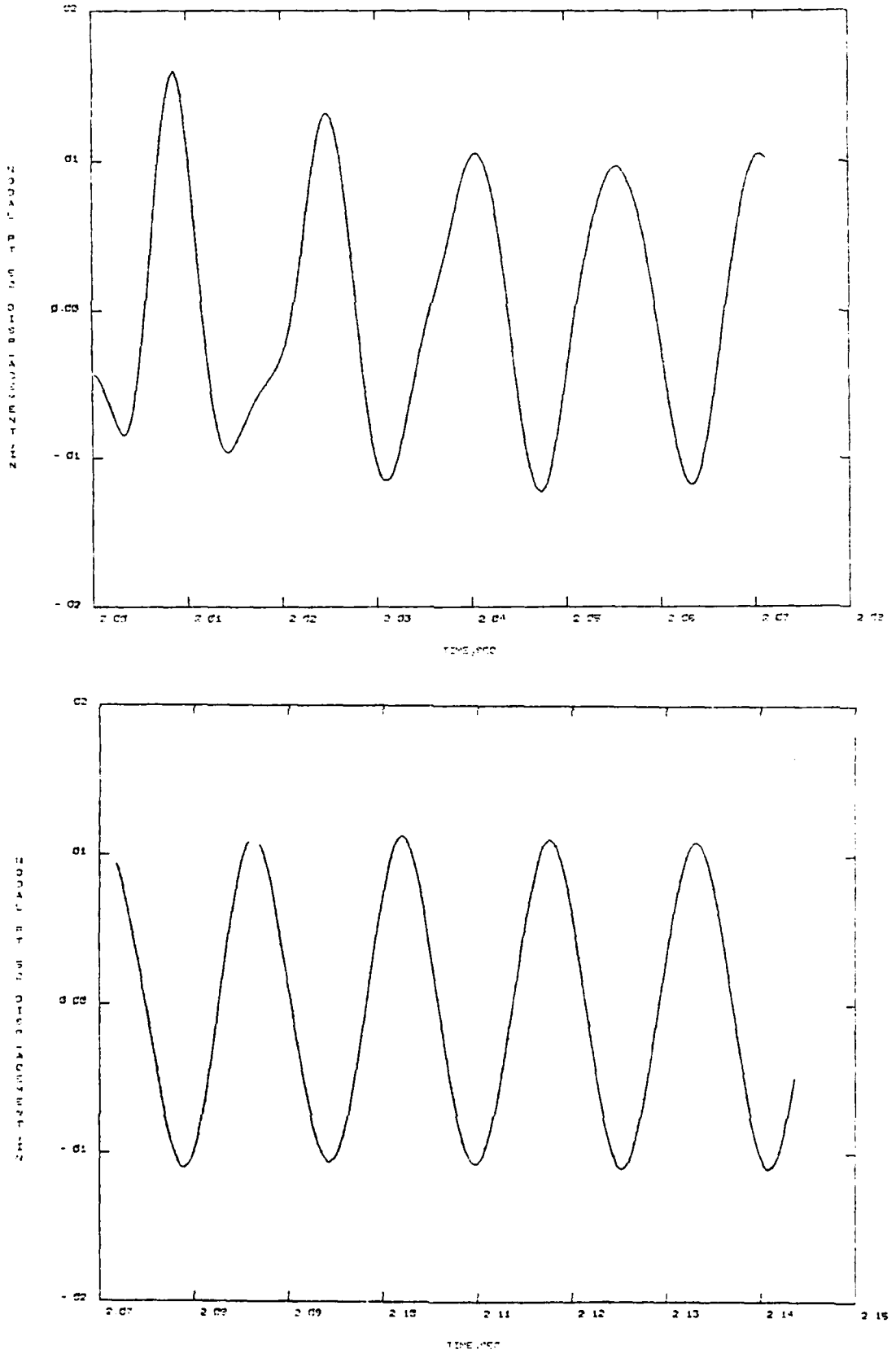

Figure A-11. (continued)

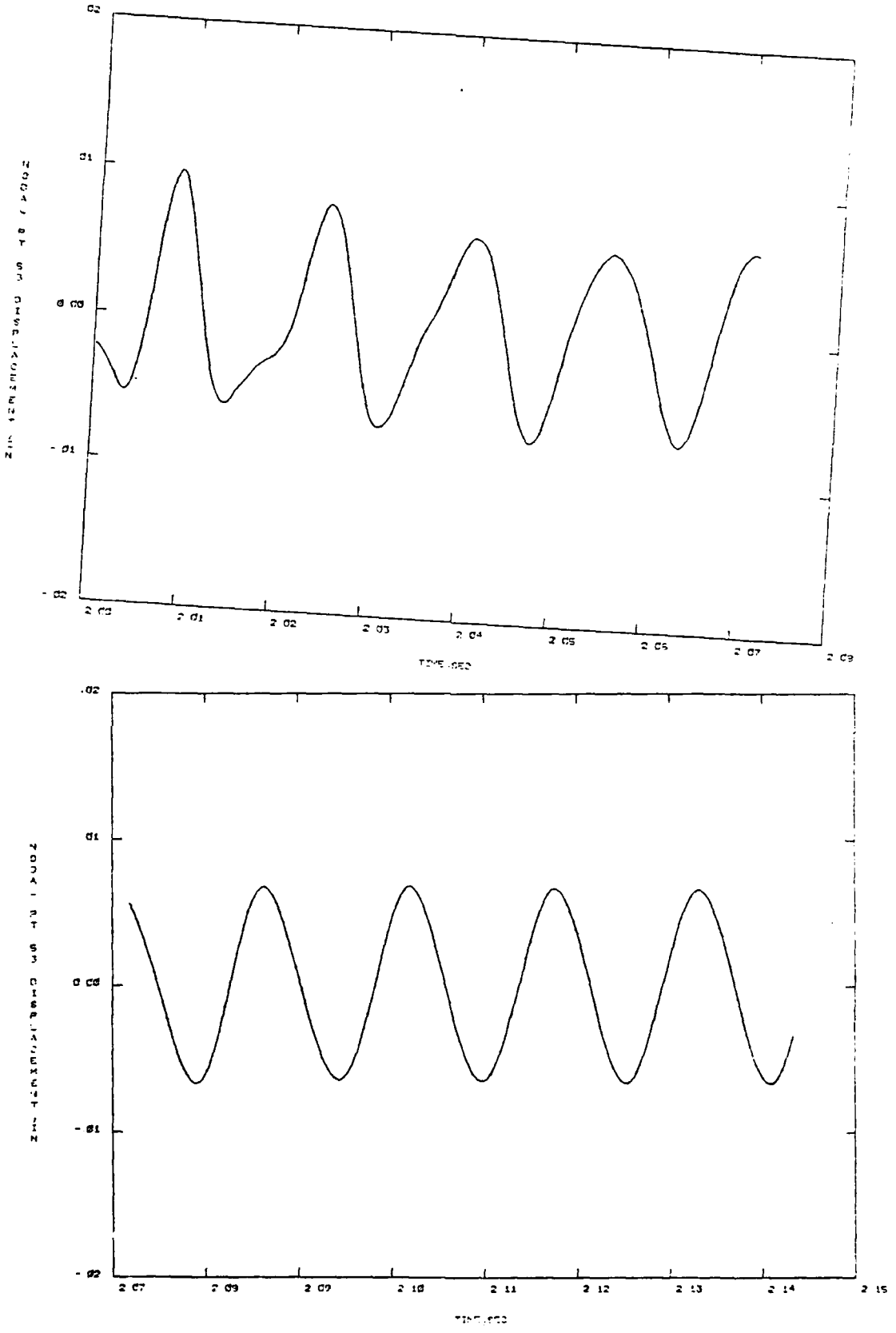

Figure A-11. (continued)

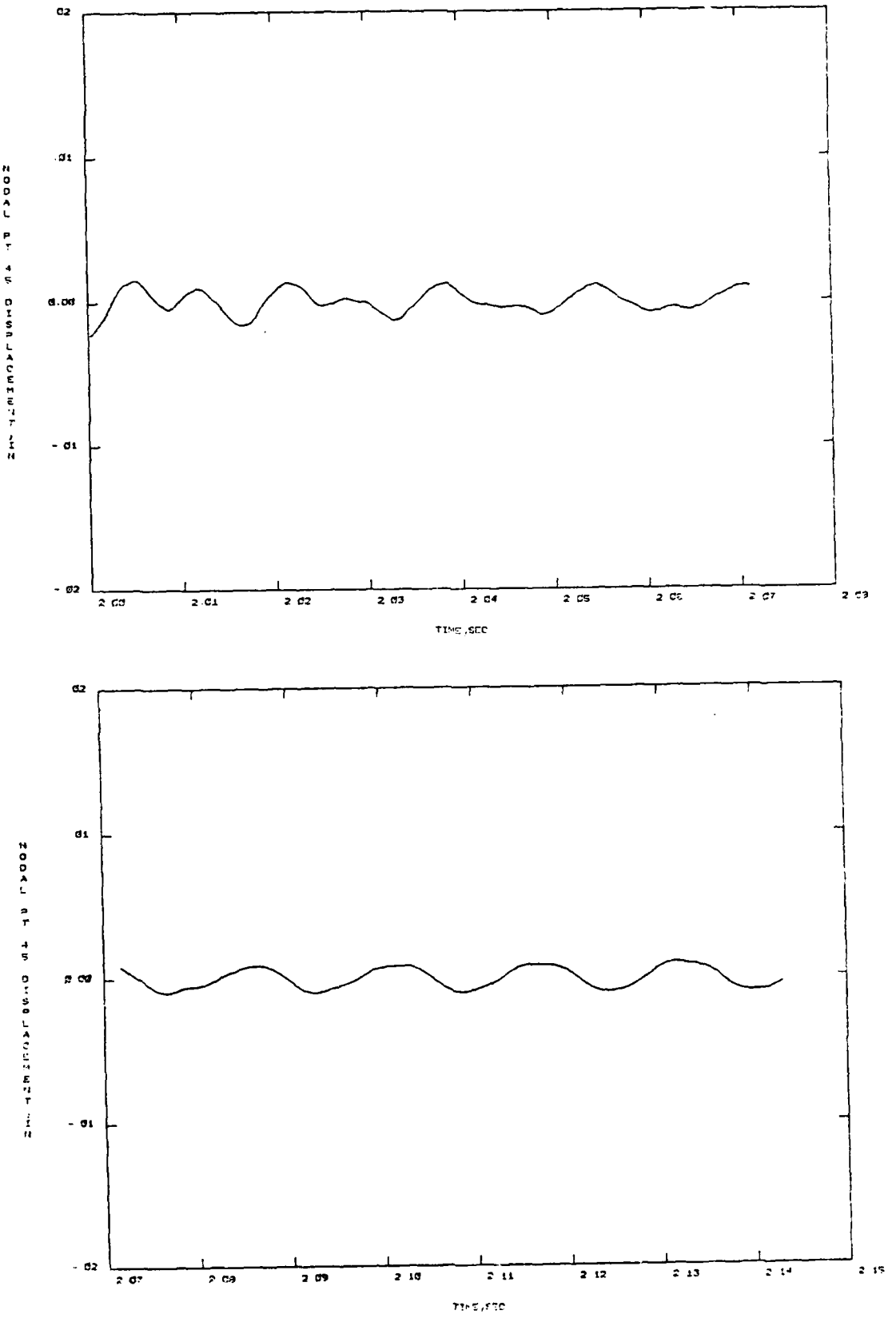

Figure A-12. Transient Dynamic Response to ID#3 (λ = 300, u/M = .013, M = 0.8)

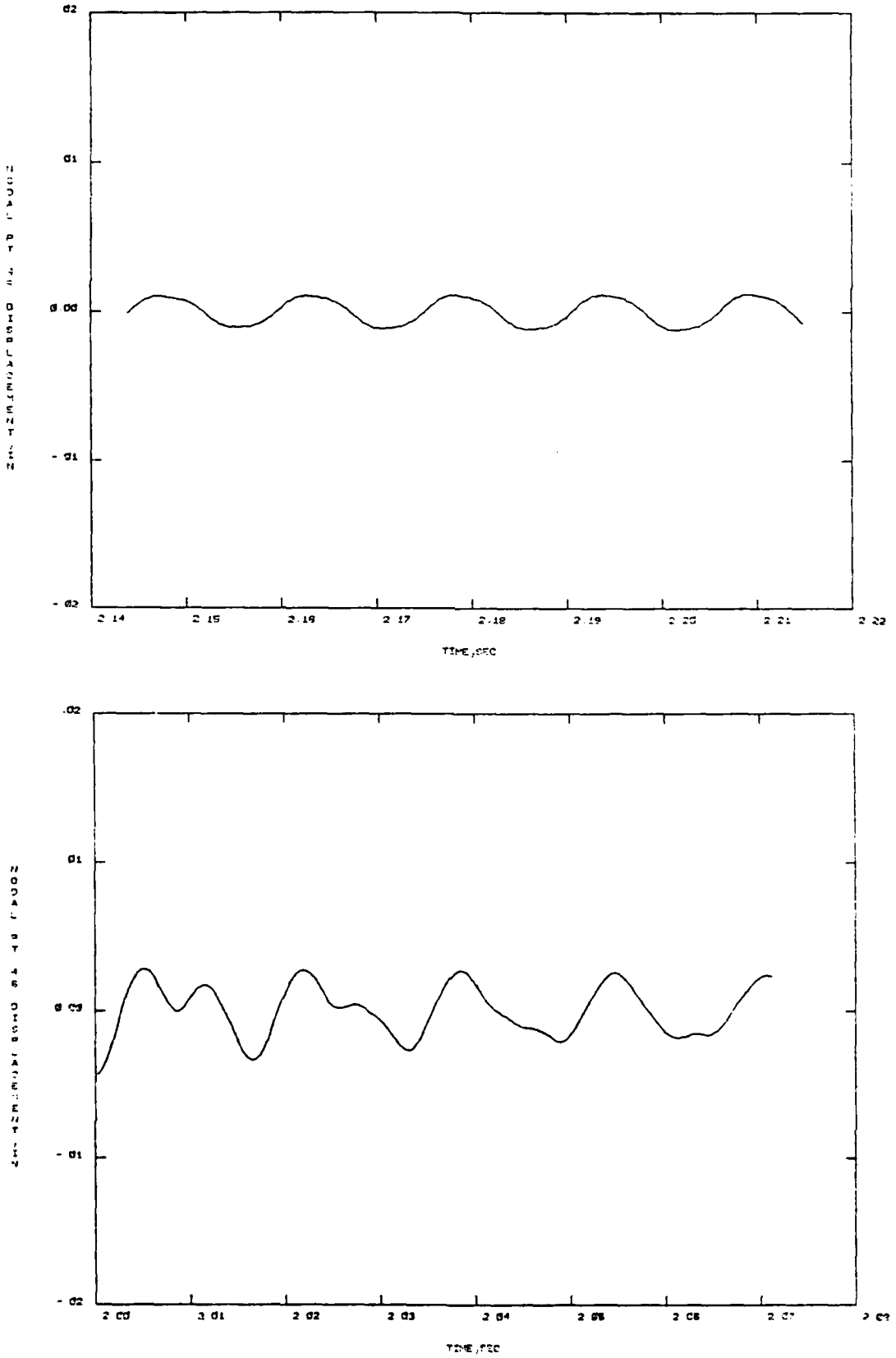

Figure A-12. (continued)

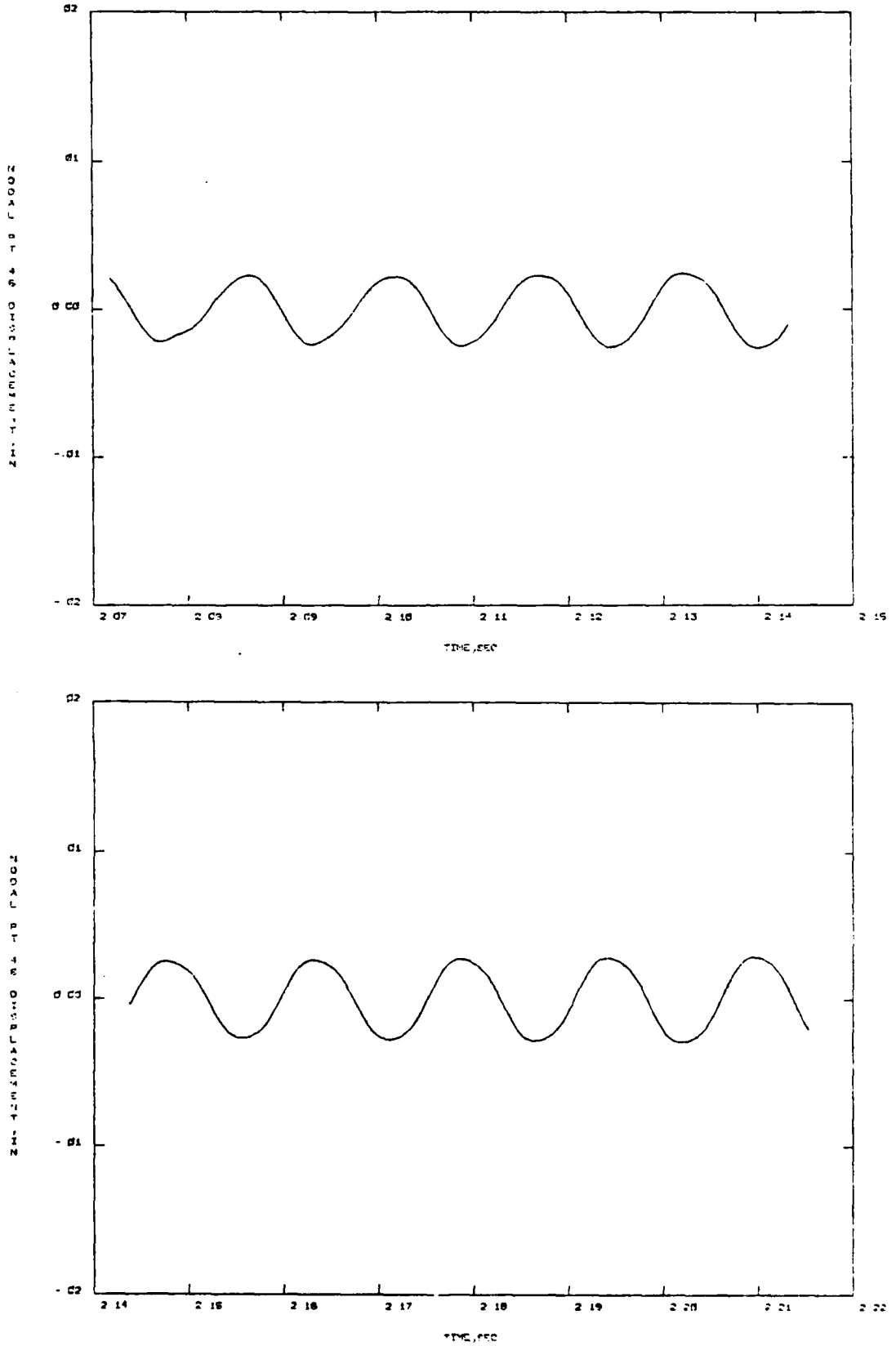

Figure A-12. (continued)

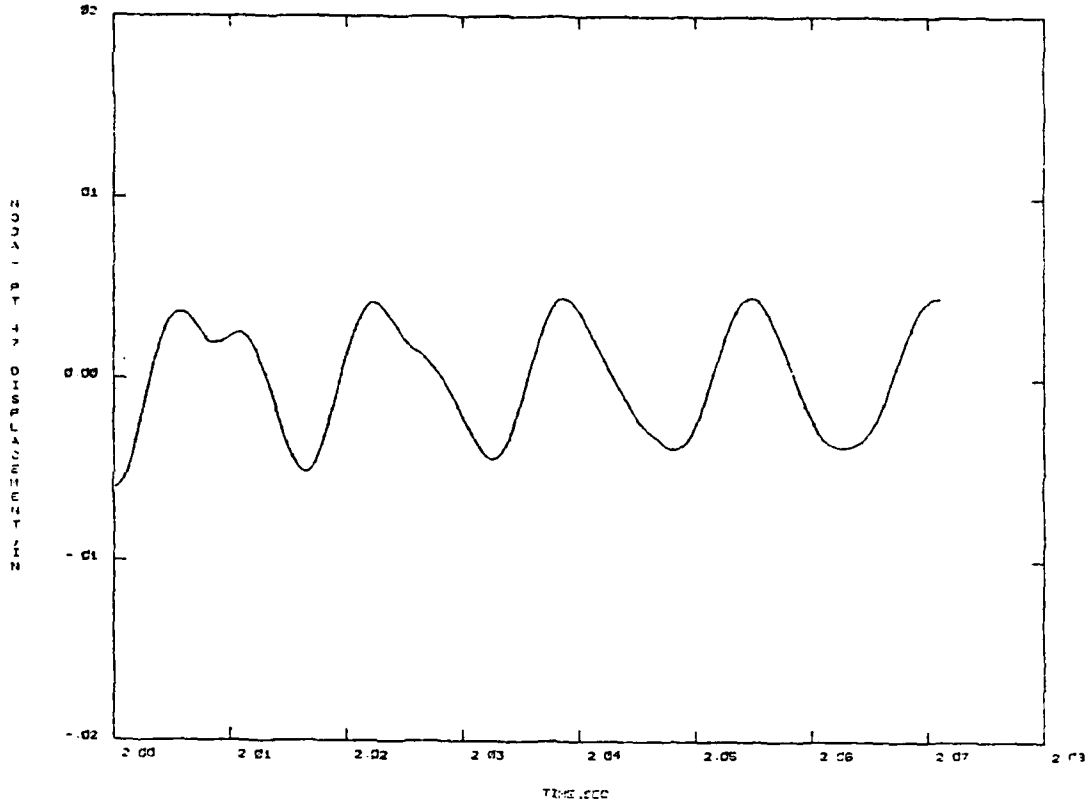

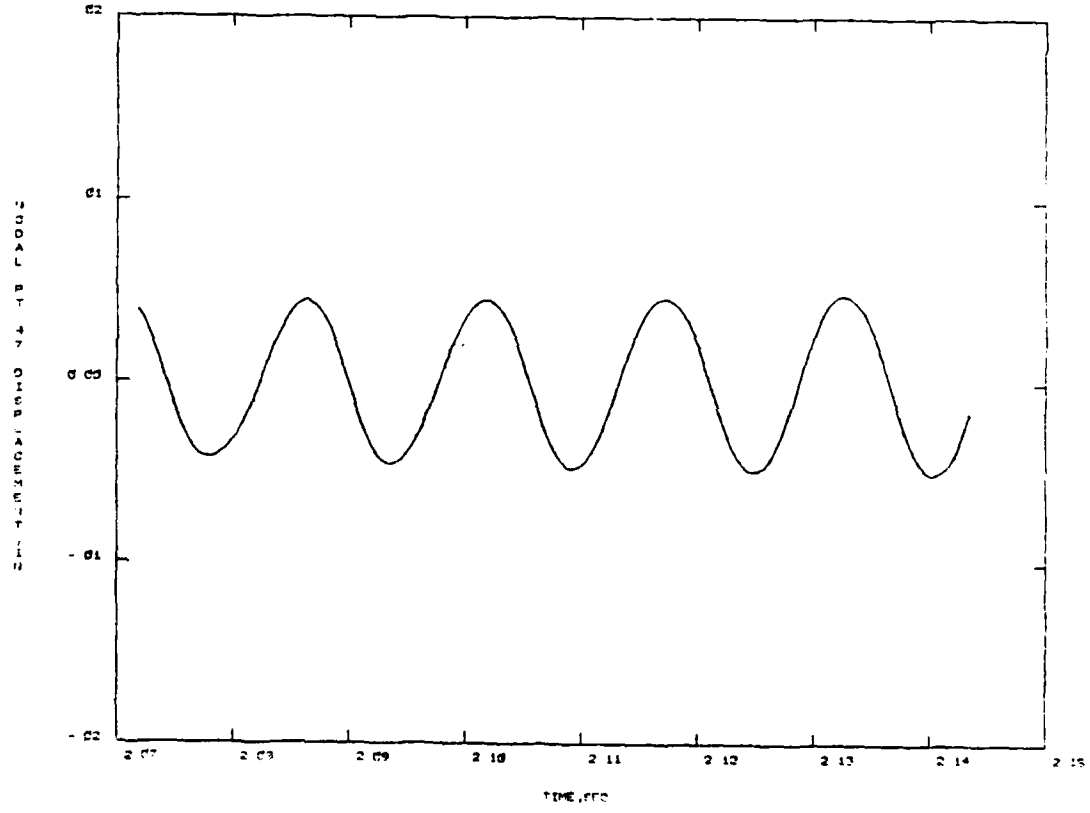

Figure A-12. (continued)

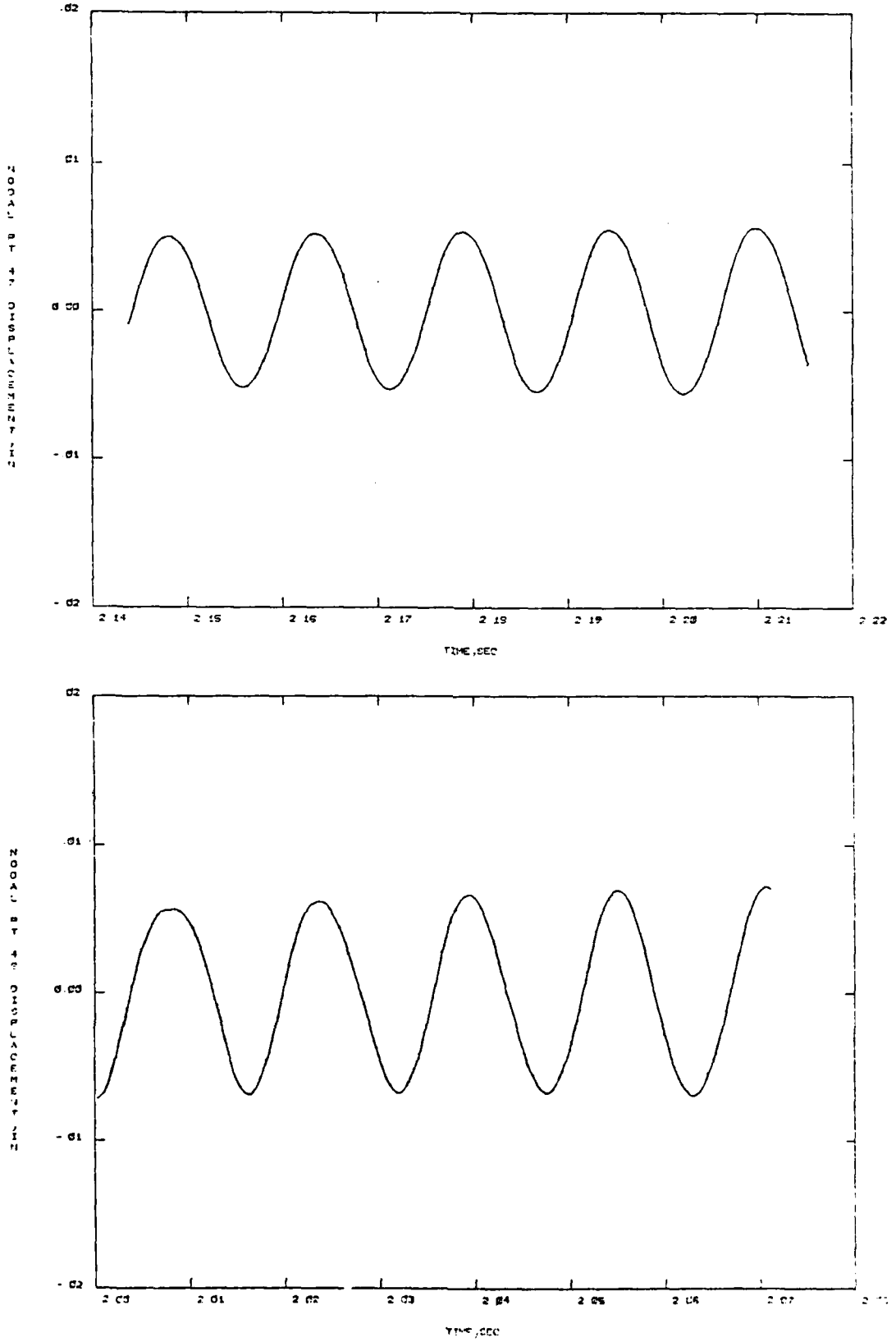

Figure A-12. (continued)

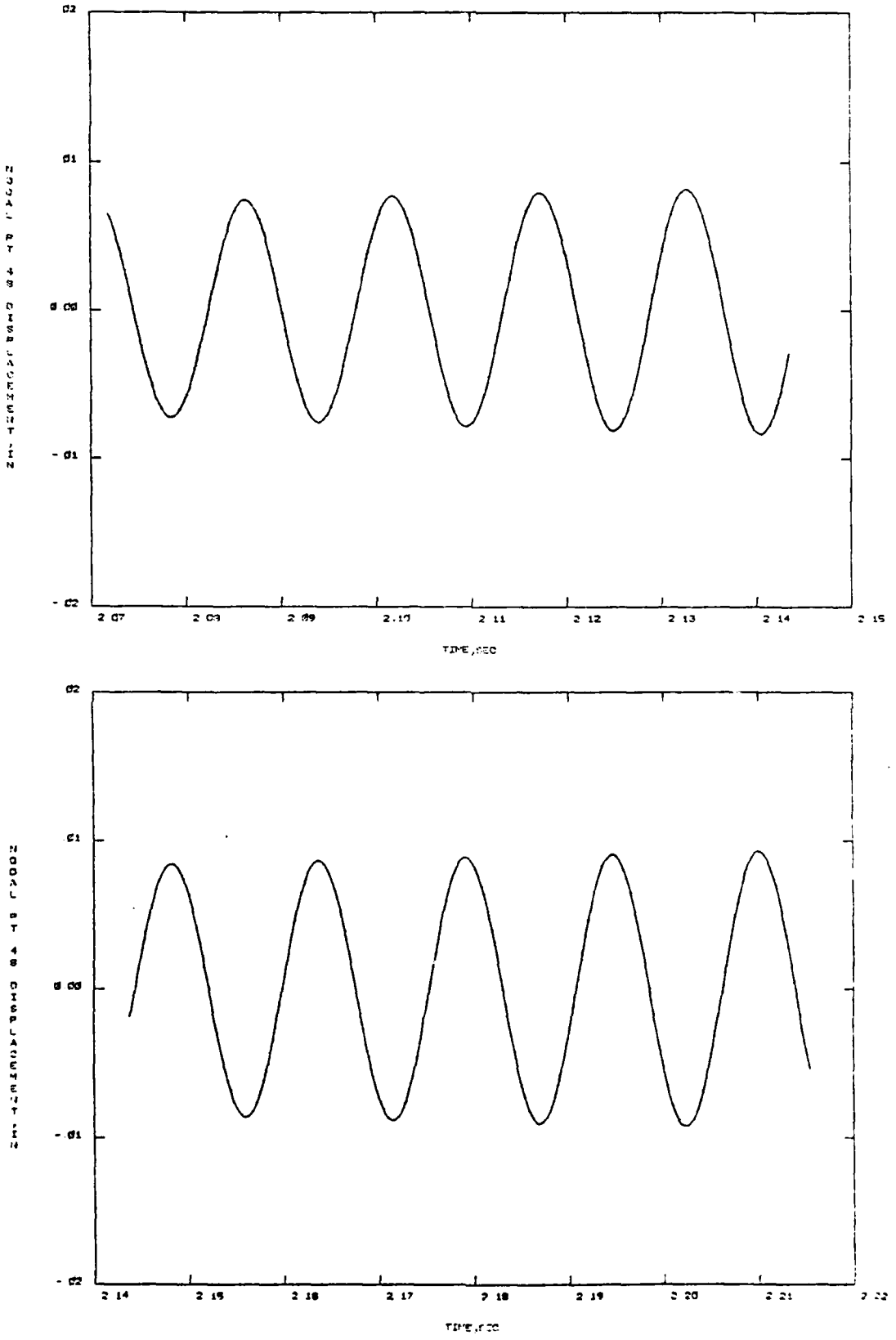

Figure A-12. (continued)

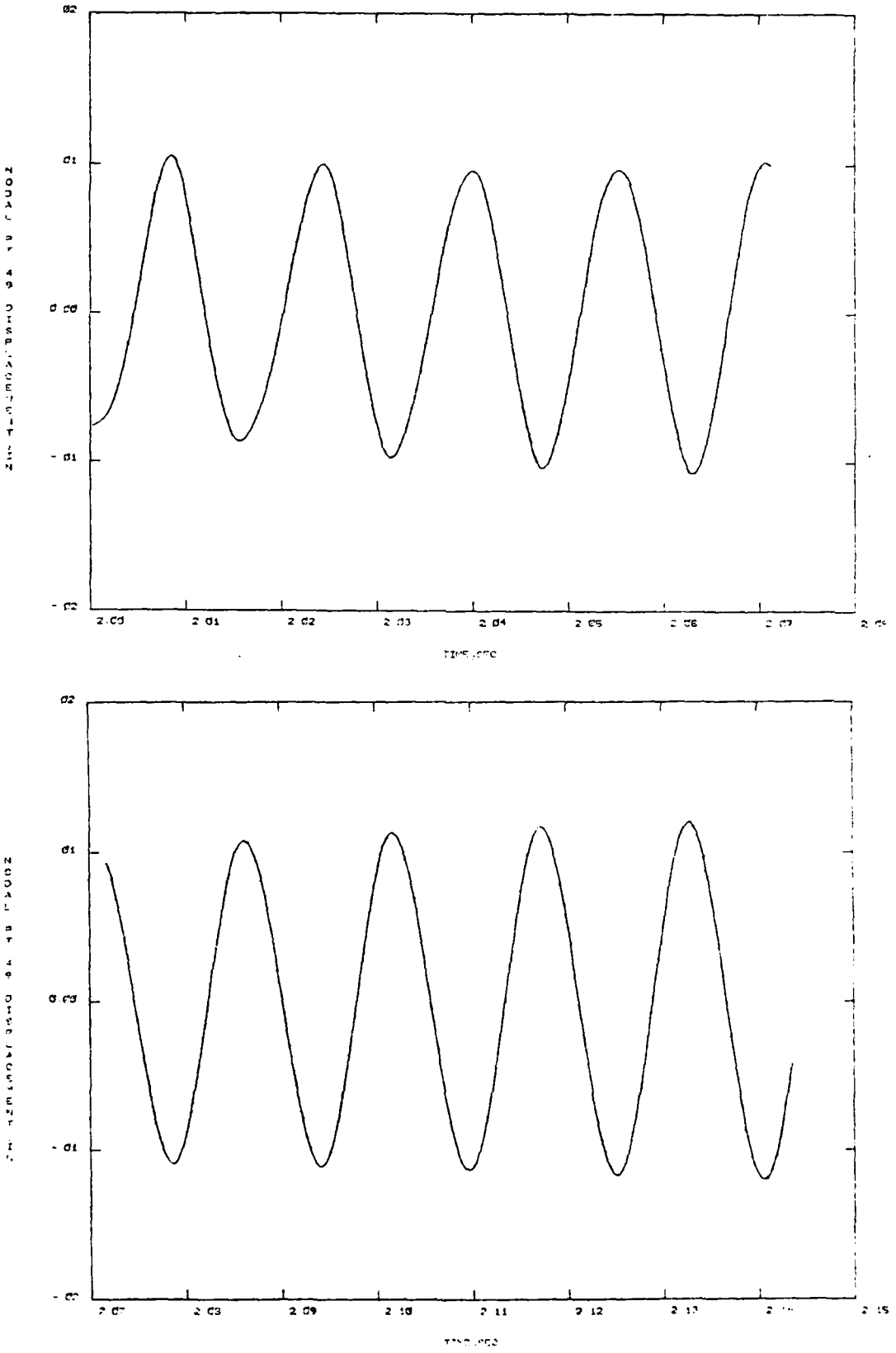

Figure A-12. (continued)

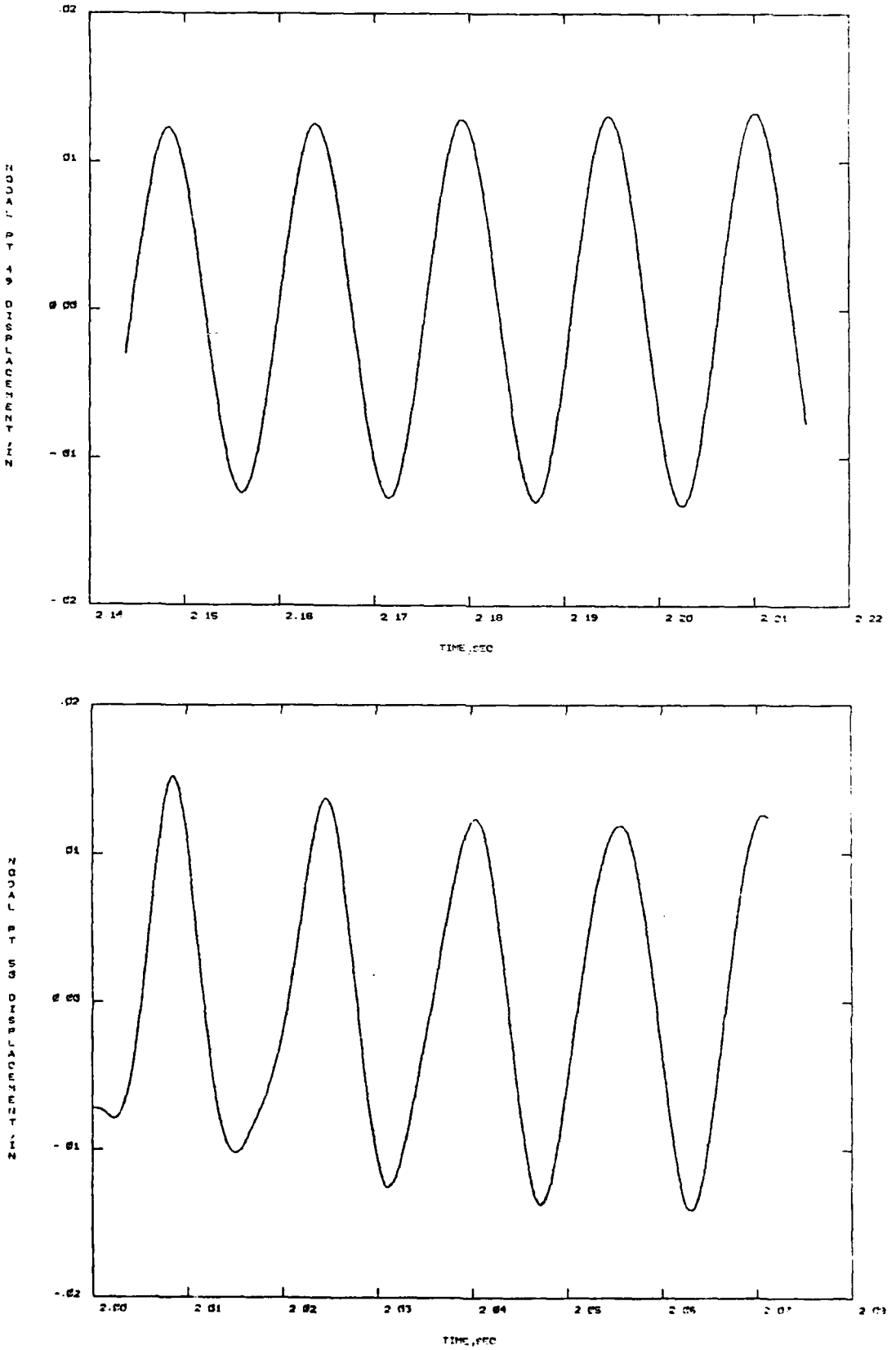

Figure A-12. (continued)

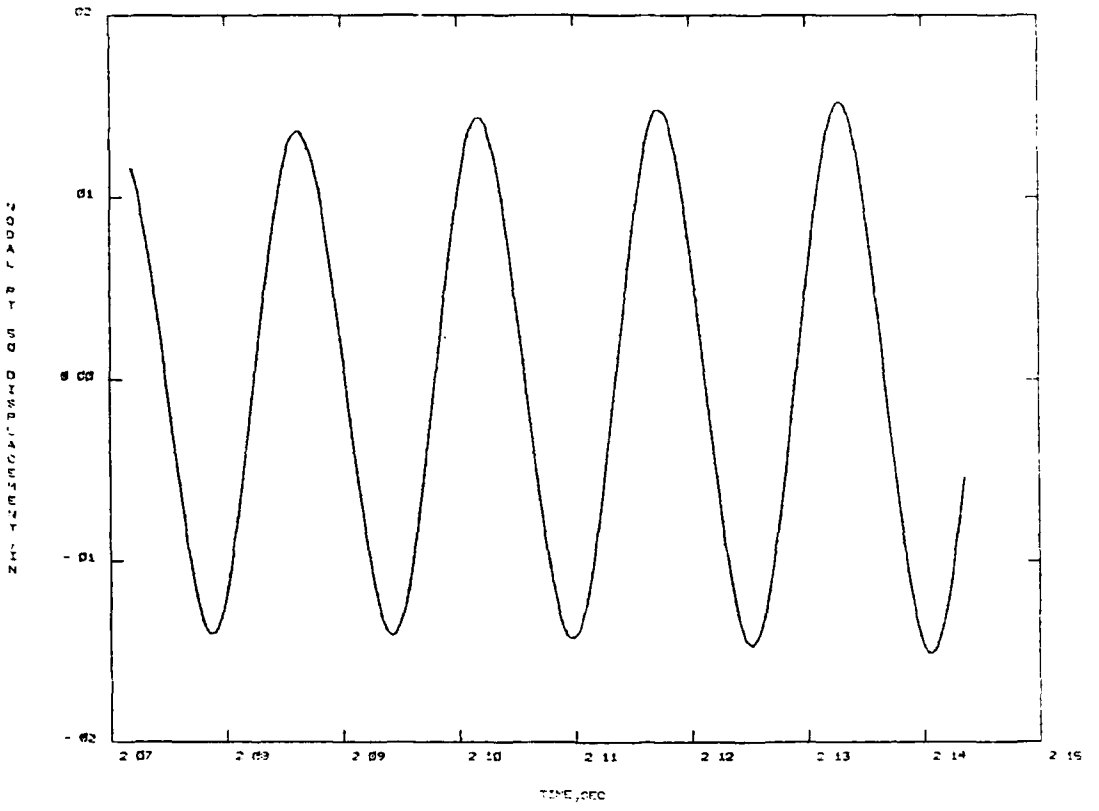

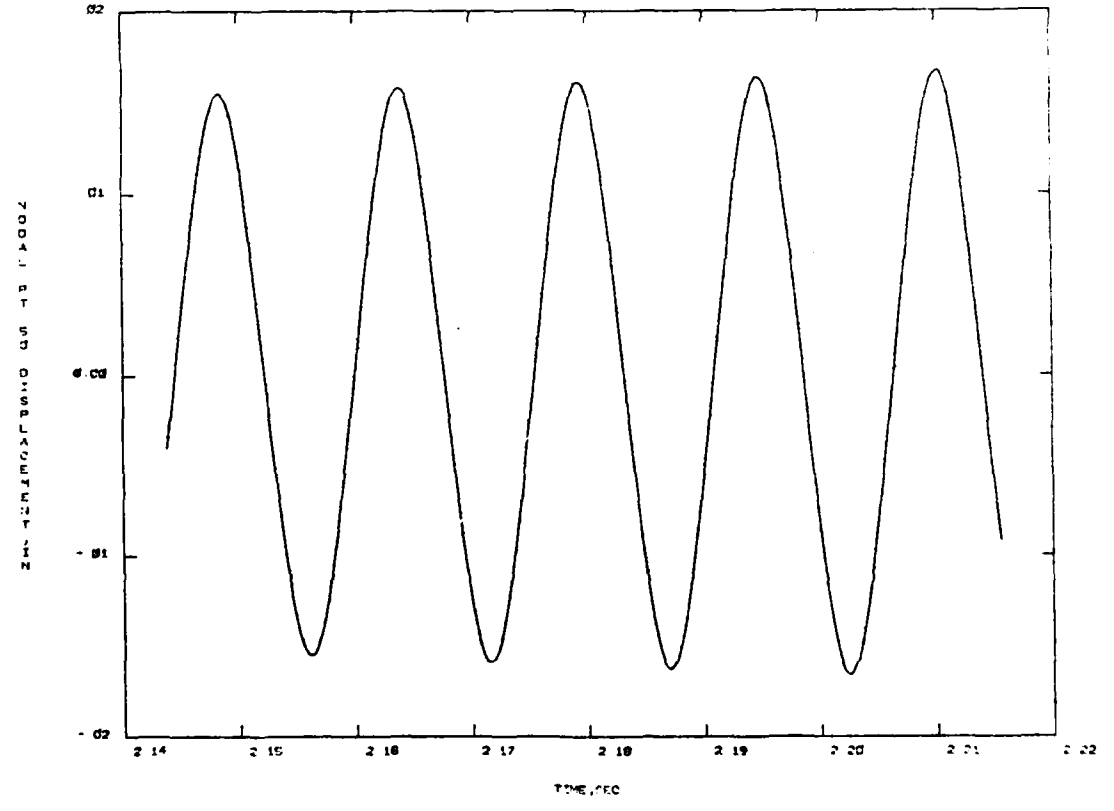

Figure A-12. (continued)

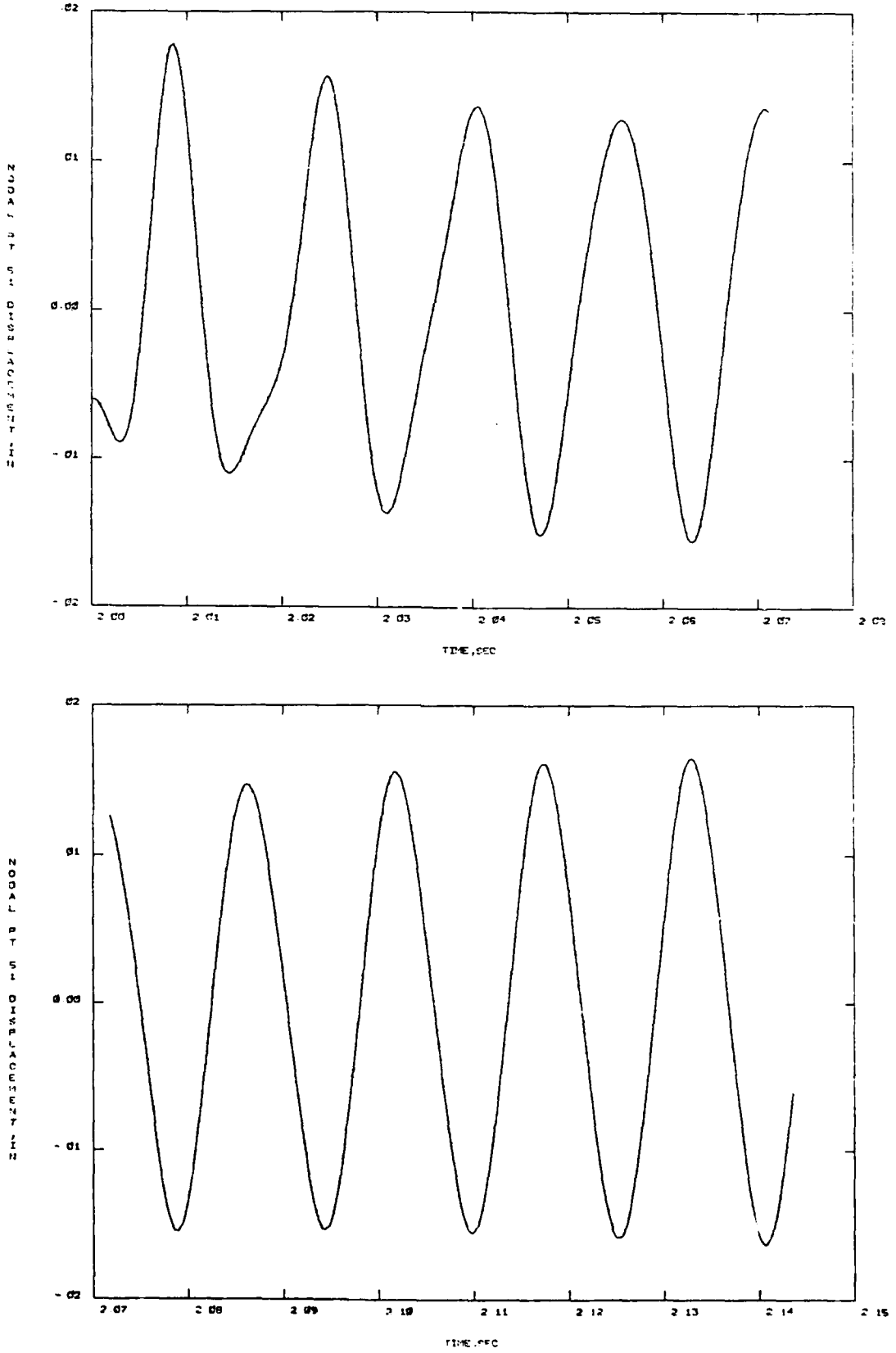

Figure A-12. (continued)

AD-A133 918 NONLINEAR OSCILLATIONS OF A FLUTTERING PANEL IN A TRANSONIC AIRSTREAM(U) DAYTON UNIV OH SCHOOL OF ENGINEERING F E EASTEP APR 83 UDR-TR-83-43 2/2

UNCLASSIFIED AFOSR-TR-83-0858 AFOSR-81-0134 F/G 20/4 NL

END
DATE FILMED
11 83
DTIC

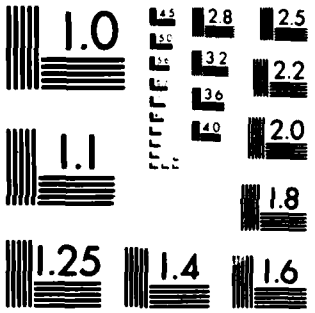

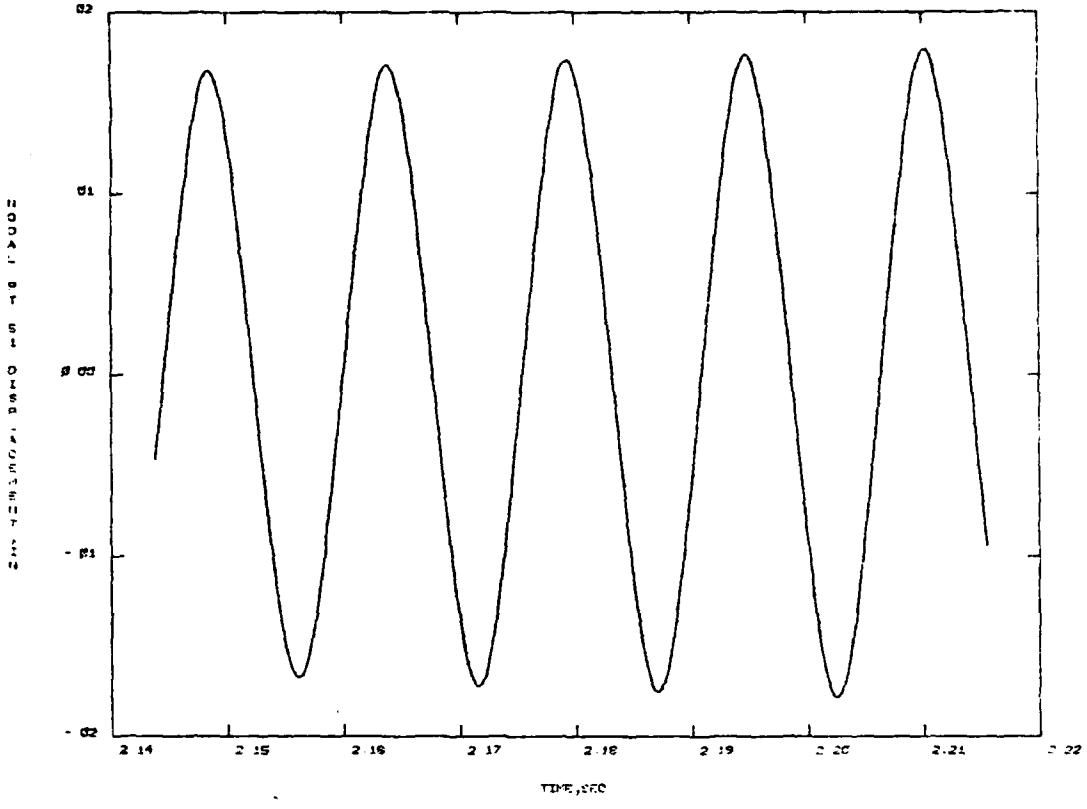

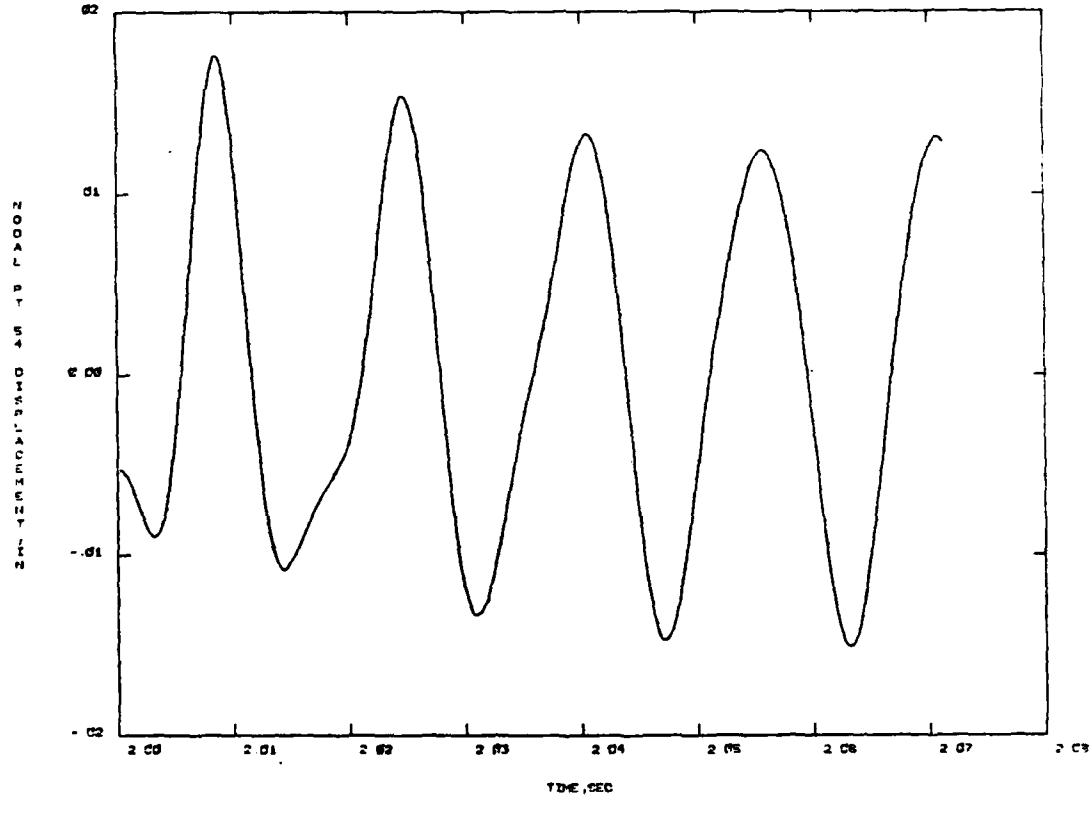

Figure A-12. (continued)

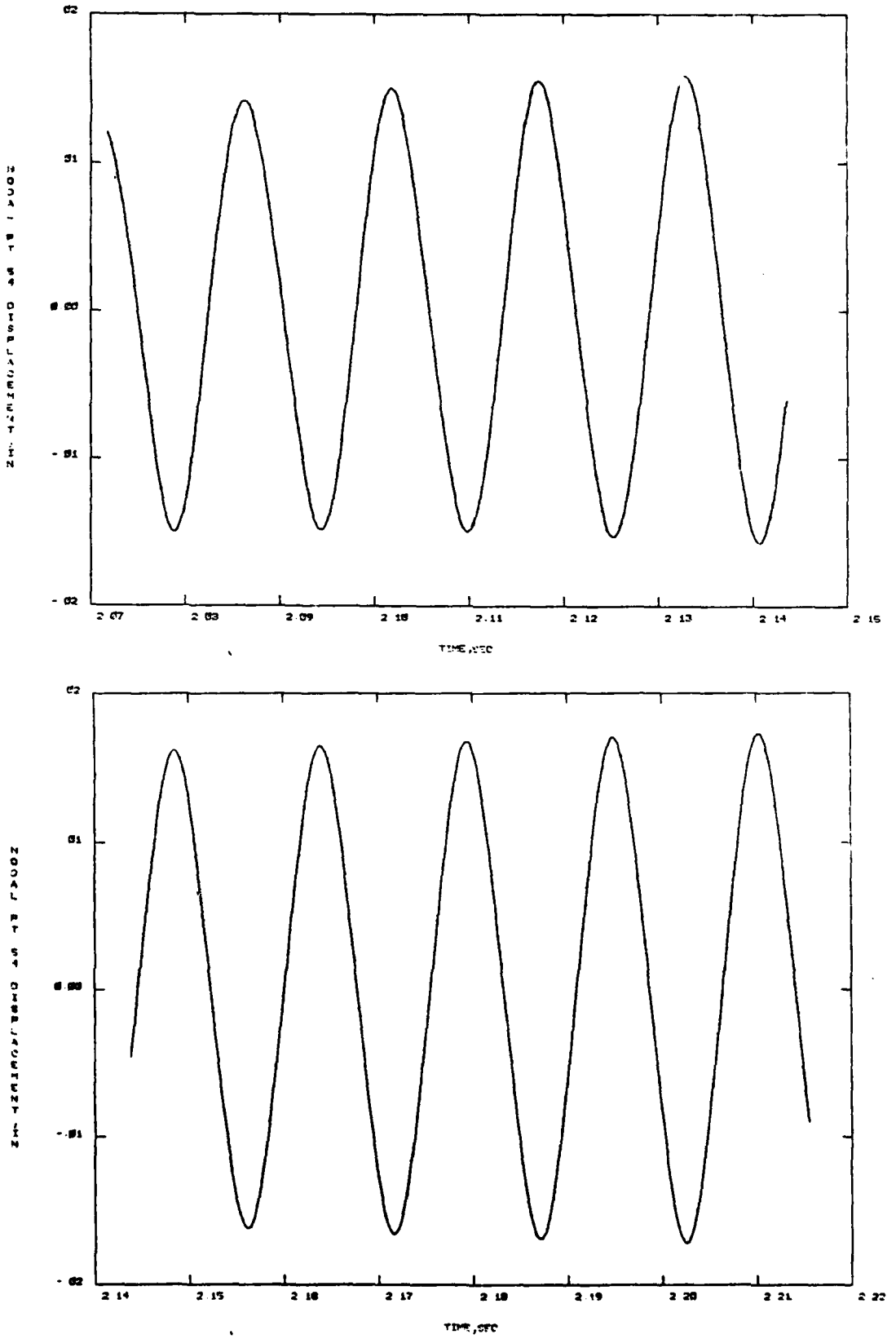

Figure A-12. (continued)

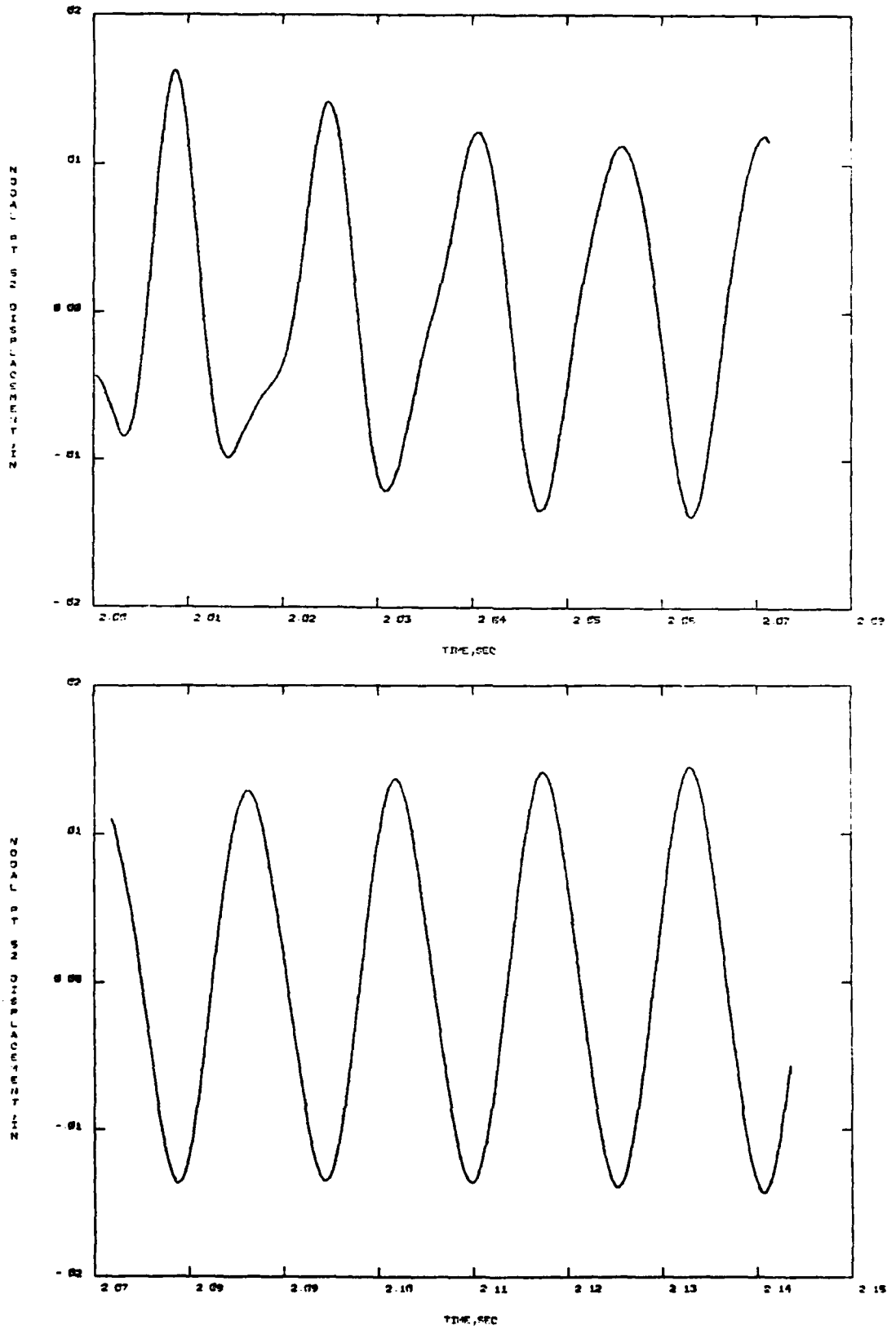

Figure A-12. (continued)

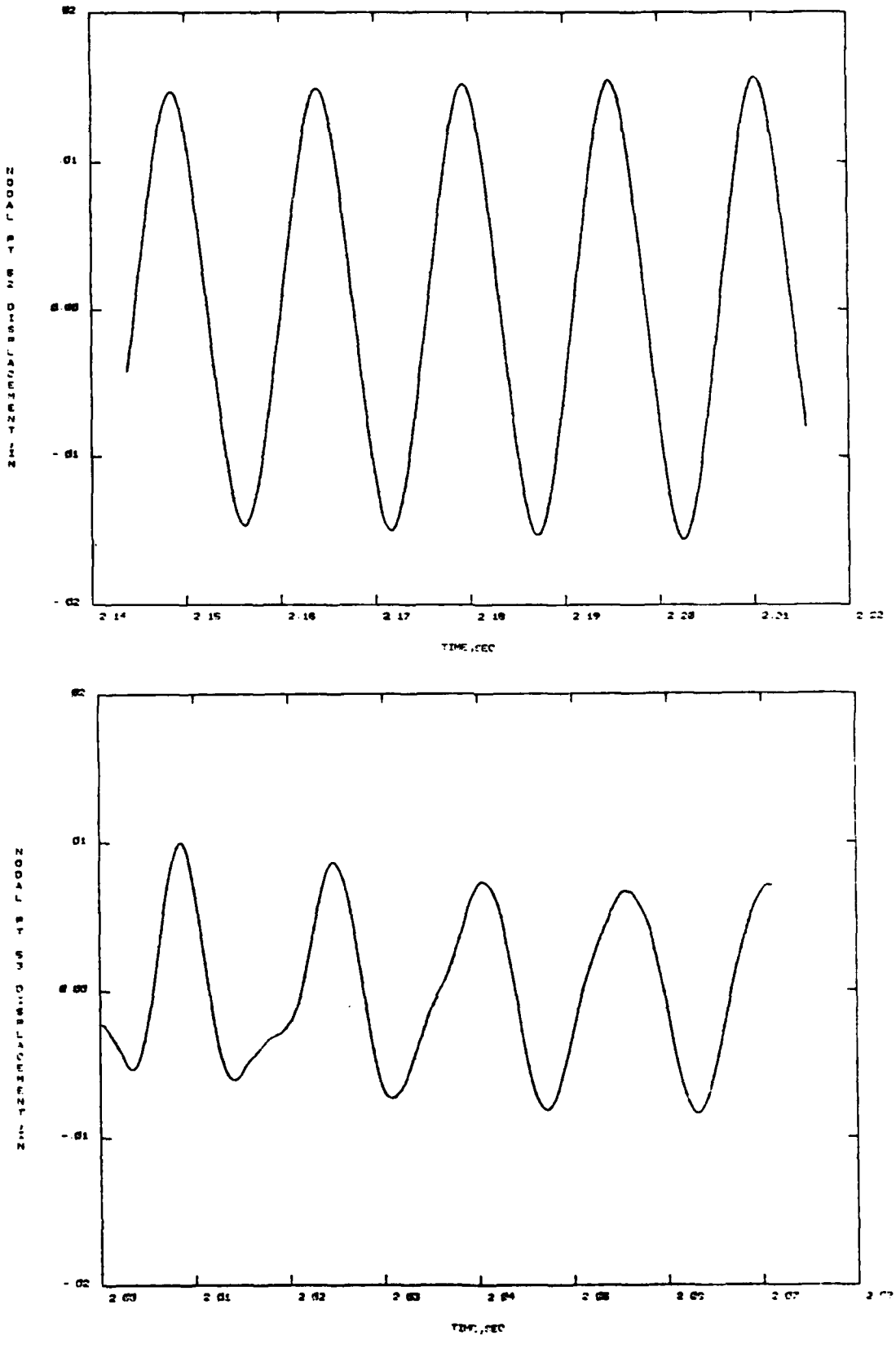

Figure A-12. (continued)

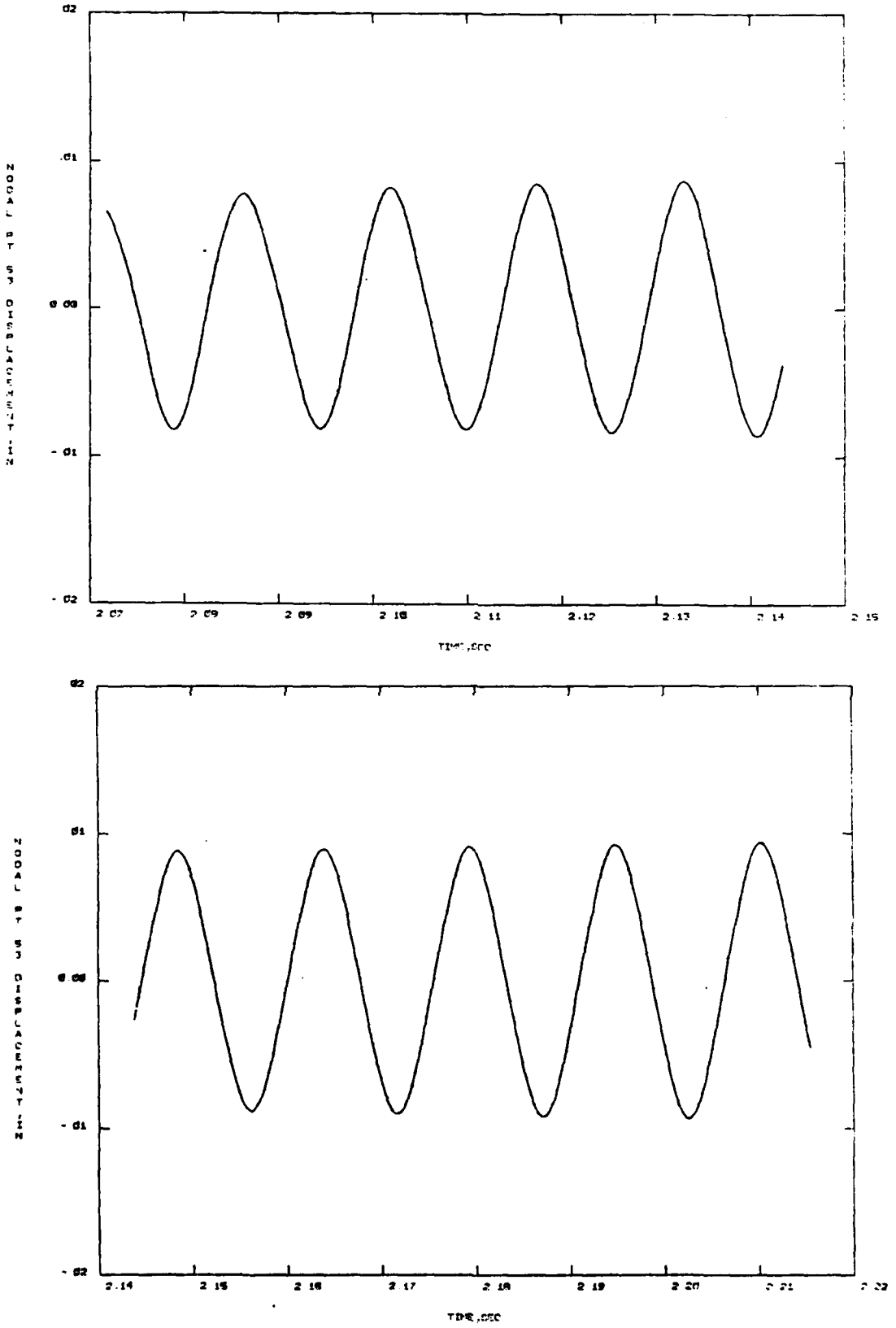

Figure A-12. (continued)

APPENDIX B

ELEMENT #9 ROUTINE MODIFIED FOR PLANE STRAIN

```
      SUBROUTINE INP09 (NELEM,NMAT,NONLIN,IOYN)
C-VAX      IMPLICIT REAL*8 (A-H,O-Z)
      COMMON/BLANK/X(4,1)
      COMMON  /VCPARAM/ NCD(9),NP(9),IPAR(15)
      COMMON/PCOM1/E(3,3),RHO,RATIO,EPSINC,G,AA(3,3),
     +             THICK,XK,TEC
      COMMON/FILNAM/NIN,NOUT,NTK,NTVC,NTEK,NTEM,NTCON,NTEC,
     +       NTPR,NTST
      DIMENSION PROP(25),ALFA(20)
      DIMENSION EE(20),PR(20),CNS(20),YLD(20)
      DIMENSION DEMAX(20),GAMMA(20),IHARD(20),ISSC(20)
      DIMENSION EC(18),IOUTAX(2)
      EQUIVALENCE (E(1,1),PROP(1))
      DATA HISO,HKIN,HCOM,BLANK,IOUTAX
     +     /3HISO,3HKIN,3HCOM,3H   ,3HLOC,3HGLC /
C
C     INPUT AND ELEMENT FILE INITIALIZATION
C     ELEMENT 9 - VARIABLE (4-9) NODE PLANE STRESS ELEMENT
C
      CALL PPROP (2,3,0,NELEM,I4,R1)
      NPRMD=25
      DO 1 I=1,NPRMD
    1    PROP (I)=0.
      IPAR(1)=0
      IPAR(2)=24
      IPAR(3)=24
      IPAR(4)=2
      IPAR(5)=2
      IPAR(6)=NPRMD
      DO 2 I=7,15
    2    IPAR(I)=0
      NTP2=NTST
      WRITE(NOUT,1000)
      WRITE(NOUT,1010)
C
C     MATERIALS DATA
C
      DO 5 I=1,NMAT
         READ(NIN,1020) EE(I),PR(I),CNS(I),YLD(I),DEMAX(I),
     +      GAMMA(I),IHARD(I),ISSC(I),ALFA(I)
         IF(NONLIN.GT.0) GO TO 4
C
C     LINEAR MATERIAL PROPERTIES
C
         WRITE(NOUT,1030)I,EE(I),PR(I),CNS(I),ALFA(I)
         GO TO 5
C
C     NONLINEAR MATERIAL PROPERTIES
C
    4    IF(YLD(I).LE.0.) YLD(I)=1.E2
         IF(DEMAX(I).LE.0.0)DEMAX(I)=0.
         IF(IHARD(I).LE.0) IHARD(I)=1
         SH=BLANK
         IF(IHARD(I).EQ.1) SH=HISO
         IF(IHARD(I).EQ.2) SH=HKIN
         IF(IHARD(I).EQ.3) SH=HCOM
      WRITE(NOUT,1040)I,EE(I),PR(I),CNS(I),ALFA(I),YLD(I),
```

```
     +                    DEMAX(I),GAMMA(I),SH,ISSC(I)
    5      CONTINUE
C
C     READ ELEMENTS
C     WRITE =        1.CONNECTIVITY FILE
C                    2.ELEMENT COORDINATES FILE
C                    3.PROPERTIES FILE
C                    4.INTEGRATION POINT FILE
C
      ITYPE=1
C ------------------------------------
C
C ---- MODIFICATION FOR PLANE STRAIN ---
C
                ITYPE = 2
C
C ------------------------------------
      IELPR=0
      IPRPR=0
      DO 8  I=1,9
         NOD(I)=0
    8    NP(I)=0
C
      WRITE(NOUT,116 )
   11 READ (NIN,105) IELNO,IPR,INT,KGEN,NOD,THICK
      IF(IELNO.LE.0) GO TO 51
      IF(KGEN.LE.0) KGEN=1
      IPAR(14)=IPR
      IF (THICK.LE.0.0) THICK=1.0
      IF (INT.LT.2) INT=2
      IF(INT.GT.3) INT=3
      IF((IELNO-IELPR).GT.1) GO TO 13
      DO 11  I=1,9
   11    NP(I)=NOD(I)
      KGEN=0
   12 CONTINUE
C
C     GENERATE ELEMENTS IELPR+1 THROUGH  IELNO
C
      NE=IELNO-IELPR
      DO 34 IE=1,NE
         IELPR=IELPR+1
         DO 14  I=1,9
            IF (NP(I).GT.0) NP(I)=NP(I)+KGEN
   14       CONTINUE
         IF(KGEN)15,150,15
C
C     KGEN.EQ.0 : SET UP NEW PROPERTIES
C
   15    CONTINUE
      IPAR(5)=INT
      IPAR(7)=1
      IFLAG=IPR-IPRPR
      IPRPR=IPR
      IF(IFLAG.EQ.0) GO TO 18
      IPAR(9)=ISSC(IPR)
      IPAR(10)=IHARD(IPR)
```

```
115                EEE=EE(IPR)
                   PRT=PR(IPR)
                   CALL GET2D (E,EEE,PRT,ITYPE)
                   RHO=DNS(IPR)
                   XK=YLD(IPR)
120                TEC=ALFA(IPR)
                   RATIO=GAMMA(IPR)
                   EPSINC=DEMAX(IPR)
                   G=.5*EEE/(1.+PRT)
                 180 IF(NCNLIN.GT.0) IPAR(7)=
125             C
                C     ELEMENT COORDINATES AND TRANSFORMATION
                C
                   NPI=NP(1)
                   ZMAX=X(3,NPI)
130                ZMIN=X(3,NPI)
                   ZTOL=1.0E-5
                   DO 185 I=2,9
                      NPI=NP(I)
                      IF (NPI.LE.0) GO TO 185
135                   ZZ=X(3,NPI)
                      IF (ZZ.GT.ZMAX) ZMAX=ZZ
                      IF (ZZ.LT.ZMIN) ZMIN=ZZ
                 185  CONTINUE
                   DO 195 I=1,3
140                   DO 190 J=1,3
                 190      AA(I,J)=0.0E0
                 195   AA(I,I)=1.0E0
                   IPLANE=1
                   IF ((ZMAX-ZMIN).LE.ZTOL) IPLANE=2
145                IPAR(11)=IPLANE
                   IOUTZ=ICUTAX(IPLANE)
                   IF (IPLANE.LE.1) CALL CRTMAX (AA,NP)
                   KK=0
                   DO 210 J=1,2
150                DO 210 I=1,9
                      XL=0.0
                      NPI=NP(I)
                      IF (NPI.LE.0) GO TO 205
                      DO 200 K=1,3
155                 200  XL=XL+AA(J,K)*X(K,NPI)
                    205   KK=KK+1
                    210   EC(KK)=XL
                   CALL ICINMP(NTPR,IPAR,1,15)
                   CALL IGRLMP(NTEC,EC,1,18)
160                CALL ICINMP(NTCON,NP,1,9)
                   CALL IGRLMP(NTP2,PROP,1,NPRMP)
                   WRITE (NOUT,300) IELPR,IPR,INT,KG-N,NP,THICK,IOUTZ
                   CALL PRELEM (IELPR,9,NP)
                 300  CONTINUE
165             C
                C     NEXT ELEMENT
                C
                   GO TO 1
                5     RETURN
170                1  FORMAT(4H1)
                   101  FORMAT (1X,24HINPUT FOR ELEMENT TYPE 9 ,
```

```
     +       8X,26HTWO-DIMENSIONAL, 4-9 NODE ,
     +          2?HPLANE STRESS ELEMENT      ,
     +       //1?X,19HMATERIAL PROPERTIES  ,
     +       //1?X,4HMATL,5X,23HMODULUS   POISSON RATIO  ,
     +   3X,7HDENSITY,3X,9HTHERM.EXP,3X,21HYIELD   MX.INC.STRAIN
     +       2X,5HGAMMA,6X,2?HHARDENING  S-E CURVE    ,/1X)
      1?4? FORMAT (6E1?.?,2I5,E1?.?)
      1?3? FORMAT(I13,3X,E12.5,F12.6,2E12.6)
      1??? FORMAT(I13,3X,E12.5,F12.6,2E12.6,3X,E11.4,1X,
     +       E11.4,F9.4,8X,A3,3X,I7)
      1?8? FORMAT(//1?X,2?HELEMENT CONNECTIVITY,
     +      WITH FOR VARIABLE-NODE PLANE STRESS ELEMENTS,
     +//1?X,24HELMT  MATL  INT  KGEN   ,
     +      3?HNODE1 NODE2 NODE3 NODE4 NODE5 ,
     +      35HNODE6 NODE7 NODE8 NODE9   THICKNESS,
     +   2X,11HOUTPUT AXES                    ,/1X)
      1 9? FORMAT (I14,2I5,I7,2X,9I6,3X,E1?.3,5X,A3)
      1?E? FORMAT (13I5,F1?.?)
      END
```

APPENDIX C

USER ROUTINE FOR PISTON THEORY AERODYNAMICS

```
      SUBROUTINE ULOAD(P,WK,TIME,DT,NTNODV,NRDOF,NRCODE,NTDIS,
     +NRU,NRV,NIN,NOUT)
      DIMENSION P(1),WK(1)
      COMMON/MPAFT/N,IFILL(3),NWORK
      DATA FACT1,FACT2/-.5,-2./
C     LAMDA = 3.,U/M = .13
      PI = 0.
      IELE = 1
   10 NA = (IELE-1)*8+4
      NB = (IELE-1)*8+6
      NC = (IELE-1)*8+12
      CALL READMF(NTDIS,WK,N,NRU)
      DISPA = WK(NA)
      DISPB = WK(NB)
      DISPC = WK(NC)
      CALL READMF(NTDIS,WK,N,NRV)
      VELA = WK(NA)
      VELB = WK(NB)
      VELC = WK(NC)
      P(NA) = .0375*FACT1*(-3.*DISPA+4.*DISPB-DISPC)+
     1.5929E-5*FACT2*(4.*VELA+2.*VELB-VELC)+PI
      P(NB) = .075*FACT1*(-1.*DISPA+DISPC)+
     1.1186E-4*FACT2*(VELA+6.*VELB+VELC)
      PI = .0375*FACT1*(DISPA-4.*DISPB+3.*DISPC)+
     1.5929E-5*FACT2*(-1.*VELA+2.*VELB+4.*VELC)
      IELE = IELE+1
      IF(IELE.GT.10) GO TO 20
      GO TO 10
   20 CONTINUE
      P(NC) = PI
      WRITE(NOUT,31)
   31 FORMAT(1HX,*NODAL FORCES IN Y-DIRECTION ON UPPER SURFACE*)
      DO 40 I=4,84,4
      WRITE(NOUT,30) P(I)
   40 CONTINUE
   30 FORMAT(1HX,E15.8)
      RETURN
      END
```

APPENDIX D

COMMENTS ON NUMERICAL INSTABILITIES WHEN BOTH PANEL AND AERODYNAMIC EQUATIONS ARE NONLINEAR

An analysis was initiated to study the panel response represented by a nonlinear structural equation (Von Karman's large deflection) and a nonlinear aerodynamic equation represented by NLR-LTRAN2 numerical code. A time dependent response study requires the simultaneous time integration of the structural and aerodynamic nonlinear equations. Here, the panel response was represented by a linear superposition of assumed modal terms even though both the structural equations and aerodynamic equations are nonlinear. Using the Galerkin procedure, the spatial dependency in the structural equations was eliminated and were integrated simultaneously with the aerodynamic equations represented by the NLR version of LTRAN2. The NLR version of LTRAN2 included a modification to account for the changing induced angle of attack resulting from the panel deformation which was incorporated into a chord deformation option contained internal to NLR-LTRAN2.

The simultaneous time integration procedure allows one to determine panel deflection, velocities and accelerations. Once the initial conditions for the panel deformation are provided, the effective induced angle of attack and its time derivatives can be calculated for each point on the panel. The resulting aerodynamic pressures can then be calculated. The panel response or deformation at the next time increment can be determined and

the process repeated for each desired time step. Prior to releasing the panel for response to the aerodynamic pressure, the aerodynamic equations were integrated in time for an assumed simple harmonic panel deformation until the transient prediction of the aerodynamic pressures disappeared and the pressures became periodic. This assumed simple harmonic motion generally required the time for two periods of panel oscillation to insure that the convergence criteria specified in NLR-LTRAN2 was satisfied.

For the panel and airstream parameters investigated, the simultaneous integration of nonlinear structural and aerodynamic equations were unsuccessful in obtaining stable panel responses. In all cases the panel response diverged sometimes quite quickly when the panel was freed to response to the transonic aerodynamic pressure. The diverging panel response was attributed to numerical instabilities since previous investigations using a linear aerodynamic representation at greater Mach numbers (piston theory) yields a stable panel response for certain selected panel parameters. Various magnitudes of initial displacement, velocity and acceleration, both singly and in combination, were investigated. The time step for the time integration was varied to very small values within computational considerations. Also, the number of cycles for forcing the plate motion in a sinusoidal fashion was varied to assure all transients were small. In all cases considered, the panel response was divergent after a given period of time.

The following suggestions are offered as possible courses of the aforementioned numerical instabilities for consideration by future investigators.

1. The chord deformation option within NLR-LTRAN2 was a constant source of convergence problems. Even for very small panel deformations the local angles of attack (slopes of panel deformation) can become large enough to exceed the convergence criteria specified in NLR-LTRAN2. This would result in an over prediction of aerodynamic pressure with no warning from the computational code. This investigator is unaware of any verification that the chord deformation option has been accomplished and any coding errors would surely yield a source of numerical instabilities. Further investigation of the aerodynamic pressures predicted by this option of NLR-LTRAN2 for a given chord deformation would seem to be warranted to insure numerical stability.

2. Representation of the nonlinear panel response to the nonlinear aerodynamic pressures by a linear superposition of natural modes may be another source of numerical instability and is a somewhat questionable approach. As suggested in Appendix A, the representation of the large deflection structural equations with a large deflection finite element has some merit for investigation of nonlinear response.

3. In performing the simultaneous integration of structural and aerodynamic equations there is by necessity a difference in time step increments required primarily to insure convergence of the chord deformation option used in NLR-LTRAN2.

The difference in the time scaling between the structure and aerodynamic equations were not fully investigated and would be another source of numerical instability.

4. The stable response obtained using a linear aerodynamic theory were conducted at supersonic Mach numbers whereas the Mach numbers selected in this investigation were in the so called "sub-transonic" Mach number regime. The flow field characteristics are radically different than the supersonic Mach regime and would require numerical carefulness to insure numerical stability. Verification of the possibility of stable responses in this "sub-transonic" region needs to be established.

5. Another possible cause could be the time step size resulting in an instability generated by the motion of a shock wave due to the mixed numerical differencing in NLR-LTRAN2. It would be necessary to choose the time interval small enough such that shock waves do not travel more than one mesh point in the x direction over a single time step. However, very small time steps may result in prohibitive computational times.

6. Finally, the initial panel deformation and aerodynamic pressure generated initially before release of the panel to response to the aerodynamic pressure needs a more complete investigation when both nonlinear structural and nonlinear aerodynamic equations are integrated simultaneously.